Thesis/
Reports
Li,
R. M.

82-10-60

81 17

HYDRAULIC MODEL STUDY OF FLOW CONTROL STRUCTURES

FINAL REPORT

Prepared for

USDA FOREST SERVICE

ANGELES NATIONAL FOREST

Pasadena, California

and

ROCKY MOUNTAIN FOREST AND RANGE

EXPERIMENT STATION

Flagstaff, Arizona

CONTRACT NO. 16-712-CA #3 AND #4

Prepared by

Department of Civil Engineering
Engineering Research Center
Colorado State University
Fort Collins, Colorado

R. M. Li
D. B. Simons
T. J. Ward
C. J. Orvis

April 1979

CER 78-79RML-DBS-TJW-CJO 51

81 1703

HYDRAULIC MODEL STUDY OF FLOW CONTROL STRUCTURES

FINAL REPORT

Prepared for

USDA FOREST SERVICE

ANGELES NATIONAL FOREST

Pasadena, California

and

ROCKY MOUNTAIN FOREST AND RANGE

EXPERIMENT STATION

Flagstaff, Arizona

CONTRACT NO. 16-712-CA #3 AND #4

Prepared by

Department of Civil Engineering
Engineering Research Center
Colorado State University
Fort Collins, Colorado

R. M. Li
D. B. Simons
T. J. Ward
C. J. Orvis

LIBRARY COPY
ROCKY MT. FOREST & RANGE
EXPERIMENT STATION

April 1979

CER 78-79 RML-DBS-TJW-CJO 51

TABLE OF CONTENTS

Section		Page
	LIST OF TABLES	i
	LIST OF FIGURES	ii
	LIST OF PLATES	iv
	GLOSSARY	vii
	PREFACE	ix
	EXECUTIVE SUMMARY	xi
I	INTRODUCTION	1
II	FACILITY AND MODEL DESIGN	5
	GENERAL LAYOUT	5
	CALIBRATION AND ADJUSTMENT OF THE FACILITY	12
	MODEL SCALE	12
III	PROCEDURES AND FINDINGS	22
	GENERAL FINDINGS	22
	GROUP I RUNS	23
	GROUP II RUNS	23
	GROUP III RUNS	39
	PARTIAL SCOUR RUNS	65
	VEGETATIVE DEBRIS RUNS	65
	TOP-TIE PILE WALL DAMS	78
	COMPARISON OF SCOURING FOR ALL DAMS	81
IV	ADAPTION OF SPLIT DAM DESIGN MATHEMATICAL MODEL	85
	GENERAL	85
	SPLIT DAM MATH MODEL	85
	INCREMENTAL HYDROGRAPH	89
V	SUMMARY AND CONCLUSIONS	105
VI	RECOMMENDATIONS FOR FUTURE WORK	108
VII	REFERENCES	110
	APPENDIX A	111
	FORMULATION OF THE MATHEMATICAL MODEL	111
	REFERENCES FOR APPENDIX A	118
	APPENDIX B	119
	LISTING OF THE SPLIT DAM MATHEMATICAL MODEL	119

LIBRARY COPY
ROCKY MT. FOREST & RANGE
EXPERIMENT STATION

LIST OF TABLES

Table		Page
1	Scaling of the model	14
2	Group I runs listing water height on dam and discharge	27
3	Group II runs showing water discharge and sediment transport capacity for three slopes	41
4	Group III runs. Loading and unloading rates for original ogee and rectangular dams at three slopes . . .	54
5	Results of partial scour runs	68
6	Vegetative debris size distribution used in experiments	69
7	Results of vegetative debris runs	75
8	Results of top-tie pile wall loading and unloading runs	79
9	Average percent of material removed by scour	84
10	Loading and unloading rates for new ogee and rectangular dams	94

LIST OF FIGURES

Figure		Page
1	Flume facility	6
2	Original debris dams	16
3	New debris dams	17
4	Top-tie pile wall and catenary cable dams	18
5	Water height on dam and discharge for ogee-shape	28
6	Water height on dam and discharge for rectangular-shape	29
7	Model sediment size distribution	40
8	Sediment discharge Q_s compared to water discharge Q_w	42
9	Comparison of loading and unloading rates $\Delta s/\Delta t$ for ogee-shaped dam at three slopes	56
10	Comparison of loading and unloading rates $\Delta s/\Delta t$ for rectangular-shaped dam at three slopes	57
11	Comparison of loading and unloading rates for original ogee and rectangular dams at 5% slope	62
12	Comparison of loading and unloading rates for original ogee and rectangular dams at 15% slope	63
13	Comparison of loading and unloading rates for original ogee and rectangular dams at 25% slope	64
14	Partial scour rates for original ogee dam at the three slopes	66
15	Partial scour rates for original rectangular dam at the three slopes	67
16	Percent of vegetative debris trapped compared to water discharge Q_w for original ogee- and rectangular-shaped dams	76
17	Comparison of loading and unloading rates $\Delta s/\Delta t$ for top-tie pile wall dam at the three slopes	80
18	Comparison of computed and measured water level heights on dam	87
19	Comparison of computed and measured sediment transport rates using calibrated Meyer-Peter, Müller equation	88

Figure		Page
20	Comparison of measured and predicted loading and unloading rates $\Delta s/\Delta t$ for original ogee-shaped dam . . .	90
21	Comparison of measured and predicted loading and unloading rates $\Delta s/\Delta t$ for original rectangular-shaped dam .	91
22	Comparison of measured and predicted loading and unloading rates $\Delta s/\Delta t$ for new ogee-shaped dam	92
23	Comparison of measured and predicted loading and unloading rates $\Delta s/\Delta t$ for new rectangular-shaped dam	93
24	Measured filling and scouring rates compared with predicted rates from mathematical model for new ogee-shaped dam	96
25	Measured filling and scouring rates compared with predicted rates for mathematical model for new rectangular-shaped dam	97
26	Prototype incremental hydrograph	99

LIST OF PLATES

Plates		Page
1	General layout of experimental flume facility	7
2	Belt conveyor sediment feed system with sediment hopper	8
3	Stilling basin used with calibrated weir for water surface elevation measurements	9
4	Artificial gravel roughness and model structure	10
5	Overall view of flume facility looking upstream along flume axis	11
6	Flume facility with modified sediment feeding system	13
7a	Original ogee and rectangular debris dam scale models	19
7b	New ogee and rectangular debris dam scale models	20
7c	Top-tie pile wall dam and catenary cable dam scale models	21
8	Discharge-water depth rating experiment looking upstream to ogee-shaped dam on 15% slope with 8-foot prototype depth	24
9	Discharge-water depth rating experiment looking downstream to ogee-shaped dam on 15% slope with 8-foot prototype depth	25
10	Side view discharge-water depth rating experiment for ogee-shaped dam at 15% slope with 8-foot prototype depth	26
11	Pre-run channel surface for sediment transport capacity experiment	31
12	Upstream view during sediment transport capacity experiment	32
13	Side view of run during sediment transport capacity experiment	33
14	Post-run channel surface for sediment transport capacity experiment	34
15	Sampler collecting sediment during sediment transport capacity experiment	35
16	Leveling of sample before measurements in sediment transport capacity experiment	36
17	Measurement of sample during sediment transport capacity experiment	37

Plates		Page
18	Emptying of sampler during sediment transport capacity experiment	38
19	Top view of rectangular dam during loading rate experiment at approximately 1400 cfs	44
20	Upstream view of rectangular dam during loading rate experiment at approximately 1400 cfs	45
21	Top view of rectangular dam after loading rate experiment	46
22	Upstream view of rectangular dam after loading rate experiment	47
23	Top view of rectangular dam during unloading rate experiment	48
24	Downstream view of rectangular dam during unloading rate experiment	49
25	Oblique upstream view of rectangular dam after unloading rate experiment	50
26	Downstream view of rectangular dam after unloading rate experiment	51
27	Low sediment storage capacity behind ogee dam on 25% channel slope	58
28	Horizontal backwater surface behind ogee dam on 25% channel slope	59
29	Armor layer developed on sediment deposit behind dam	61
30	Vegetative debris run at low water level	70
31	Vegetative debris run at medium water level	72
32	Vegetative debris run at high water level	73
33	Sampling of vegetative debris	74
34	Split dam opening clogged by vegetative debris	77
35	Adverse bed slope developed behind top-tie pile wall dam on 25% channel slope	82
36	Erosion at the upstream end of the deposited sediment behind top-tie pile wall dam occurring on 25% channel slope	83

Plates		Page
37	Incremental hydrograph run at 1500 cfs	100
38	Incremental hydrograph run at 4400 cfs	101
39	Incremental hydrograph run at 500 cfs	102
40	Deposited sediment behind new ogee dam after an incremental hydrograph run for 15% channel slope . . .	104

GLOSSARY

adverse slope--bed of channel sloping in upstream direction

aggradation--deposition in or filling of a stream's channel with sediment

bulking factor--ratio of the sediment volume or rate with voids in the clear water discharge volume or rate

catenary cable dam--a porous debris dam constructed of wire netting to temporarily trap sediment while allowing water to flow through

debris--rock, soil and vegetative material transported during flood flows

degradation--erosion of a stream's channel

ephemeral stream--a stream channel which does not contain flowing surface water most of the year

equilibrium--the state in a channel reach where erosion and deposition occur at equal rates thus not producing overall changes in the gradient of that channel reach

loading (filling)--deposition of debris behind a flow control structure

mathematical model--a model where processes in the system being studied are represented by mathematical formula

model--a representation of a planned or existing object

physical model--a scale model of a structure or a stream reach

prototype--a planned object that is to be built or modeled

sediment--inorganic rock or soil material transported by water

sediment debris--inorganic rock and soil material transported during flood flows

self-cleaning--design of a flow control structure that permits low flow erosion of a sizable portion of deposited debris

split dam--a water and sediment detention dam that is separated in two halves by a center vertical cut of varying shape

top-tie pile wall dam--a solid dam composed of vertical H-beams with timbers that slide into the grooves in the beams, with cable placed between the dam's crest and upstream anchors to prevent overturning of the dam

transport capacity--maximum rate at which a stream can carry sediment above which deposition occurs

unloading (scouring)--erosion of material through the port of a flow control structure by water flow

vegetative or organic debris--organic material, such as trees and brush, transported during flood flows

PREFACE

This model study was conducted for the Angeles National Forest, Pasadena, California through Research Agreement Nos. 16-712-03-CA and 16-712-04-CA between USDA Forest Service, Rocky Mountain Forest and Range Experiment Station and Colorado State University. Ron S. Aygarn is the authorized project coordinator and D. Ross Carder is the authorized project officer for the USDA Forest Service. Daryl B. Simons and Ruh-Ming Li are the principal investigators at Colorado State University. The project was divided into two phases. The period of agreement for the two phase study was from August 25, 1977 to September 30, 1978. According to the agreement, the completion report on the experimental designs, findings, and recommendations is submitted.

Problems of sedimentation and structures for controlling it have attracted the attention of scientists and engineers throughout the world in recent decades. Millions of dollars have been spent to collect laboratory and field data to quantify the transport rate, erosional and depositional characteristics and performance of hydraulic structures. The increasing need to manage rivers and watersheds has led to increased use of convenient and less costly laboratory flumes for developing timely specific information. Most previous studies have been concentrated toward solving sediment problems in relatively flat gradient channels. Very few studies have been conducted that simulate steep mountain channels. Knowledge of watershed management and system response in steep mountain channels is urgently needed.

This model study is the first attempt at Colorado State University, possibly the first major attempt in the world, to study the hydraulics, sediment transport and response of hydraulic structures in steep

mountain channels using physical and mathematical models. Because a tremendous amount of sediment must be fed and/or cleaned out of the model, many staff members, graduate students and undergraduate students were involved in assisting the writers with these difficult experiments. The writers wish to acknowledge Ms. Tammy McFall, Mr. Craig Goodwin, Mr. Chuck Lurvey, Mr. Ming-Sing Huang, and Ms. Carla Worley for their excellent assistance and great patience in working overtime and long hours. Mr. Ewald Patzer, machine shop foreman, and his excellent crew helped a great deal in designing and fabricating the experimental facility. Without their assistance this study would not be possible. Special thanks are due to Ms. Annette Ward for editing this final report. Finally, the writers are indebted to Mr. Ron Aygarn and Mr. David McCauley of the U.S. Forest Service for their guidance and constructive suggestions.

EXECUTIVE SUMMARY

Angeles National Forest personnel, Pasadena, California are currently investigating efficiency of the split dam prototype structures and catenary cable dams to control water and sediment flows in mountain channels of the San Gabriel Mountains in southern California. The overall purpose of such structures is to reduce the peak of water and sediment flows during heavy storms, and to eventually pass most of the stored sediment through the system during periods of smaller flows. A hydraulic model study of these structures was conducted at Colorado State University.

The primary objective of this model study was to identify the efficiencies of selected flow control structures in altering normal sediment movement through steep ephemeral channels below highly erodible watersheds. The other objective of this study was to establish recommendations regarding design modifications that will improve functioning of selected structures.

The study was divided into two phases. Phase I included the design of experimental facilities and models, the initial findings, the results of initial flume runs and recommendations for the Phase II study. In the Phase I study, a total of 57 flume runs were completed. In the Phase II study, approximately 100 additional runs, implementation of a mathematical model capable of predicting the hydraulic response of a proposed structure for different structural and hydraulic conditions, and testing of the structure response to vegetative plugging and a variable discharge hydrograph were conducted.

Results of Phase I and Phase II of this study suggest that a split dam prototype with the desired self-cleaning capability performs very

well. However, efficiency of the self-cleaning feature is dependent on the shape of the structure's opening, the rate and duration of low flows and corresponding sediment loads, the channel slope, the sediment size and size distribution, and the amount of vegetative debris carried in the channel. Top-tie pile wall and catenary cable dams are not as efficient. Top-tie pile wall dams, once filled, do not provide storage for incoming sediments. The catenary cable dam was found to be too porous to produce sediment trapping and scouring conditions needed for adequate functioning. Dam porosity precluded development of backwater where deposits could take place. Sediments had to be trapped in the openings or piled up behind the plugged openings. During low flows, the porous dam did not permit flow concentration and attendent scour.

I. INTRODUCTION

The Angeles National Forest, Pasadena, California, through the Rocky Mountain Forest and Range Experiment Station contracted with the Engineering Research Center, Colorado State University to investigate the efficiency of the proposed prototype split dam and catenary cable dam in controlling water and sediment debris flows in mountain channels of the San Gabriel Mountains in southern California. A top-tie pile wall dam (solid dam) was also studied as a reference of existing conditions. The overall purpose of the proposed self-cleaning structures is to reduce the peak of water and sediment through the system during periods of high flows, a result that is not often attained by top-tie pile wall dams. A hydraulic model study of these structures was conducted at Colorado State University.

The first objective of this physical model study was to identify the relative efficiencies of the selected flow control structures that favorably alter the normal sediment movement through steep ephemeral channels draining highly erodible watersheds. The second objective of this study was to establish recommendations regarding design modifications that would improve the functioning of the selected structures.

Proposed structures to be studied were designed to adjust sediment transport during rare runoff events. When functioning ideally, these structures 1) pass all of the water and rock debris during runoff events that are less than a stipulated rare runoff event, 2) partially impound water and rock debris during the stipulated rare runoff event, and 3) pass impounded rock debris during subsequent runoff events that are less than the stipulated rare runoff event. To accomplish the two

objectives, structure modeling and flume runs were performed to determine the hydraulic response of the natural channel system to the design of the proposed cross-channel structures. Hydraulic response of the natural channel system required determination of water velocity, depth, discharge, sediment transport, sediment size, degradation, and deposition. Design of each structure involves the size of the structure, its shape, the opening configuration, channel shape, and channel slope. General questions pertinent to the proposed structures were: 1) changes in energy concentration, 2) changes in water and rock debris storage and flow, 3) rock debris deposition and transport, and 4) the most effective shape of structures for efficient self-cleaning.

On October 11-12, 1977, Mr. Ron Aygarn and Mr. David McCauley of the Forest Service visited Colorado State University and observed preliminary flume runs using models under examination. The catenary cable model proved to be inefficient because low flows are too dispersed to facilitate self-cleaning. A modified version of this model was used in limited testing in Phase II. The Phase I study was then revised before completion (Li, Simons, Ward, and Steele, 1977). Under the revised Phase I study requirements, the two original split dam configurations were examined further. One model contained a scaled down opening representing a 5-foot wide by 7-foot high vertical hole below a 3-foot wide vertical outflow port. This is called the ogee model because it incorporated the double conical transition from the larger to the smaller opening. The second original split dam model contained a scaled down dimension representing a 4-foot high by 8-foot wide horizontal hole below a 3-foot wide vertical outflow port. This is called the rectangular model. In Phase II of this study the solid top-tie pile wall dam

was analyzed to develop data that could be compared with the data of the split dam models. In addition, two new split dams, one ogee and one rectangular, were constructed and tested based on the findings of Phase I and the initial results of Phase II.

Three channel slopes of 5 percent, 15 percent and 25 percent were used in this study. Only one modeled sediment size distribution and one modeled vegetative debris distribution were used in Phase I and Phase II. The basic flume runs required are classified into the following three groups: 1) Group I determines clear water discharge rate for two split dam shapes, each on three slopes with various model flow depths, 2) Group II determines the maximum natural sediment transport rates for various water discharges in open channel flow without models, and 3) Group III determines sediment loading and unloading rates of the two split dam shapes. The Phase I study included the flume runs of Groups I and II and included flume runs of Group III for one structure shape and one slope.

Phase II began with completion of testing of the ogee and rectangular dams for Group III runs. The top-tie pile wall dam was tested to determine its loading and unloading rates. The ogee and rectangular dams were tested with respect to vegetative clogging using clear water flow. Results of Phase I and Phase II runs provided needed information for implementing a mathematical model that describes split dam functioning. This model was verified by experiments on two new split dam shapes as agreed to in a May 2, 1978 meeting attended by Mr. Ron Aygarn, Mr. Dave McCauley and the Colorado State University investigators at National Forest Region 5 headquarters in San Francisco, California. At that time the original Phase II objectives were amended to include

mathematical model verification using two new designs instead of one. Other changes included elimination of one of two combination hydrograph runs, production of two movies of 15 to 20 minutes in duration, and a later modification and limited retesting of a catenary cable structure.

Several useful results have been developed in this study. First, split dams do have a self-cleaning capability that depends on water flow rate, sediment size and distribution, sediment inflow rate, channel slope, split opening configuration and vegetative plugging. Second, it is possible to implement a mathematical model that realistically describes loading and unloading of split dams. Third, catenary cable dams do not provide the needed sediment retention and self-cleaning attributes. Finally, a better understanding of steep channel hydraulics and structure interaction has been developed.

II. FACILITY AND MODEL DESIGN

GENERAL LAYOUT

To conduct the experiments required innovation. In order to simulate the field situation, a unique flume capable of a large range of slopes was constructed in Phase I. The outstanding feature of the flume is that it is pivoted at the downstream end and attached to a stationary forklift at the upstream end. Slopes from zero to approximately 30 percent are possible. The general layout used in Phase I is shown in Figure 1 and Plate 1. Besides the pivot and lift system for changing slope, the flume layout includes:

1. A flexible water supply hose system that allows the flume to be raised and lowered,
2. A sediment settling tank (at downstream end of flume in Plate 1),
3. A belt conveyor with a calibrated variable speed feeder hopper (Plate 2),
4. A calibrated weir with stilling basin measurement gage (Plate 3),
5. A six, 650-watt bulb lighting system for photography,
6. Artificial gravel roughness cemented to the bed (Plate 4),
7. Model structures (Plate 4), and
8. Instrument carriage for measuring the bed profile.

An overall upstream view of the facility showing weir, stilling basin, flume and structure is shown in Plate 5.

The flume facility constructed in Phase I was modified for Phase II. Experiments conducted for Phase I showed that modification of the sediment feed system was needed to allow reasonable prototype scale

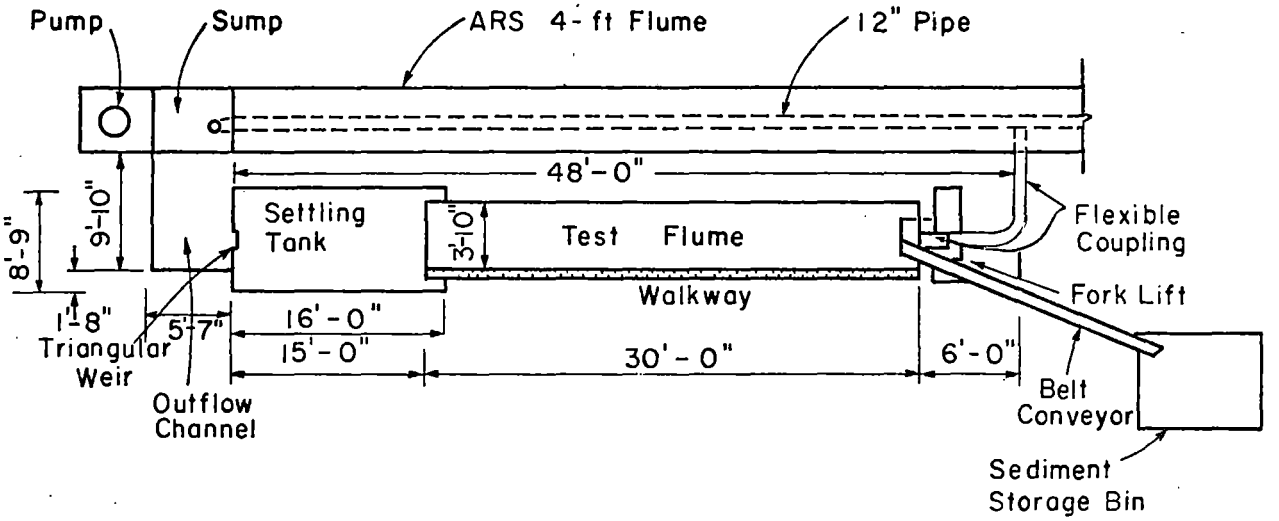

Top View

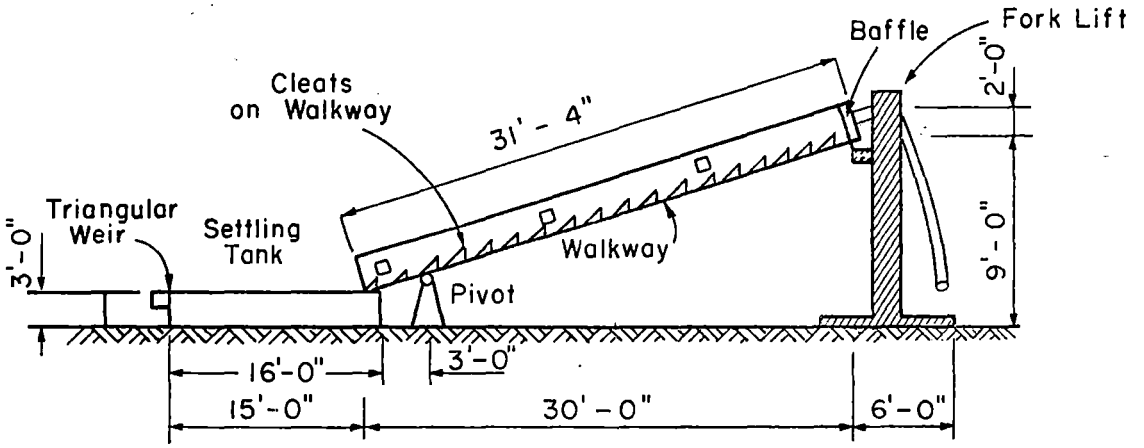

Elevation

Figure 1. Flume facility (not to scale).

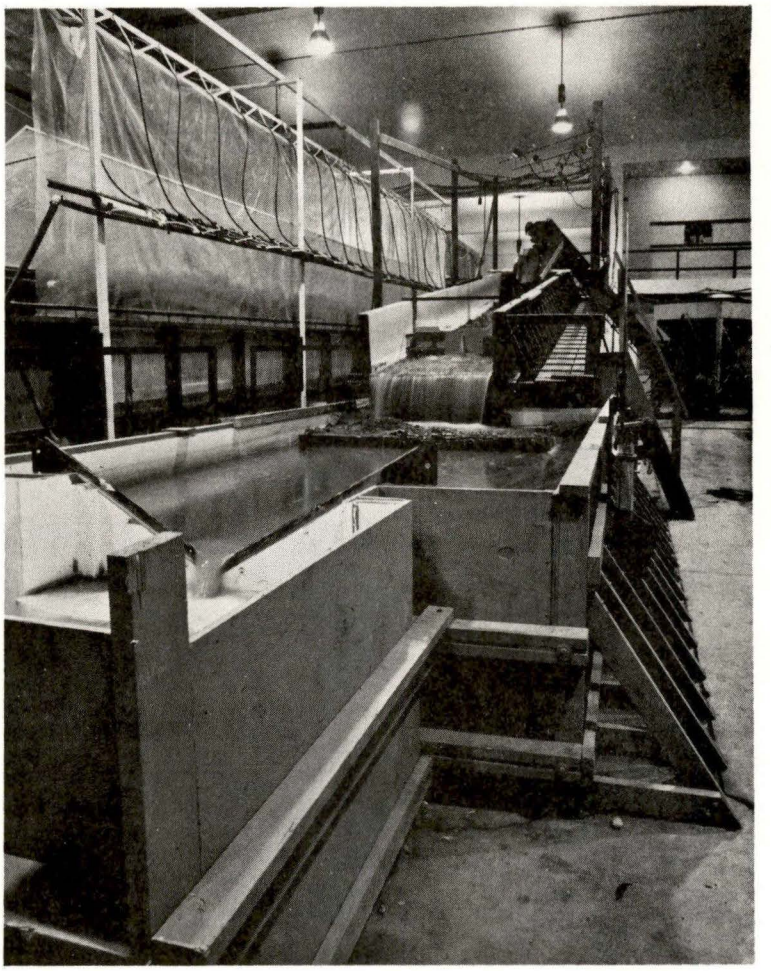

Plate 1. General layout of experimental flume facility.

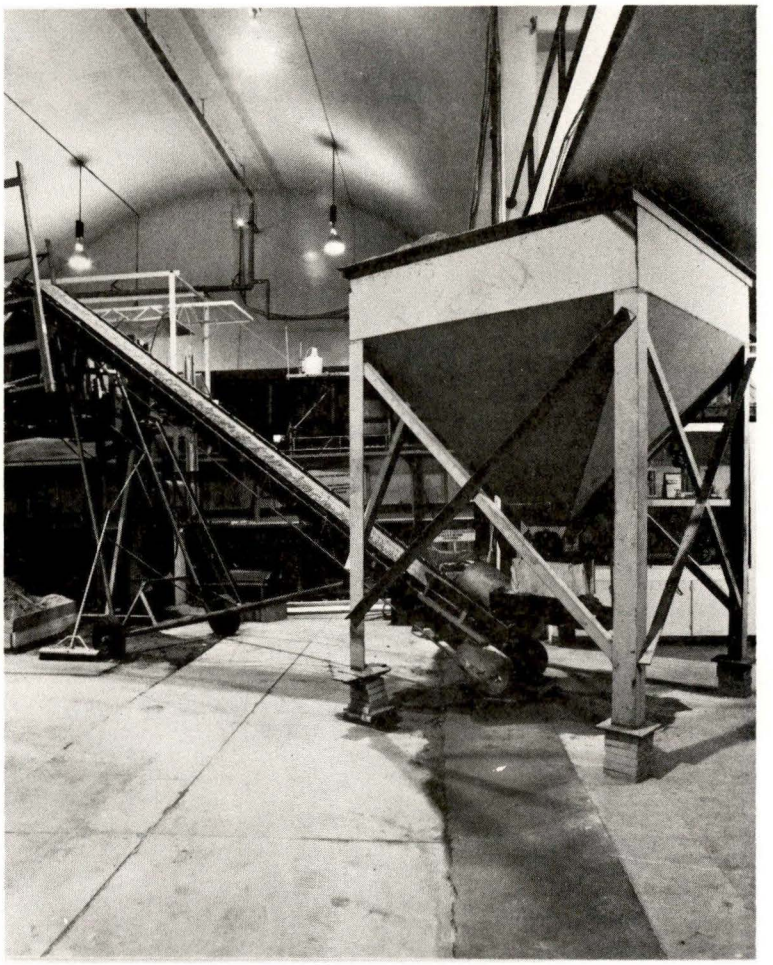

Plate 2. Belt conveyor sediment feed system with sediment hopper.

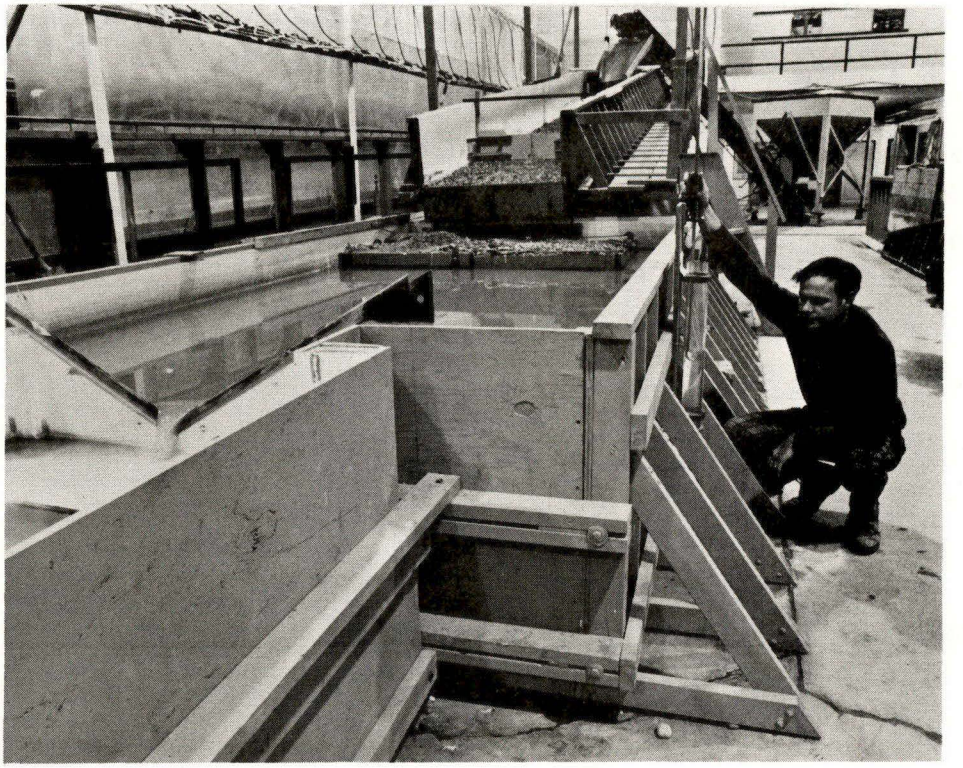

Plate 3. Stilling basin used with calibrated weir for water surface elevation measurements.

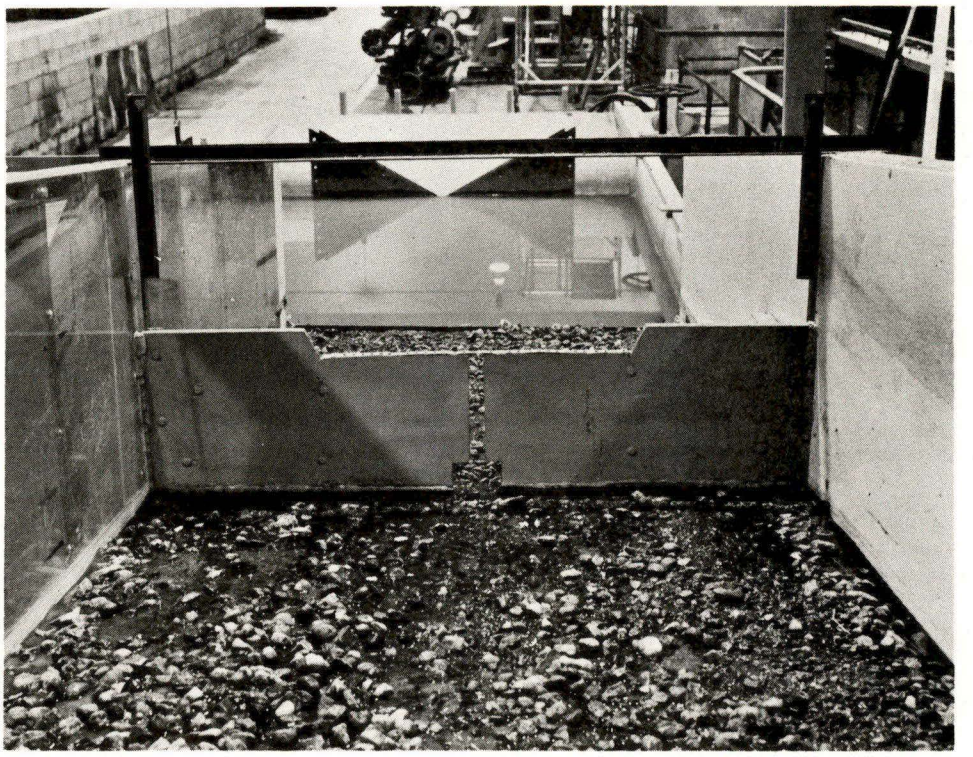

Plate 4. Artificial gravel roughness and model structure.

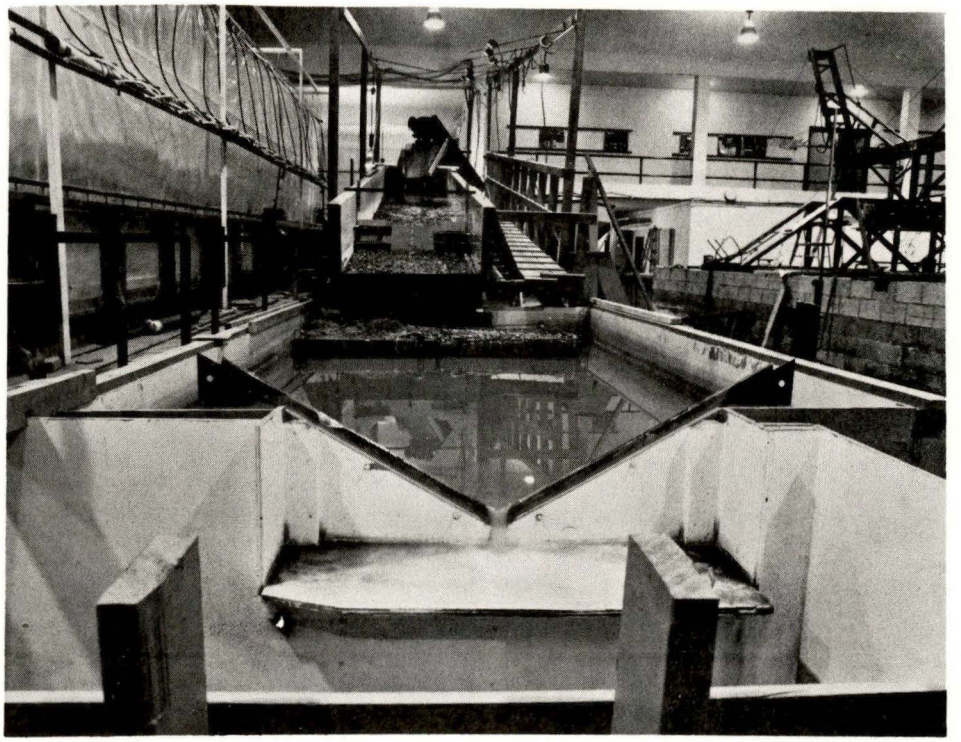

Plate 5. Overall view of flume facility looking upstream along flume axis.

water and sediment discharges to be used in evaluation of the split dams. These modifications provided increased sediment feed rates at all flume slopes. Modifications included the addition of a secondary sediment hopper, used to supply the primary feed hopper, and elevation of both hoppers with leg extensions. The new, modified feed system includes a primary feed hopper and conveyor belt that supplies sediment to the flume, and a secondary hopper and conveyor belt that supplies sediment to the primary hopper (Plate 6).

In addition, removable sediment collection boxes were added to the stilling basin to facilitate sediment removal. These new boxes substantially decreased clean out time.

CALIBRATION AND ADJUSTMENT OF THE FACILITY

Three items required calibration or adjustment before flume runs were made. First, the flume was raised to the prescribed slope and leveled cross channel. Braces were then used to support the flume at each slope. Second, the weir was installed and the stilling basin gage surveyed in order to give direct readings of hydraulic head over the previously calibrated weir (Plate 3). The weir was then used to find approximate control valve positions for selected water inflow rates. Third, sediment feed rate from the hopper was calibrated at different motor speeds and hopper throat openings by noting the length of time necessary to discharge a measured volume of sediment. These calibrations and adjustments allowed accurate measurement of both water and sediment inflow rates and channel slopes.

MODEL SCALE

The purpose of a scale model is to simulate the prototype or field situation as closely as possible. Numerous model scales can be devised

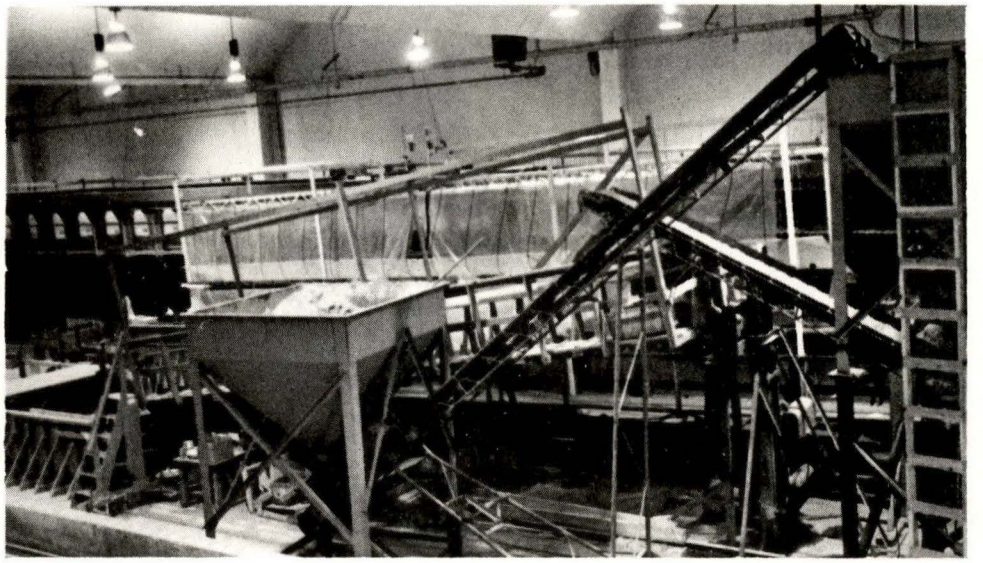

Plate 6. Flume facility with modified sediment feeding system. Secondary hopper at left of center feeds primary hopper at far right via conveyor belt. Primary hopper feeds flume via second conveyor belt, far center right.

depending the conditions of the system being modeled. In this study, Froude number similarity was used. The Froude number is the dimensionless ratio of gravity force to inertia force, often defined as water flow velocity divided by the square root of water depth per second times the gravitational acceleration, i.e., 32.2 feet per second squared at sea level. Froude number similarity coupled with the length scaling factor used in the model permitted determination of the necessary length, volume, velocity, and time. In the study the following dimensions were used with a 1/25-length scale.

Table 1. Scaling of the model.

Prototype	Model
1 foot	1/25 = .04 feet = 0.48 inch
1 cfs	$1/(25)^{5/2}$ = 0.00032 cfs
1 hour	$1/(25)^{1/2}$ = 0.20 hrs = 12 mins
1 Manning's n unit	$1/(25)^{1/6}$ = 0.58 unit

Using the model scaling factor the flume width of 46 inches represents a 96-foot wide channel and a 1.92 cfs flume discharge represents a flow of 6000 cfs in the prototype. The estimated Manning's n of 0.07 in the prototype was reduced and verified equal to 0.041 in the model (Plate 4). Verification was made by using Manning's equation with measurements of flow depths for certain discharges in the model. The dimensionless slopes of 5 percent, 15 percent, and 25 percent were unchanged.

The length scale was used to reduce six prototype dams and the sediment dimensions to model sizes. The two new split dams were similar

in configuration to the original prototype dams except the split opening dimensions were larger. The new ogee dam had split dimensions of a 6-foot wide and 7-foot high slot resting on an 8-foot wide by 14-foot high opening. The new rectangular dam had a 10-foot wide by 17.5-foot high slot resting on a 15-foot wide by 3.5-foot high opening. The weir crest width was slightly shortened for both.

The top-tie pile wall dam is solid with no opening. The modified catenary cable dam has an 8-foot radius semi-circular opening. Another catenary cable dam was examined but is not shown here. This dam was rectangular in shape measuring (in prototype dimensions) 25 feet high and about 100 feet wide with mesh openings about 1 foot on a side. After one run this dam configuration was deemed unsuitable because it filled but would not scour and was eliminated from further experiments. Dimensions of the original ogee and rectangular, new ogee and rectangular, top-tie pile wall and modified catenary cable dams are shown in Figures 2, 3, and 4. Plate 7 shows the scale model structures.

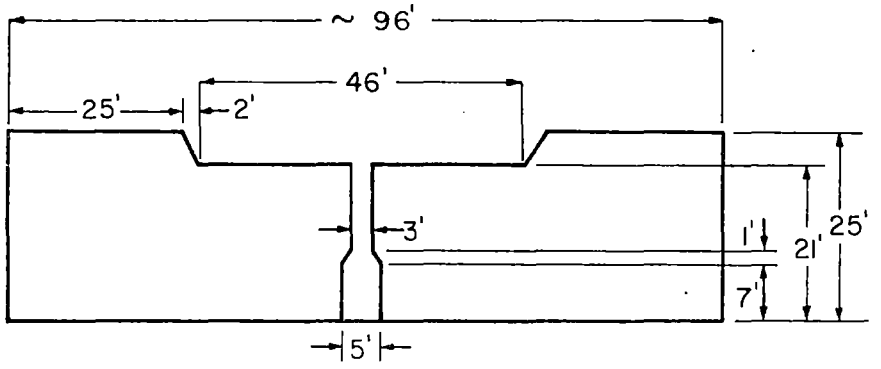

Ogee Shape

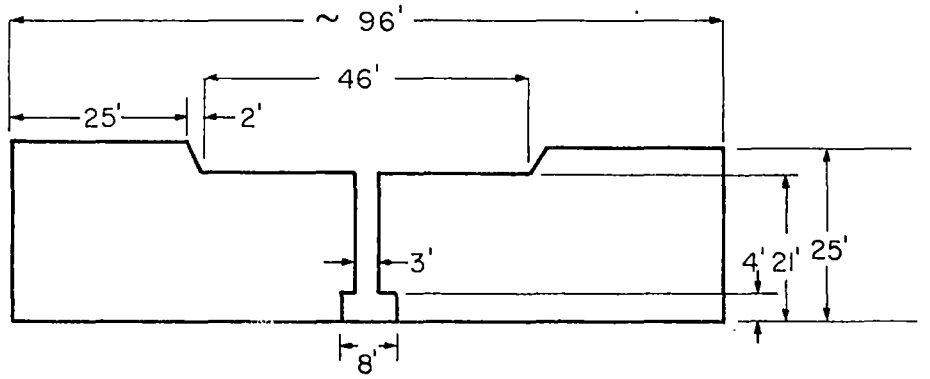

Rectangular Shape

Figure 2. Original debris dams (prototype dimensions).

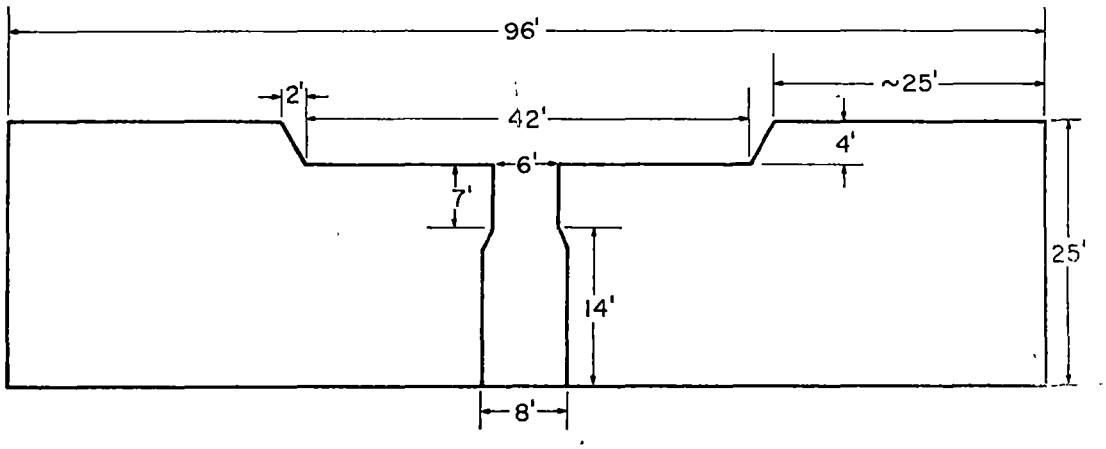

Ogee Shape

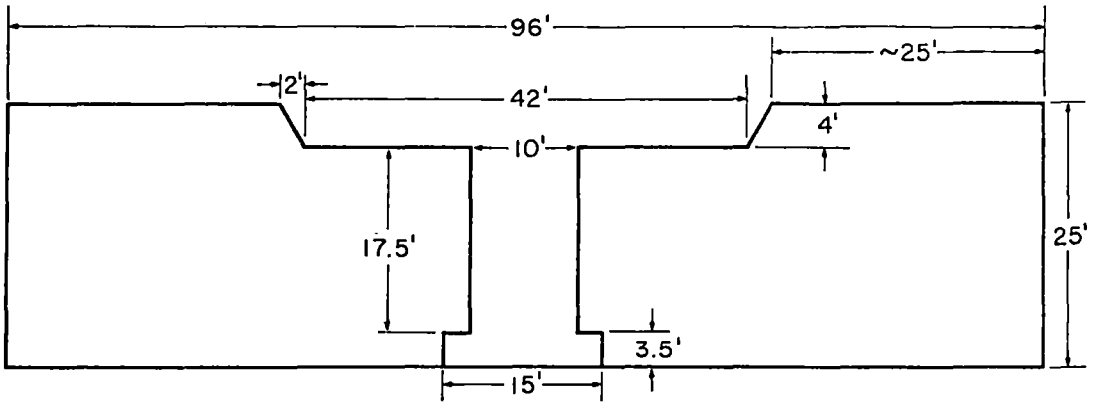

Rectangular Shape

Figure 3. New debris dams (prototype dimensions).

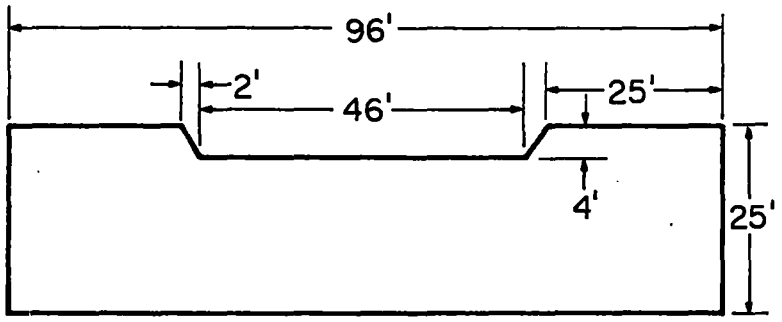

Top Tie Pile Wall Dam

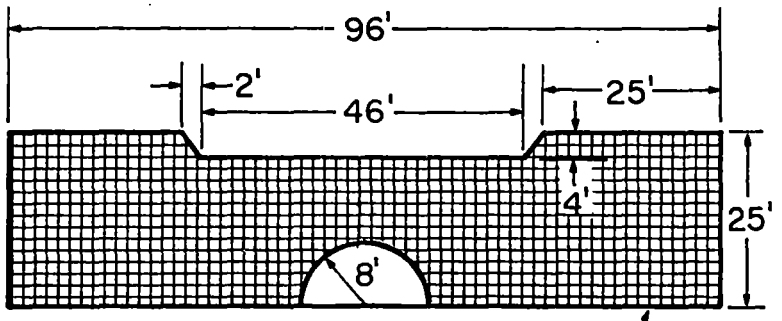

Wire mesh lines representing one foot square openings

Catenary Cable Dam

Figure 4. Top-tie pile wall and catenary cable dams (prototype dimensions).

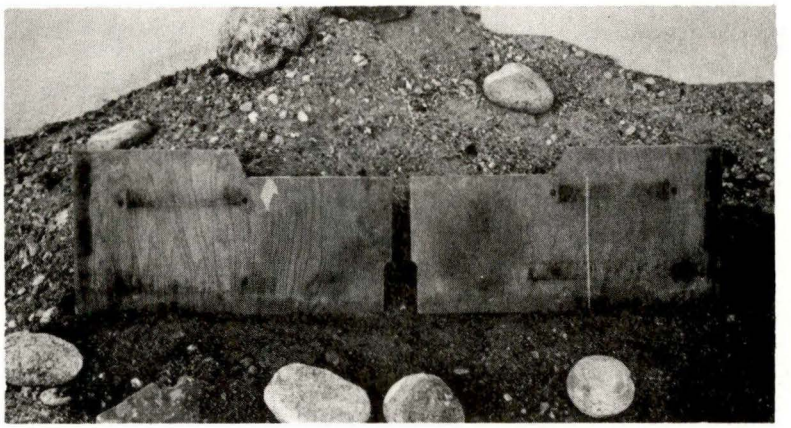

Ogee Shape

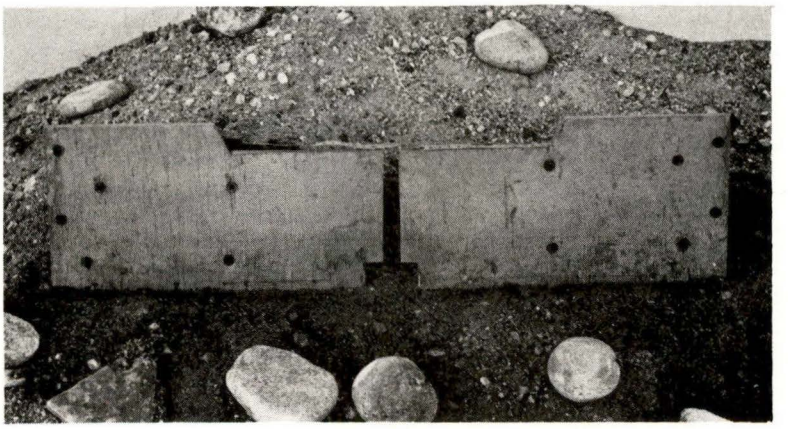

Rectangular Shape

Plate 7a. Original ogee and rectangular debris dam scale models.

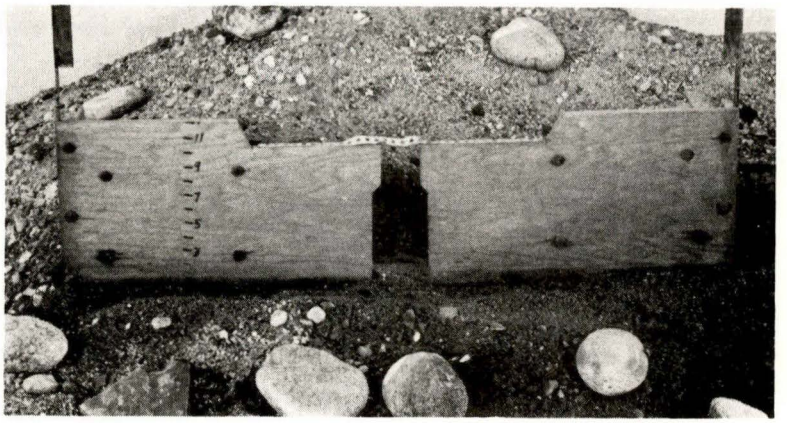

Ogee Shape

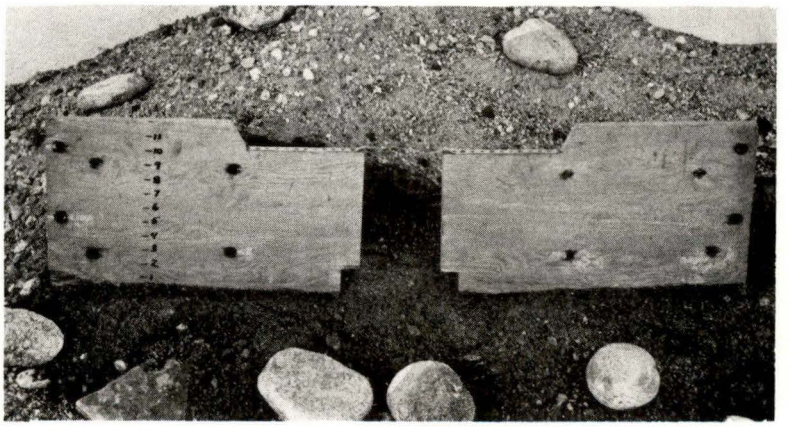

Rectangular Shape

Plate 7b. New ogee and rectangular debris dam scale models.

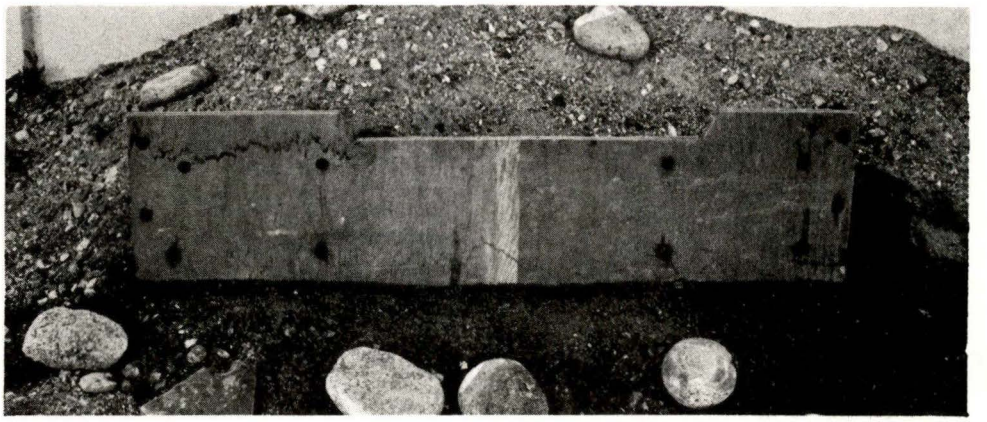

Top-tie Pile Wall Dam

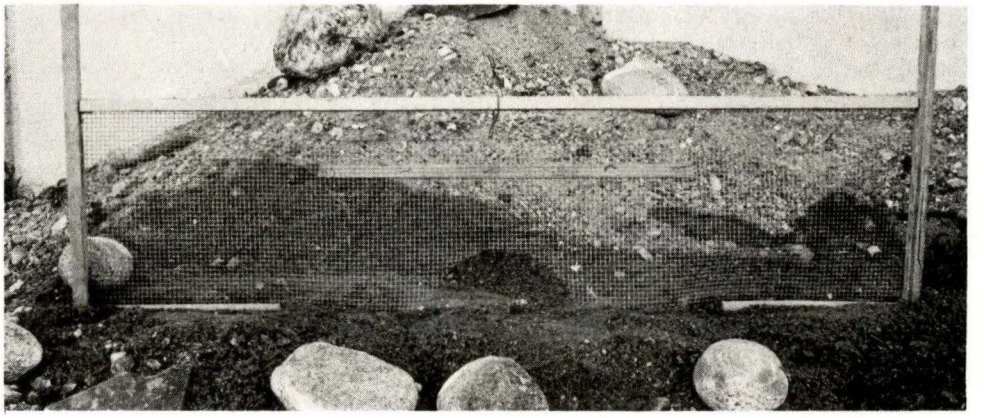

Catenary Cable Dam

Plate 7c. Top-tie pile wall dam and catenary cable dam scale models.

III. PROCEDURES AND FINDINGS

Procedures for conducting the model study and the results of Phase I and Phase II flume runs and mathematical model are summarized.

GENERAL FINDINGS

The catenary cable model does not significantly retard water or a sediment debris flow composed of material ranging from clay to cobble unless holes in the cable network are quite small. When the holes are small, selected size of debris will readily plug the holes and induce deposition behind the structure. However, self-cleaning is not possible with this model because subsequent water flow is not concentrated sufficiently to transport the debris through the holes. Therefore, further analysis of this model was eliminated.

From the flume runs, it is concluded that the split dam configuration has the desired self-cleaning features. However, efficiency of the self-cleaning feature is dependent on the shape of the structure's opening, the rate and duration of low flow and corresponding sediment loads, the channel slope, and sediment size and size distribution. Low flows with very little or no sediment load are able to remove a significant percent of the stored sediment because the bed slope on the downstream face of the prism of the stored sediment is much steeper than the channel bed slope. Depending on slope, split opening shape, and discharge, anywhere from less than 10 to over 80 percent of the fill material may be removed. There are two potential problems involved if the low flow is small and of short duration. First, low flow may be entirely contained in the porous media as subsurface flow, thus greatly reducing sediment erosive capacity. In addition, it was observed that

the scour potential downstream of the split dam port during high flows is very large. Appropriate size riprap forming the downstream apron is needed to preserve the integrity of the structure. Conversely, during low flows, the sediment discharged through the structure will form an alluvial fan below the structure due to the deposition of sediment. Most of this alluvial fan may be transported downstream by subsequent high flows, adding to the sediment load. If a series of the split dams are contemplated, analysis of the erosional and depositional response of the whole system is needed to evaluate the self-cleaning efficiency.

GROUP I RUNS

This set of runs was conducted to determine the depth of water at a dam for various clear water discharges. Five water depths at three channel slopes for the two original split dams were used. The depths, in prototype dimensions, were approximately 2', 8', 21', 25', and 27' above the channel bottom. After a dam was set in place, water was released down the flume. The discharge valve was adjusted until the depth became steady at or near a predetermined level. Discharge was then determined by reading the steady gage height in the stilling basin. Plates 8, 9, and 10 show upstream, downstream and side views of the original ogee dam at 15 percent slope and a prototype water depth of about 8 feet. Results for the two split dams are presented in Table 2. Discharges are given in the prototype values for easier interpretation. Results are plotted in Figures 5 and 6 indicating that the two structures have a similar hydraulic performance.

GROUP II RUNS

Group II runs determined the channel's sediment transport capacity for various water flows and slopes. Volumetric sediment rates were

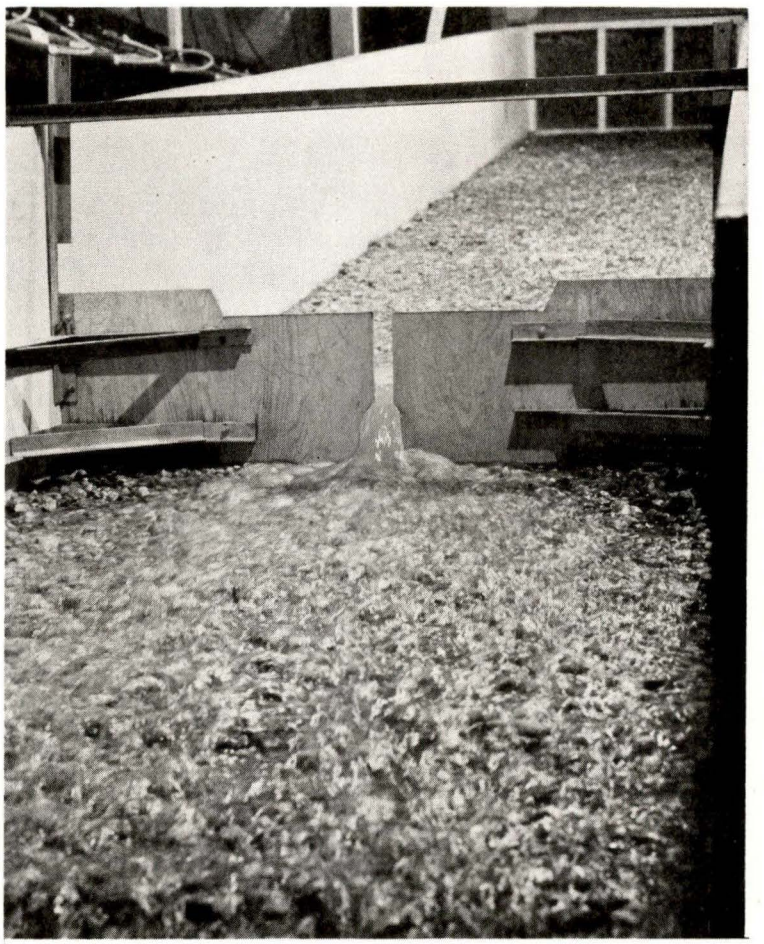

Plate 8. Discharge-water depth rating experiment looking upstream to ogee-shaped dam on 15% slope with 8-foot prototype depth. Discharge approximately 400 cfs (prototype).

Plate 9. Discharge-water depth rating experiment looking downstream to ogee-shaped dam on 15% slope with 8-foot prototype depth. Discharge approximately 400 cfs (prototype).

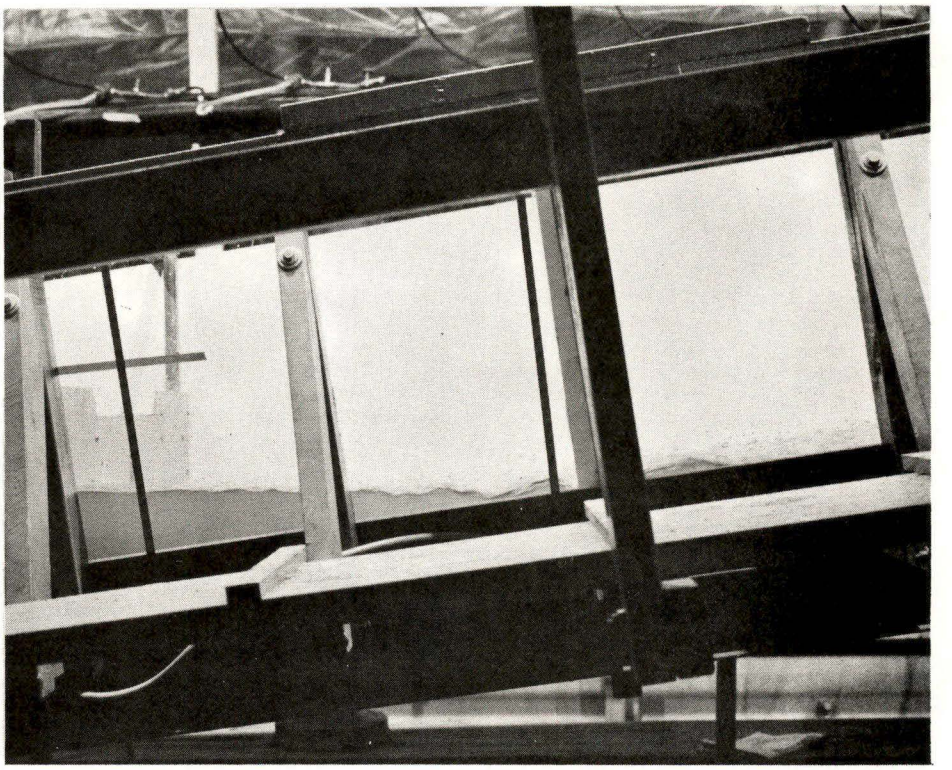

Plate 10. Side view of discharge-water depth rating experiment for ogee-shaped dam at 15% slope with 8-foot prototype depth. Discharge approximately 400 cfs (prototype).

Table 2. Group I runs listing water height on dam and discharge (prototype values for the three slopes).

Ogee Shape

5%		15%		25%	
Height feet	Discharge cfs	Height feet	Discharge cfs	Height feet	Discharge cfs
2.2	55	4	144	5.5	173
4.7	181	11.7	662	8	371
8	420	21	1486	21	1441
21	1559	25	2739	25	2294
25	2951	27	5116	27	5268
27	5023				

Rectangular Shape

5%		15%		25%	
Height feet	Discharge cfs	Height feet	Discharge cfs	Height feet	Discharge cfs
3.3	106	4.8	222	3.6	71
3.8	181	9.6	571	8.0	460
8.2	492	20.6	1388	20.7	1371
21	1432	25	2548	25	2318
25	2831	27	4641	27	4985
27	4784				

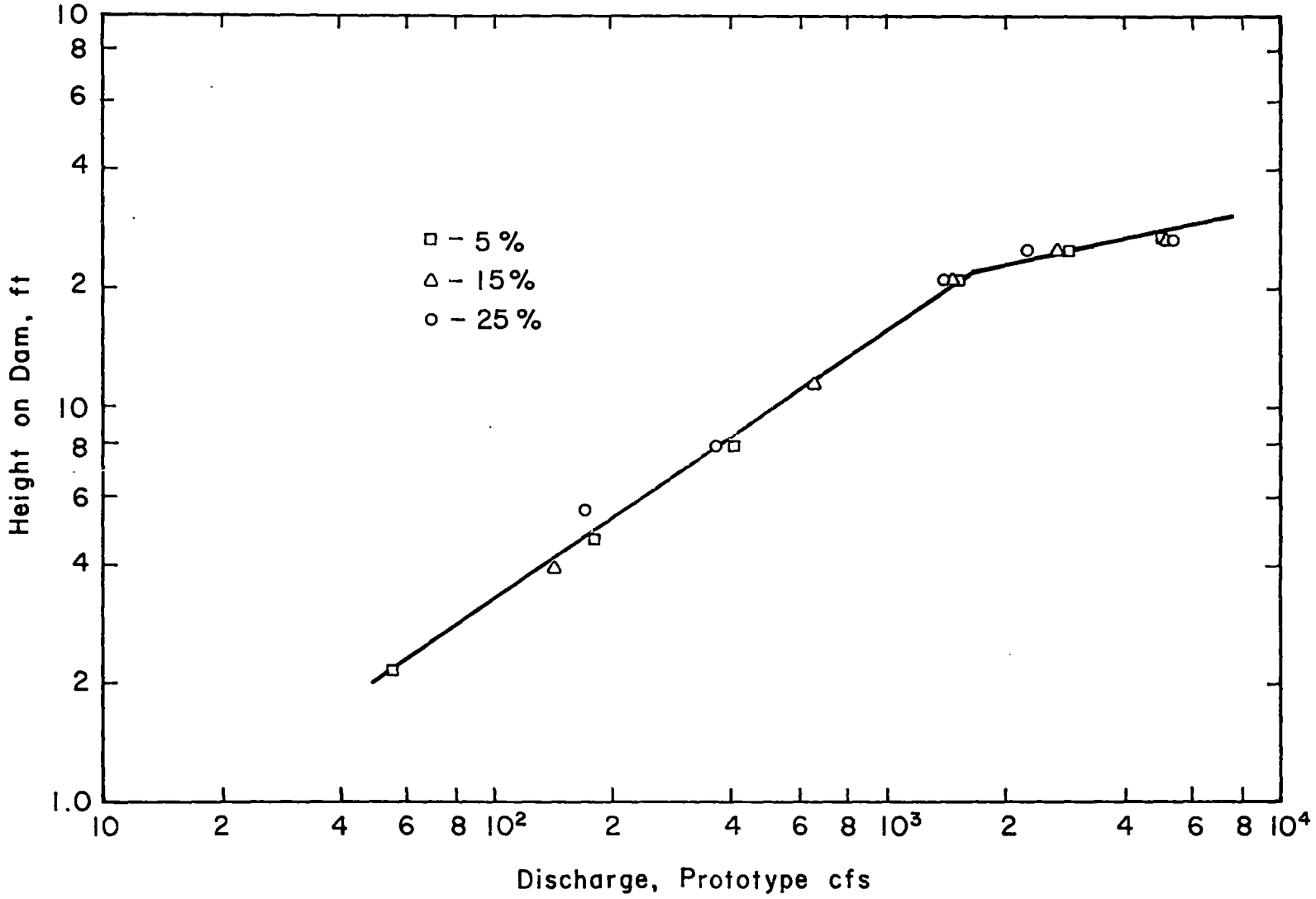

Figure 5. Water height on dam and discharge for ogee-shape (prototype values).

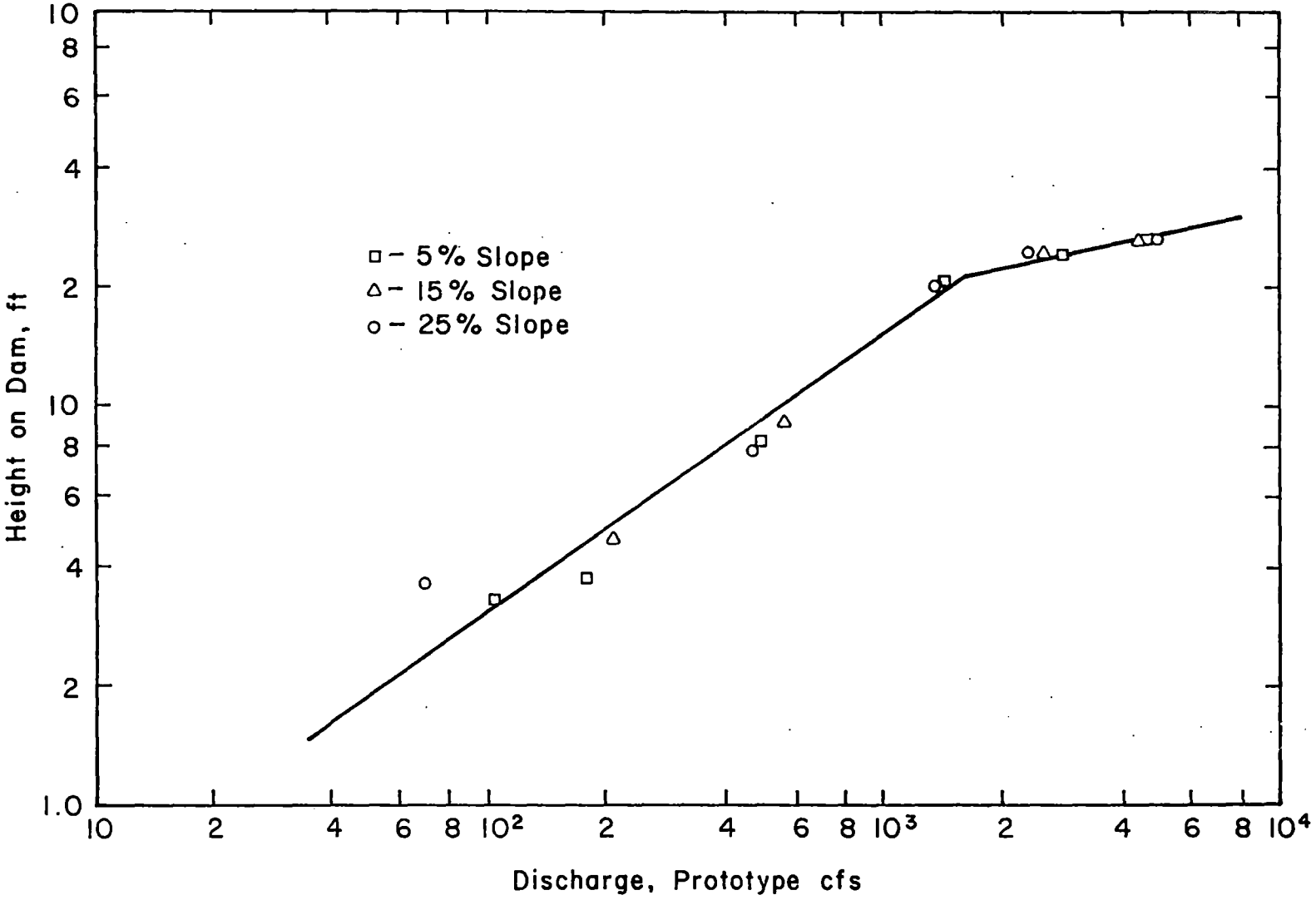

Figure 6. Water height on dam and discharge for rectangular-shape (prototype values).

measured for the various flow conditions. For discharges on five percent slope, the sediment feeder could be adjusted to supply adequate sediment to avoid significant aggradation or degradation of the 3-inch hand-laid sediment bed, thereby maintaining an equilibrium condition. For 15 percent and 25 percent slopes, the rate that sediment could be supplied was inadequate and a 6-inch bed was necessary. In the 15 percent and 25 percent runs, transport capacity was quickly reached allowing short run times. The bed on these steep slopes was checked constantly to assure that the sediment supply was adequate for the flow conditions.

The run was stopped before complete scour of the bed took place. Plates 11, 12, 13, and 14 show the channel before the run, looking upstream during the run, from the side during the run, and after the run looking upstream. These photographs show that under these conditions the bed was in equilibrium with the flow.

During each run, volumetric sediment samples were collected as shown in Plates 15, 16, 17, and 18. Plate 15 shows the sediment collector in place catching a timed sample. Sediment was then leveled (Plate 16), measured (Plate 17), and dumped in preparation for the next sample (Plate 18). Samples of supply and outflow sediment were periodically collected for sieve analysis. The collected samples were converted to volumetric rates and checked to determine if a steady rate was achieved. The average representative rate was determined from a set of carefully measured samples. Water discharge was measured for the sediment discharge where necessary. Data from these runs consisted of water and sediment flow rates at the different slopes. Sieve analysis of the sediment supply and sediment outflows showed the fine sediments not caught

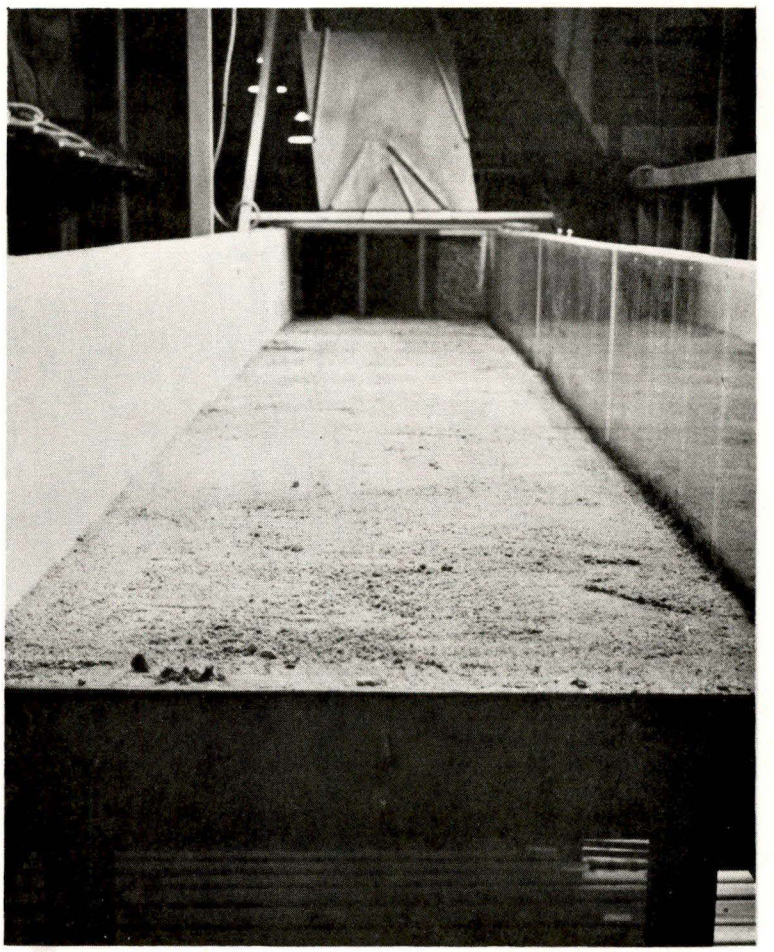

Plate 11. Pre-run channel surface for sediment transport capacity experiment.

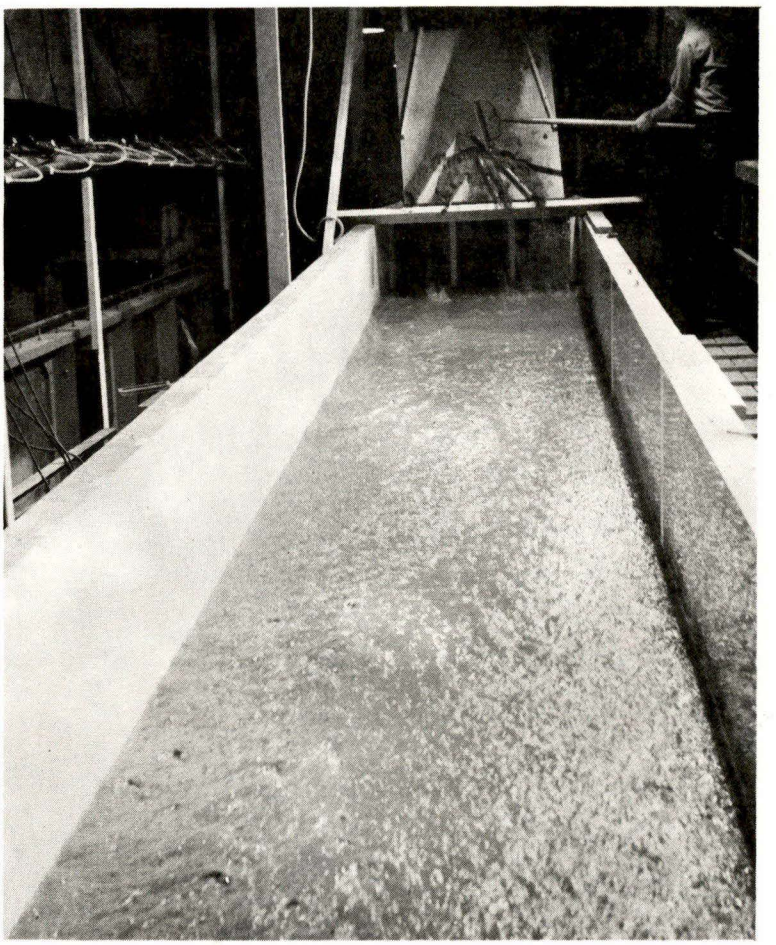

Plate 12. Upstream view during sediment transport capacity experiment.

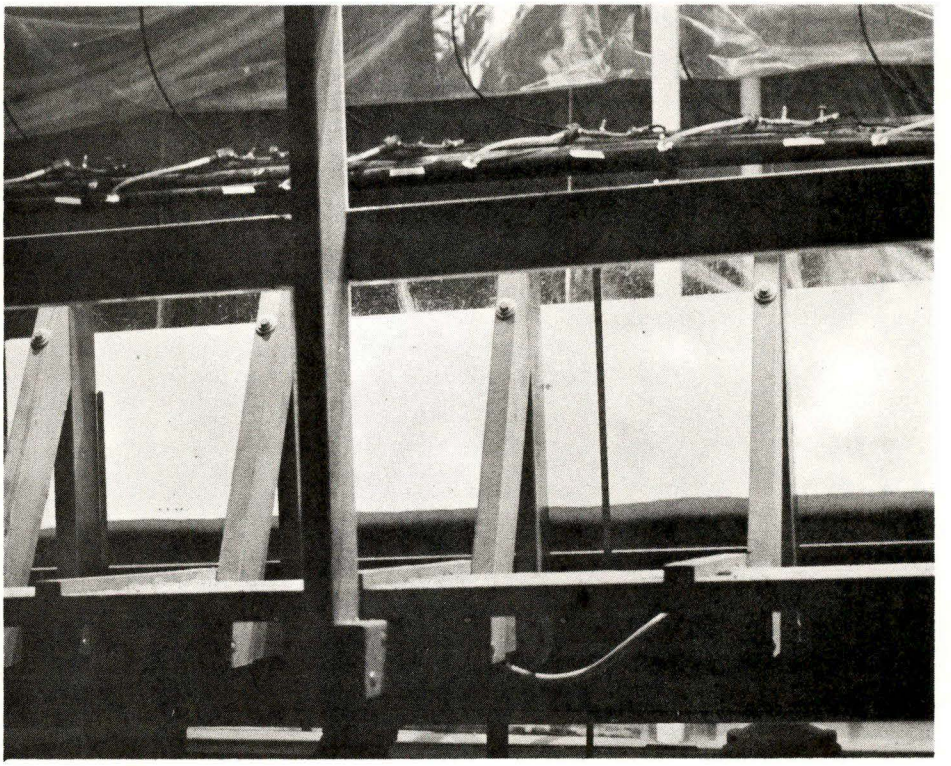

Plate 13. Side view of run during sediment transport capacity experiment. Sediment is black layer beneath gray water.

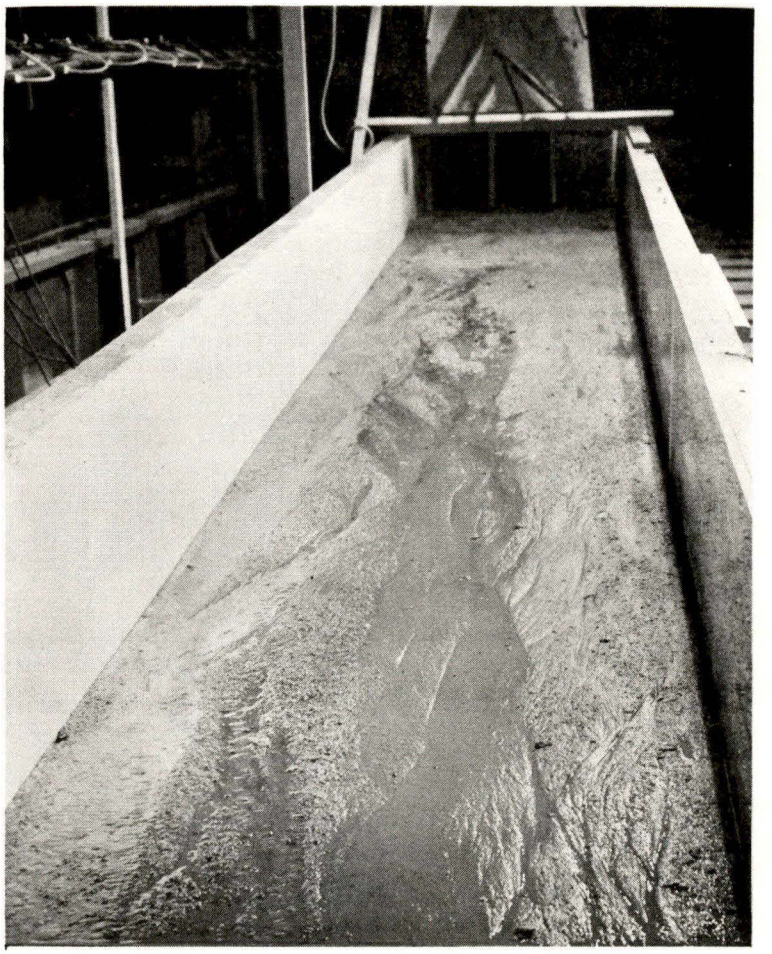

Plate 14. Post-run channel surface for sediment transport capacity experiment.

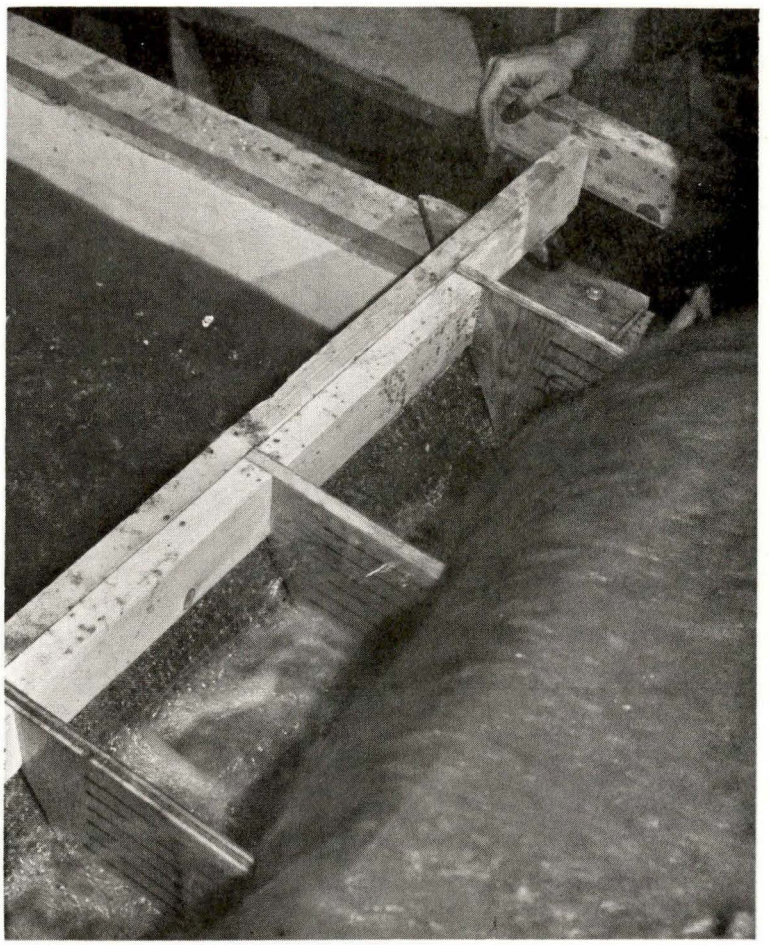

Plate 15. Sampler collecting sediment during sediment transport capacity experiment.

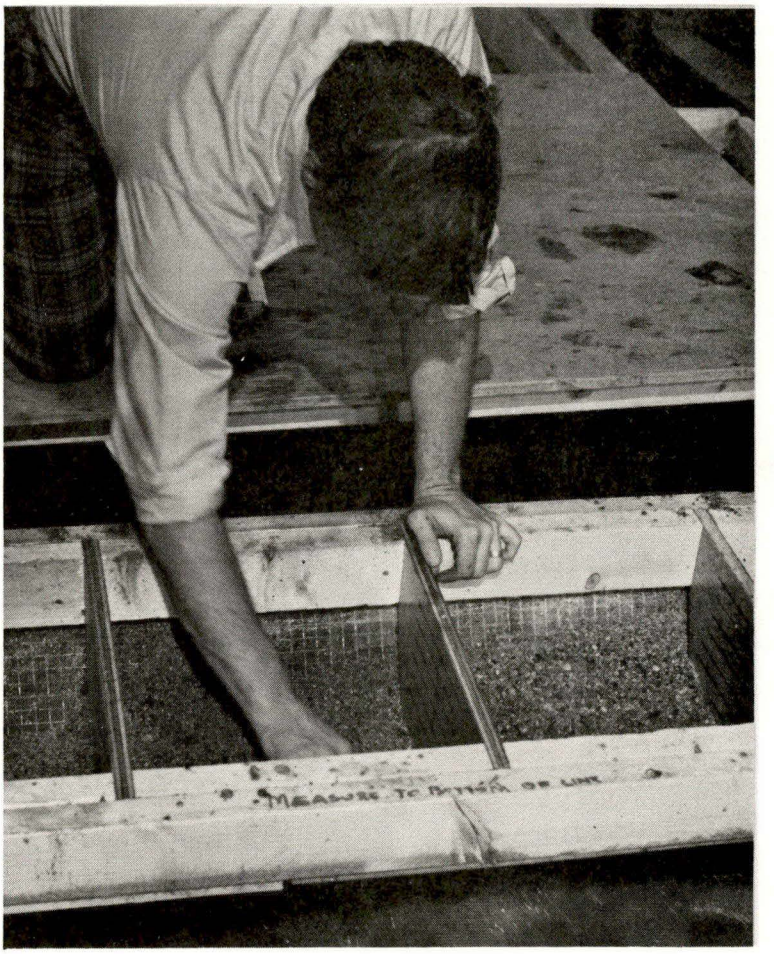

Plate 16. Leveling of sample before measurements in sediment transport capacity experiment.

Plate 17. Measurement of sample during sediment transport capacity experiment.

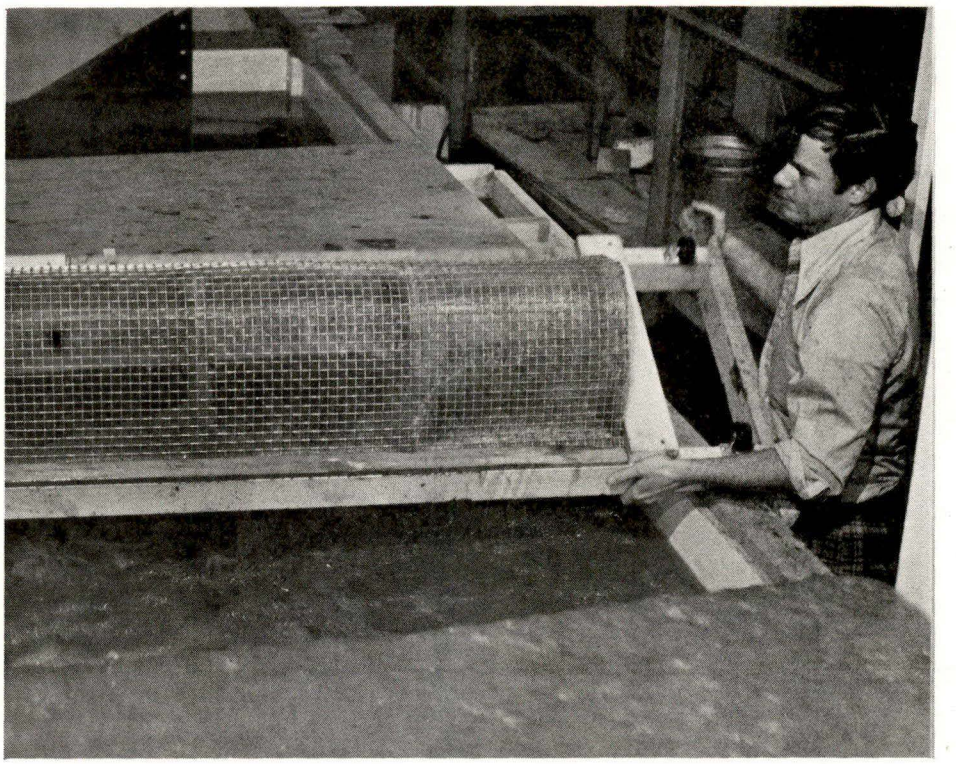

Plate 18. Emptying of sampler during sediment transport capacity experiment.

in the sediment sampler represented about one percent of the total transport, well within sampling error (see Figure 7). Therefore, corrections for minor amounts of fine materials not measured were not computed. Model sediment sizes represent prototype debris size ranging from very fine gravel to small boulders. Smaller sizes of prototype sediment cannot be efficiently modeled.

Sediment transport capacities are the equilibrium channel sediment transport rates for each respective water discharge, i.e., sediment supplied to the flow per unit time equals sediment passing out the bottom of the flume per unit time at a constant water discharge. The range of prototype water discharges studied was from 400 cfs to 5000 cfs. The 400 cfs prototype discharges were fixed by the limitations of the model facility at different slopes. In these runs, vegetative debris was not added. The results of Group II flume runs are presented in Table 3 and Figure 8. Transport rates are expressed as volume of porous sediment (with voids) per unit time. Porosity averaged about 0.44 for feeder and transported sediment. Transport values are the maximum sediment transport rates for the selected size distribution (see Figure 7) and bed slope. According to the data obtained, the maximum bulking factor is about 92 percent which is similar to that determined by the Los Angeles County Flood Control District Hydrology Manual, December 1971. It is important to note the direct proportionality of the sediment discharge to the water discharge as determined by the flume runs is within reasonable agreement with the Meyer-Peter, Müller sediment transport equation.

GROUP III RUNS

Group III runs determined the loading (filling) and unloading (scouring) rate of the sediment in the prism upstream of the model

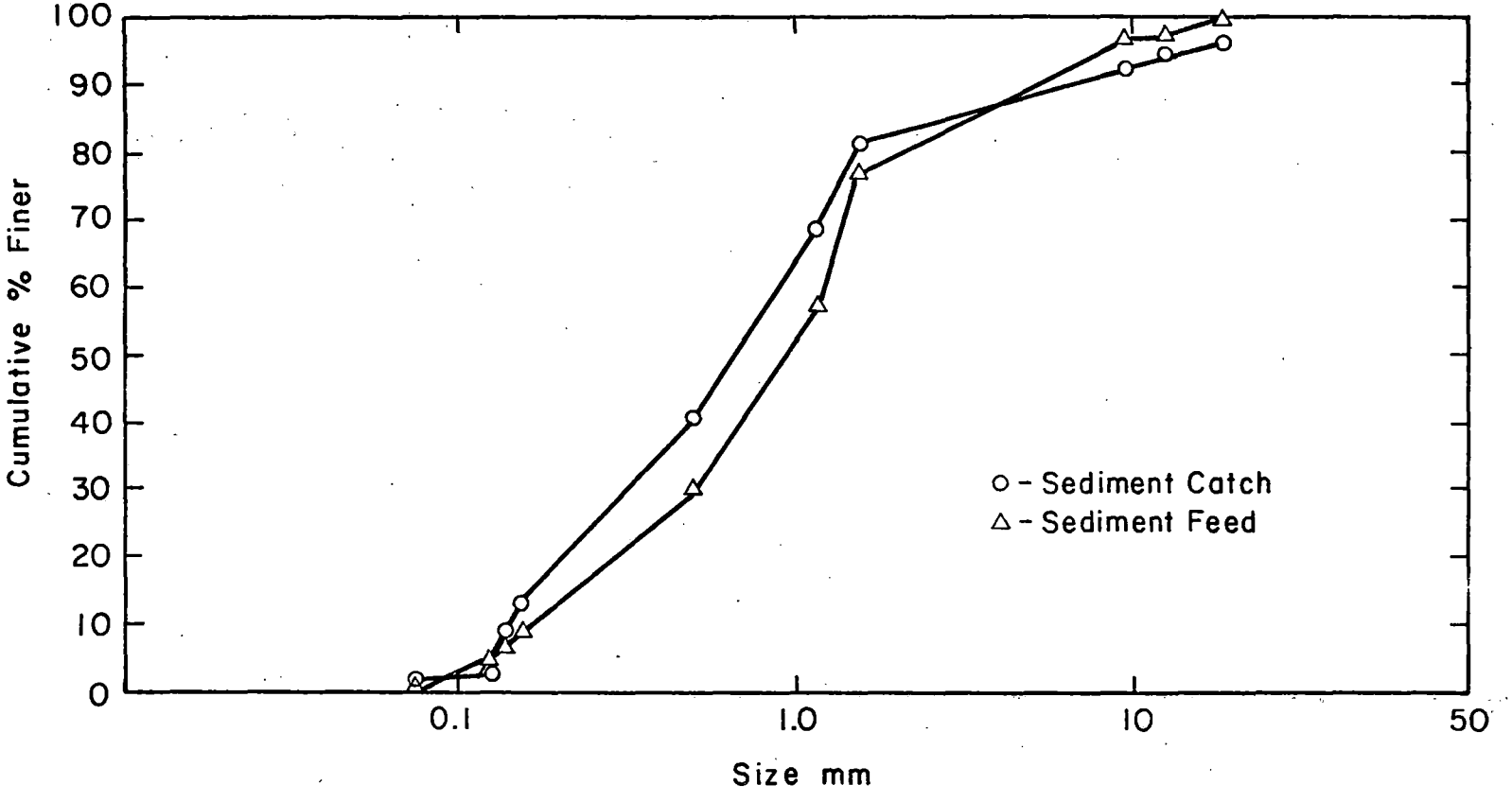

Figure 7. Model sediment size distribution.

Table 3. Group II runs showing water discharge and sediment transport capacity for three slopes (prototype values).

5%		15%		25%	
Qw	Qs	Qw	Qs	Qw	Qs
1259	59	425	166	556	641
1969	88	1088	594	1406	1075
2584	103	1762	819	2281	1966
3300	125	2559	1256	2559	2290
4719	247	4447	1753	4125	4019

Qw is without sediment
Q is in cubic feet per second
Qs is the sediment flow rate, measured as porous volume (with voids)

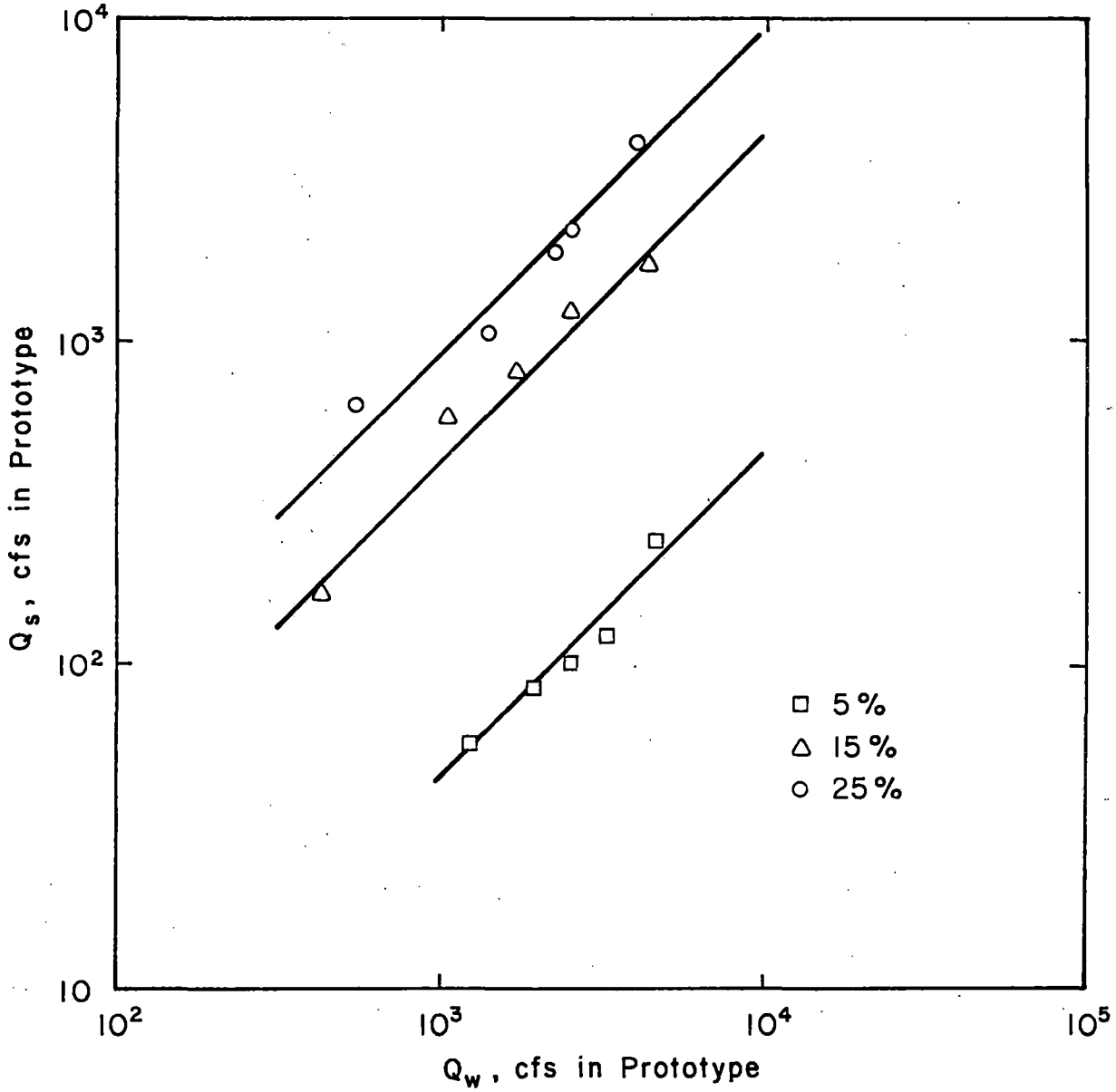

Figure 8. Sediment discharge Q_s compared to water discharge Q_w.

structure under different sediment and water discharges. In Phase I, a 6-inch bed of sediment was placed in the flume. The debris dam was placed on top of this bed attached to a 6-inch high cutoff wall. Experiments conducted in Phase II utilized a fixed, rigid bed that differed from the 6-inch sediment bed used in Phase I. This procedure was adopted to provide better control on sediment inflow rate to the structure and to shorten experimental preparation time. Water and corresponding equilibrium sediment discharges were run through the dam for the time required to fill the dam to the spillway level or until no significant change in the volume of deposited sediment was observed. The volume of deposited sediment was then profiled and computed. The bed was leveled at the dam and a clear water discharge was allowed to scour the sediment until approximately one-half of the volume of stored sediment was eroded or until changes were insignificant. Similar scouring runs were also conducted at one-half of the channel sediment transport capacity rate determined in Group II. Data from Group III runs consist of water discharge rates and rate of sediment filling or scouring. Sediment discharge samples were collected to check loading and unloading rates. Plates 19, 20, 21, and 22 show the original rectangular dam during and after filling with discharges to 1400 cfs (prototype). Note the scour hole downstream of the rectangular dam opening in Plate 19. Similar photographs document the unloading of the structure (Plates 23, 24, 25 and 26). During Phase I runs, modeled vegetative debris was introduced in the form of wood shavings, shredded plastic, toothpicks and dowels. None was added in Phase II Group III runs. Utilization of these materials to model vegetative debris is consistent with the model scaling factor and with consideration to roughness characteristics.

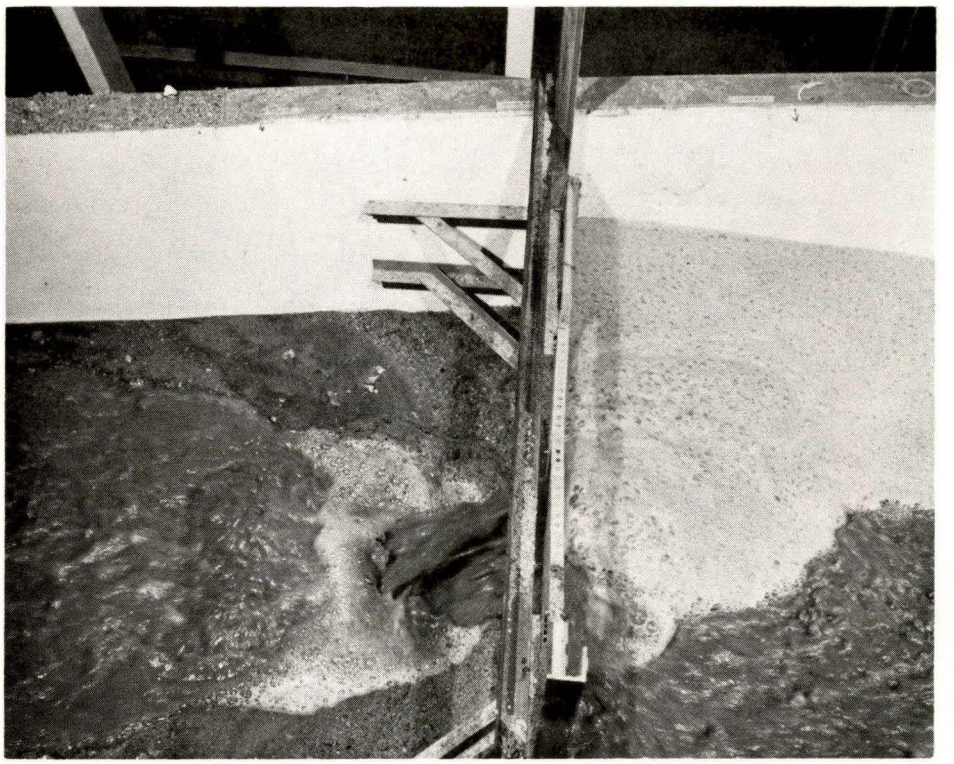

Plate 19. Top view of rectangular dam during loading rate experiment at approximately 1400 cfs (prototype value).

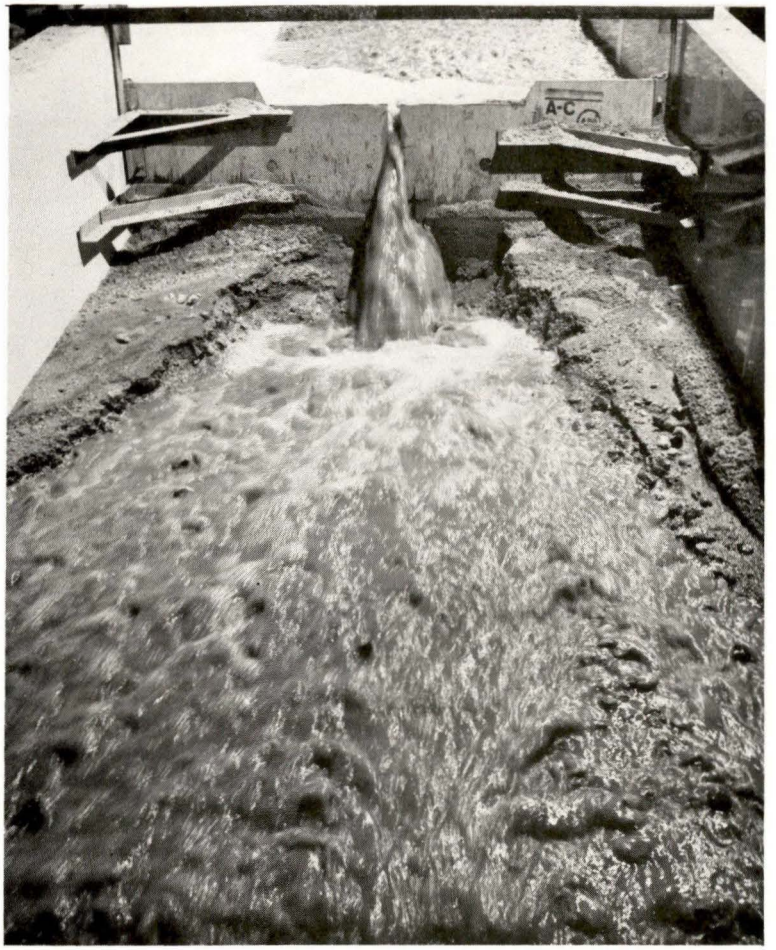

Plate 20. Upstream view of rectangular dam during loading rate experiment at approximately 1400 cfs (prototype value).

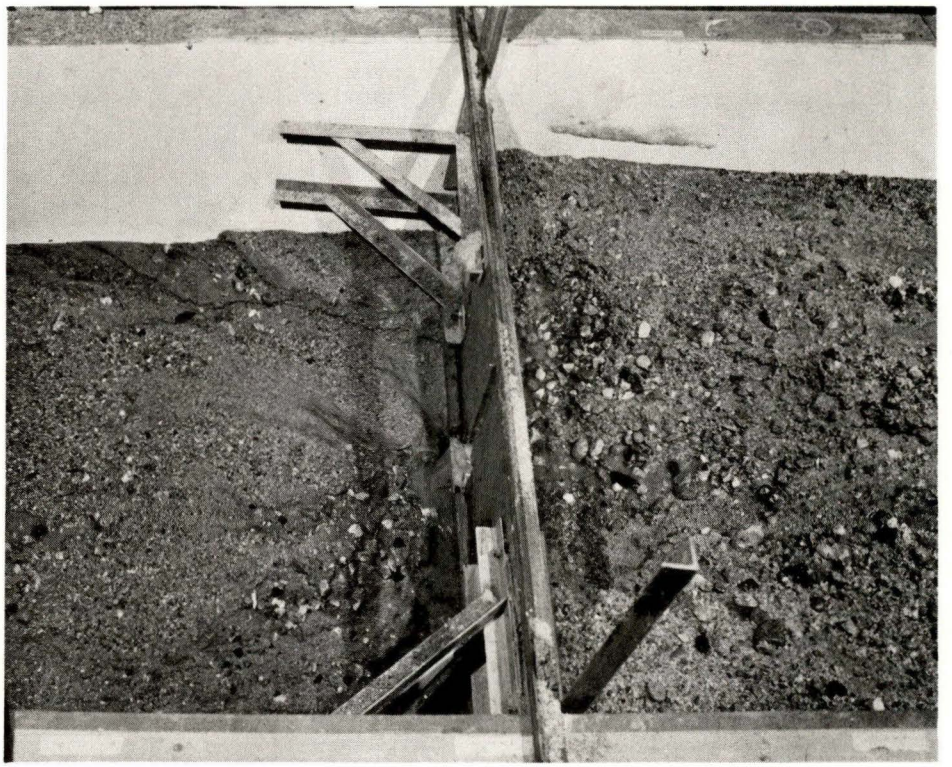

Plate 21. Top view of rectangular dam after loading rate experiment.

Plate 22. Upstream view of rectangular dam after loading rate experiment.

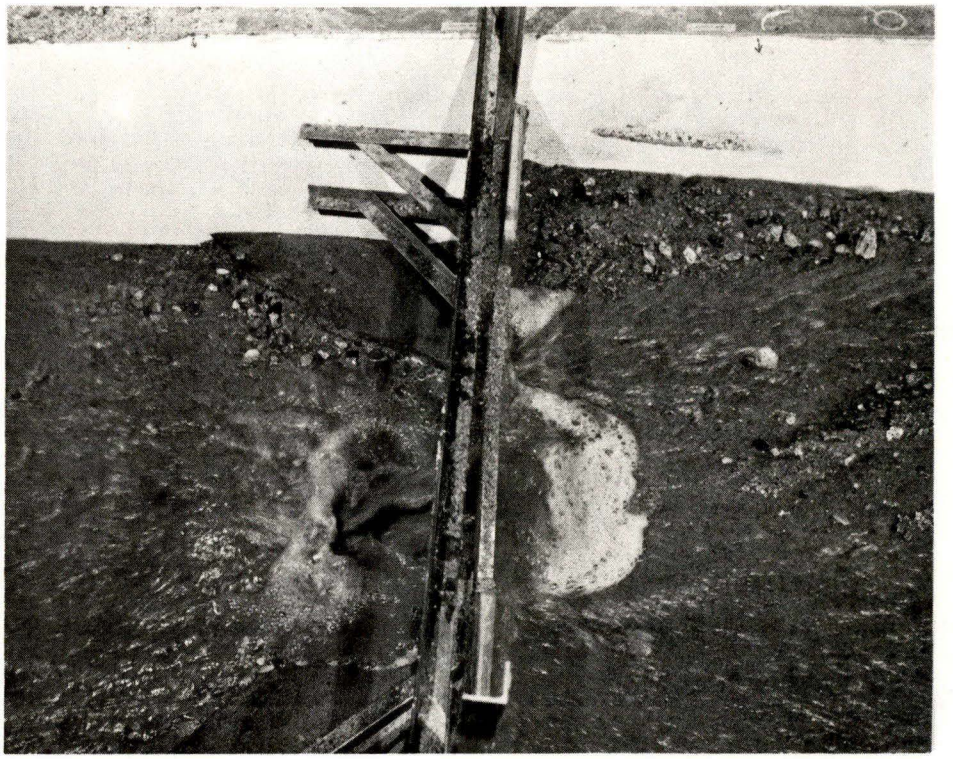

Plate 23. Top view of rectangular dam during unloading rate experiment.

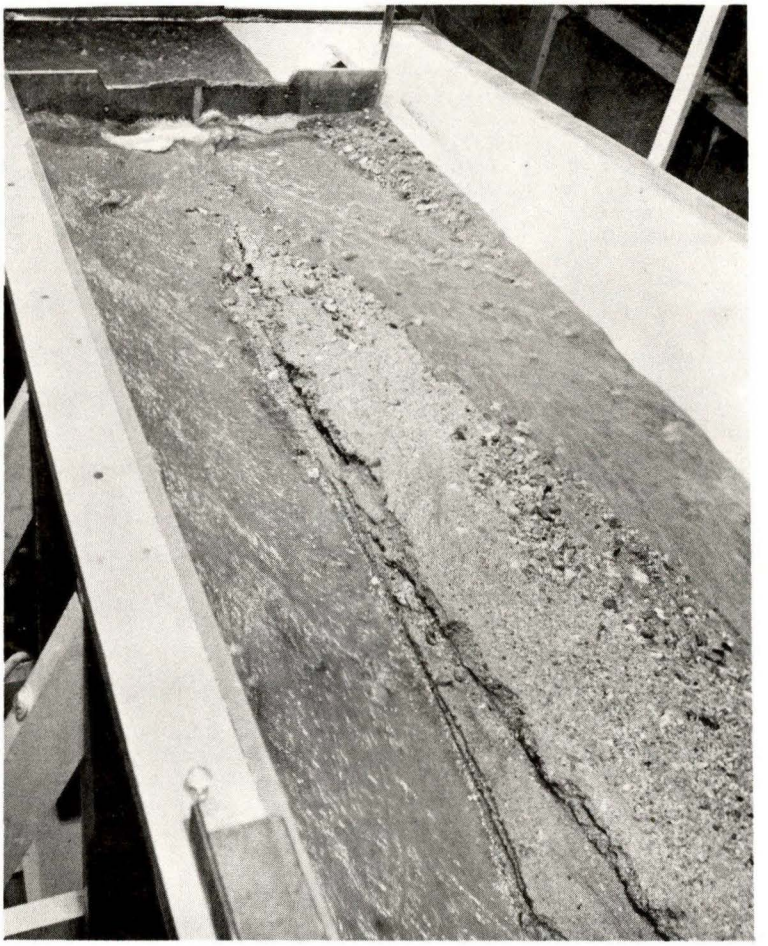

Plate 24. Downstream view of rectangular dam during unloading rate experiment.

Plate 25. Oblique upstream view of rectangular dam after unloading rate experiment.

Plate 26. Downstream view of rectangular dam after unloading rate experiment.

The Group III flume runs determined the sediment loading and unloading rates of the dams. In the Phase I study, only the original rectangular structure and a 15 percent slope were considered. Testing of the original rectangular structure and the other dams was completed in Phase II. The Group III runs were subdivided into three series: (a) Series I: maximum sediment supply is available throughout the run starting with an empty model using the sediment transport capacities determined in Group II runs, (b) Series II: no sediment is added to the flume to evaluate the debris cleaning efficiency starting with the structure loaded with sediment for various low flows (less than 1700 cfs), and (c) Series III: one-half of the debris transport capacities determined in Group II runs is fed into the flume to evaluate the debris cleaning efficiency with this sediment supply condition. The flume runs in this series start with the loaded structure. In Phase I of these runs a 6-inch layer of sediment was laid on the rigid flume bed and approximately 0.5 percent vegetative debris was added. The 6-inch bed and vegetative debris were eliminated for Phase II runs of this series.

Plate 19 shows the top view of a loading run (starting with no stored sediment upstream of the model dam) for a water discharge of about 1400 cfs. Plate 19 shows the trapping of sediment behind the model dam and a large scour hole immediately below the split dam port. Plate 23 demonstrates the top view of the unloading runs (starting with sediment stored behind the model dam) for a water discharge of about 700 cfs and no debris supplied to the flume. This plate also shows the self-cleaning feature of the split dam. Plate 25 shows formation of an alluvial fan downstream of the structure after the unloading phase. Movies were taken of loading and unloading runs. Results of the

Group III flume runs for the original ogee and rectangular shapes are tabulated in Table 4. The determined loading and unloading rates with regard to porous or bulked sediment (porosity included) for the original dams are plotted in Figures 9 and 10. Loading rates of Series I runs did not reach zero because deposition was always equal to or exceeded erosion of the prism at low flows and maximum sediment debris availability.

In all figures showing loading and unloading rates, solid lines have been added to show the trends in the data. Filling rates are strongly controlled by channel slope for at least two reasons. First, increased slope dictates higher sediment supply to the backwater area behind the dam. Second, increased slope decreases the extent of backwater behind the dam causing a much smaller local sediment storage area (Plate 27). With increased sediment inflow at higher slopes, the smaller backwater storage areas fill rapidly. During unloading or scour, the effects of slope are also evident. In runs using high slopes the limited sediment storage area is subject to more rapid erosion by greater clear water scour. At lower slopes, however, sediment transport capacity of the flow is reduced and the lower transport flow acts upon a more extensive sediment volume.

Another factor influencing transport is the gradient or slope of the sediment trapped behind the dam. As sediment deposits behind the dam, a new bed slope is established. At first the slope is nearly horizontal with the top of the dam (Plate 28). Over a period of time, however, a new bed slope would be established that represents the predominant water and sediment discharge rates. Local changes in bed slope can alter filling rates because sediment transport is roughly

Table 4. Group III runs. Loading and unloading rates for original ogee and rectangular dams at three slopes.

Number	Dam[1]	Type of Run[2]	Slope Percent	Q_{water} cfs	$\frac{\Delta s}{\Delta t}$ ft^3/sec
1	R	F	25	1302.98	1017.95
2	R	S	25	1302.98	-62.27
3	R	F	25	2317.59	1787.23
4	R	S	25	2317.59	-59.06
5	R	F	25	684.88	285.18
6	R	S	25	684.88	-27.54
7	R	F	25	936.96	426.93
8	R	F	25	749.57	202.95
9	R	F	25	618.21	145.34
10	R	F	25	798.80	434.47
11	R	S	25	798.80	-143.86
12	R	F	25	684.88	156.41
13	O	S	25	3786.75	-79.28
14	O	S	25	1833.26	-39.51
15	O	F	25	930.08	580.72
16	O	S	25	930.08	-20.16
17	O	F	25	792.55	396.58
18	O	S	25	792.55	-33.21
19	O	F	25	478.07	198.52
20	O	S	25	478.07	-23.27
21	O	F	25	415.86	216.12
22	O	S	25	415.86	-14.14
23	O	F	25	761.70	572.79
24	O	S	25	761.70	-27.87
25	O	F	15	2224.51	844.13
26	O	S	15	2224.51	-67.21
27	O	F	15	1495.02	451.70
28	O	S	15	1495.02	-79.41
29	O	F	15	978.84	354.62
30	O	S	15	978.84	-84.22
31	O	F	15	767.81	288.60
32	O	S	15	767.81	-22.56
33	O	F	15	1782.43	584.63

Table 4 (continued)

Number	Dam[1]	Type of Run[2]	Slope Percent	Q_{water} cfs	$\frac{\Delta s}{\Delta t}$ ft^3/sec
34	O	S	15	1782.43	-80.56
35	O	F	5	2236.02	98.89
36	O	S	5	2236.02	-6.36
37	O	S	5	1990.85	-5.65
38	O	S	5	1634.99	-5.66
39	O	S	5	2213.04	-6.89
40	O	S	5	5579.50	-7.46
41	O	F	5	798.80	33.93
42	O	S	5	586.38	-7.25
43	O	F	5	1495.02	58.89
44	O	S	5	930.08	-13.15
45	O	F	5	4430.54	136.74
46	O	F	5	3216.13	91.30
47	R	S	5	3216.13	-33.96
48	R	S	5	2830.51	-10.09
49	R	S	5	2236.02	-9.23
50	R	F	5	4396.07	92.52
51	R	S	5	4766.05	-19.20
52	R	S	5	317.28	-21.12
53	R	F	5	2259.15	84.51
54	R	F	5	1036.38	40.90
55	R	F	15	2406.00	741.00
56	R	F	15	378.00	38.00
57	R	F	15	972.00	228.00
58	R	F	15	400.00	78.00
59	R	F	15	1684.00	500.00
60	R	S	15	188.00	-13.00
61	R	S	15	416.00	-25.00
62	R	S	15	972.00	-72.00
63	R	S	15	381.00	-47.00
64	R	S	15	688.00	-59.00
65	R	S	15	1684.00	-97.00

[1] O = Ogee R = Rectangular

[2] F = Fill S = Scour

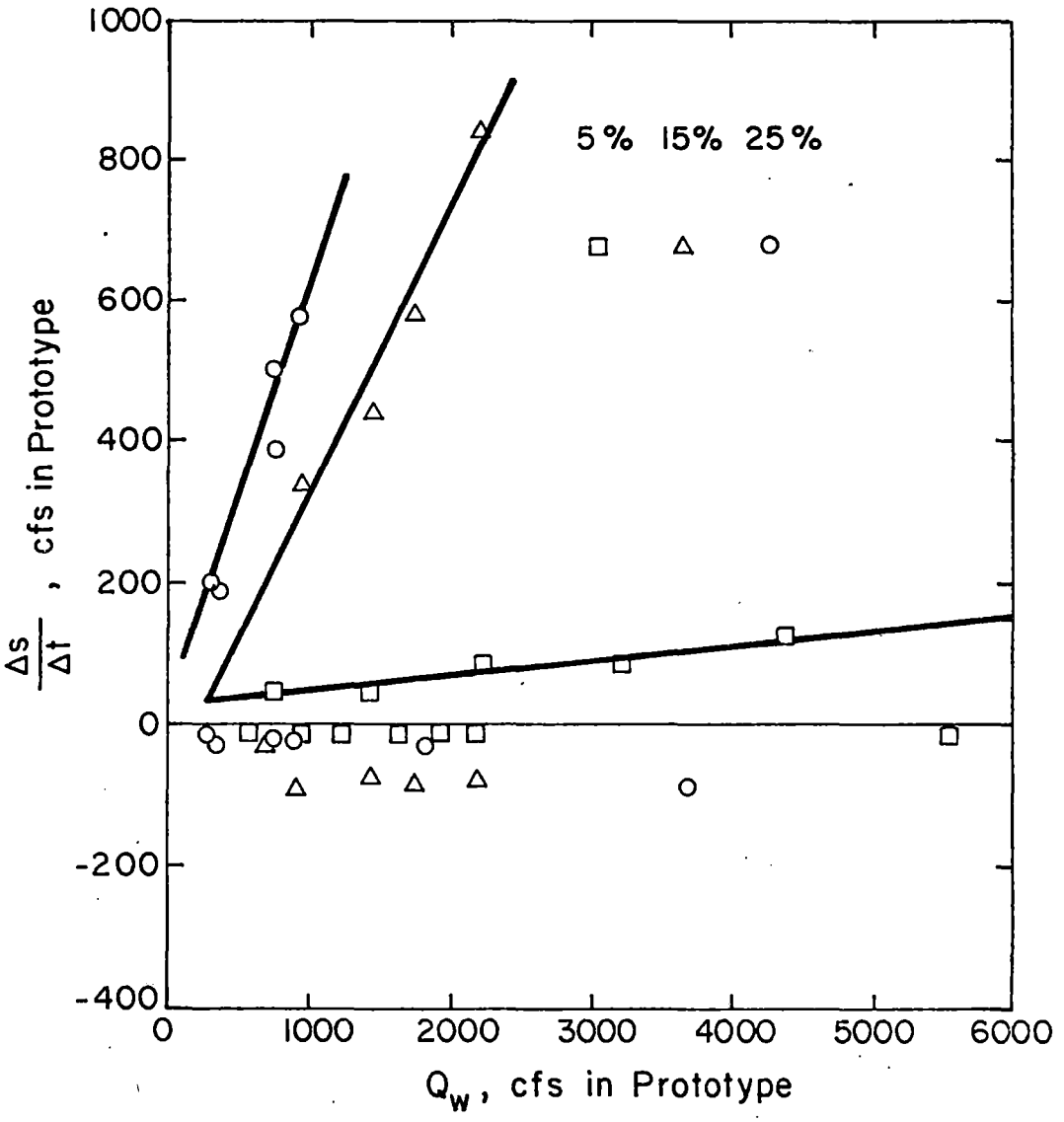

Figure 9. Comparison of loading and unloading rates $\Delta s/\Delta t$ for ogee-shaped dam at three slopes (solid lines indicate trends in data).

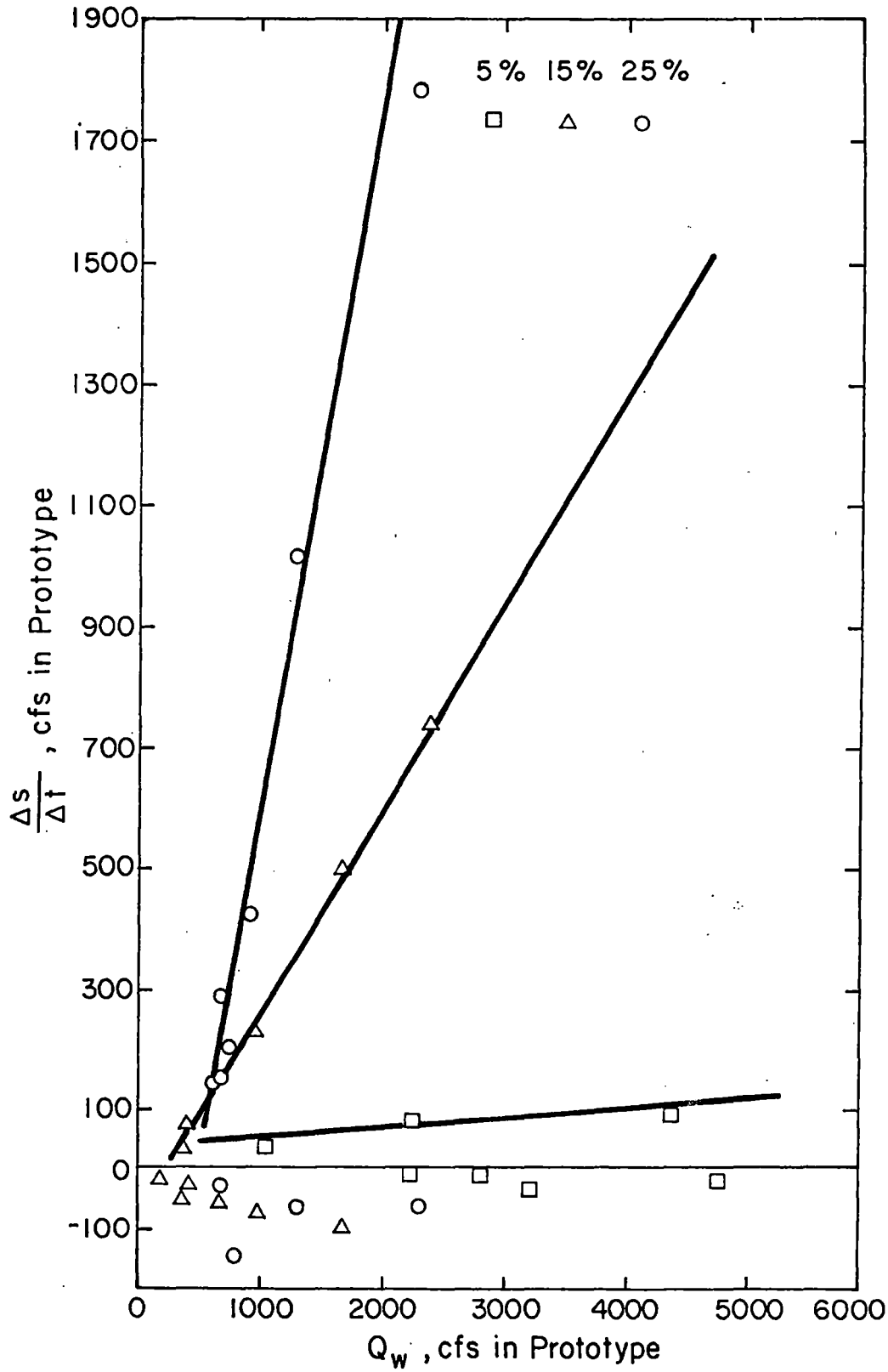

Figure 10. Comparison of loading and unloading rates $\Delta s/\Delta t$ for rectangular-shaped dam at three slopes (solid lines indicate trends in data).

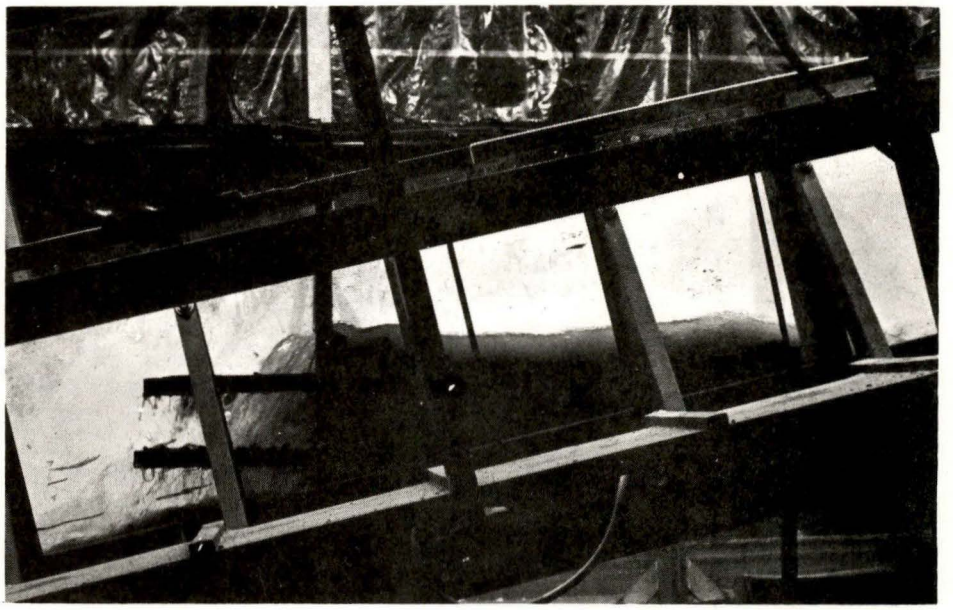

Plate 27. Low sediment storage capacity behind ogee dam on 25% channel slope.

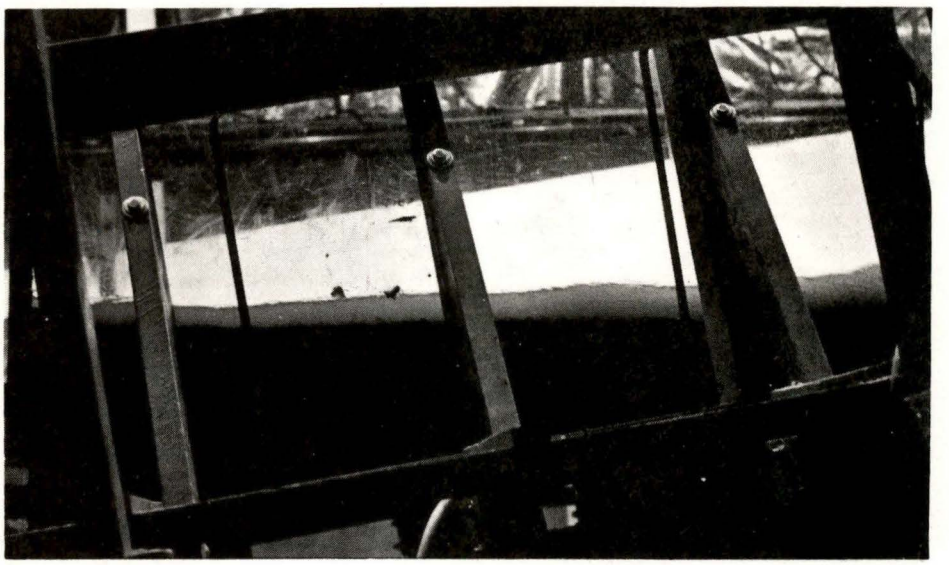

Plate 28. Horizontal backwater surface behind ogee dam on 25% channel slope.

proportional to bed slope squared. Decrease in bed slope by one-half from five to two and one-half percent therefore reduces transport to approximately one-fourth of the original value. Similarly, changes in local slope around the outflow part of the dam affect transport rates. Although the bed slope of the deposited sediments behind the dam may be nearly horizontal, the local slope of the material near the outflow port is near the angle of repose. The steepness of the deposited sediments in the vicinity of the outflow port is a result of flow through the port and response of the sediment to the flow. This steep slope in turn increases the erodibility of the material and thus material available for transport through the dam.

Another consideration is armoring or the protection from erosion provided by larger, less easily transported sediment sizes. In every run some armoring developed, a phenomena that also occurs in the field (Plate 29). Differences in slope, backwater extent, developed bed slope gradients, and armoring effects all combine to change filling and scouring rates.

Loading and unloading rates for ogee and rectangular dams are compared to all three slopes in Figures 11, 12 and 13. Generally, the ogee dam tends to fill faster. Unloading rates seem about equal for both dams with perhaps the ogee shape scouring a bit slower. The difference in filling rates between the two dams is caused by the flow areas of the two split openings. The ogee shape is tall and narrow while the rectangular shape is short and wide. The short and wide shape appears to be a better configuration as it allows passage of debris more readily and provides a better hydraulic configuration. In over 30 runs,

Plate 29. Armor layer developed on sediment deposit behind dam.

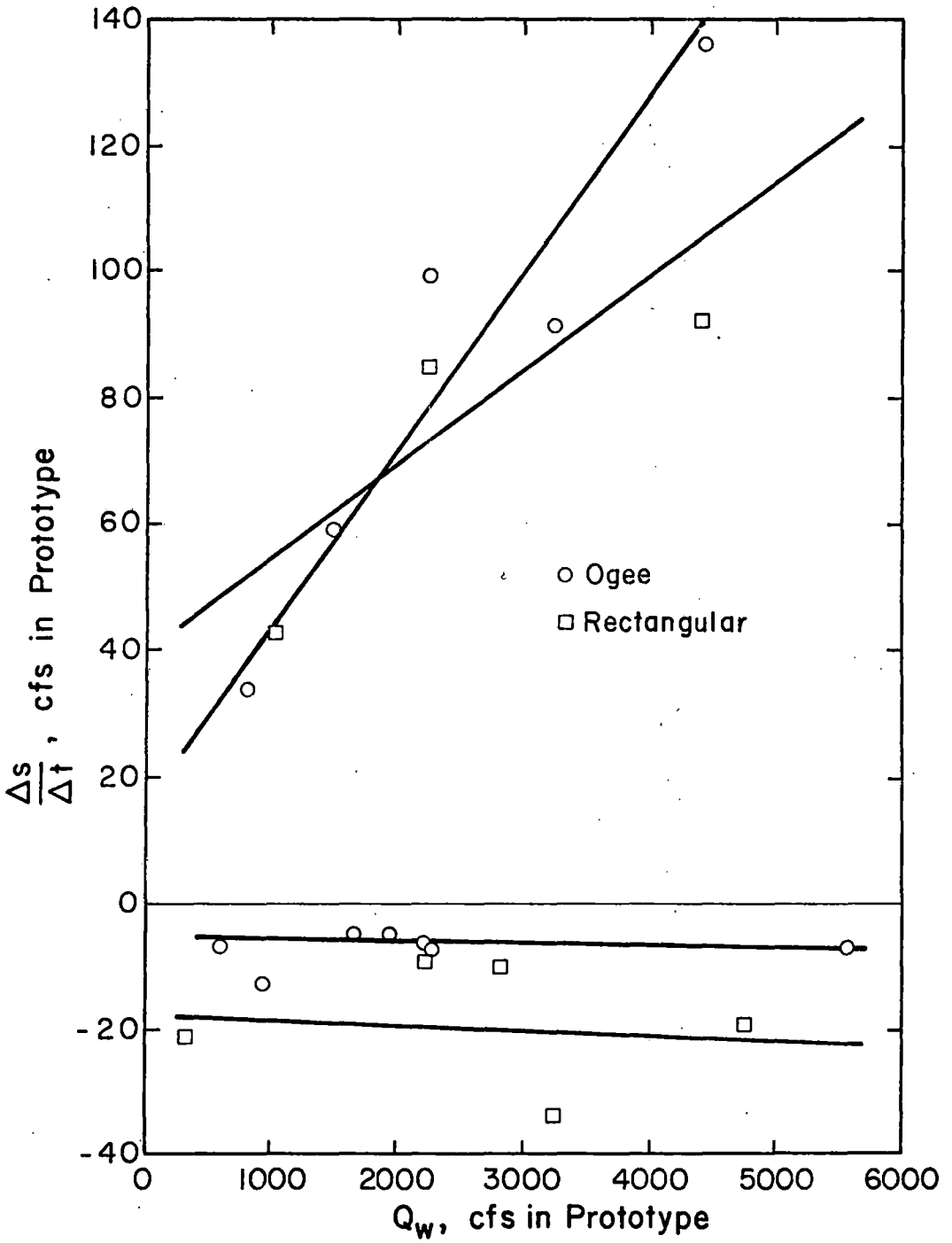

Figure 11. Comparison of loading and unloading rates for original ogee and rectangular dams at 5% slope (solid lines indicate trends in data).

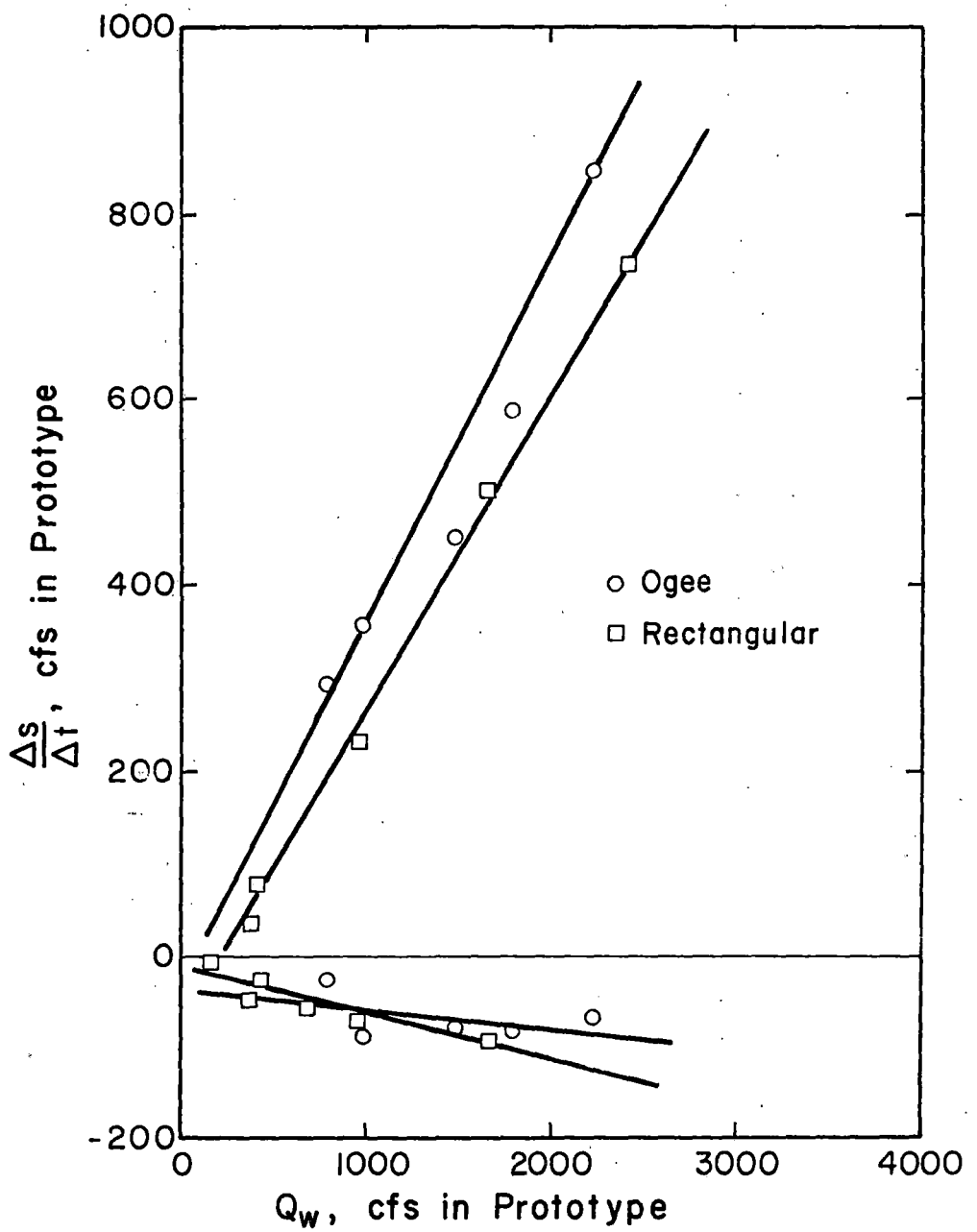

Figure 12. Comparison of loading and unloading rates for original ogee and rectangular dams at 15% slope (solid lines indicate trends in data).

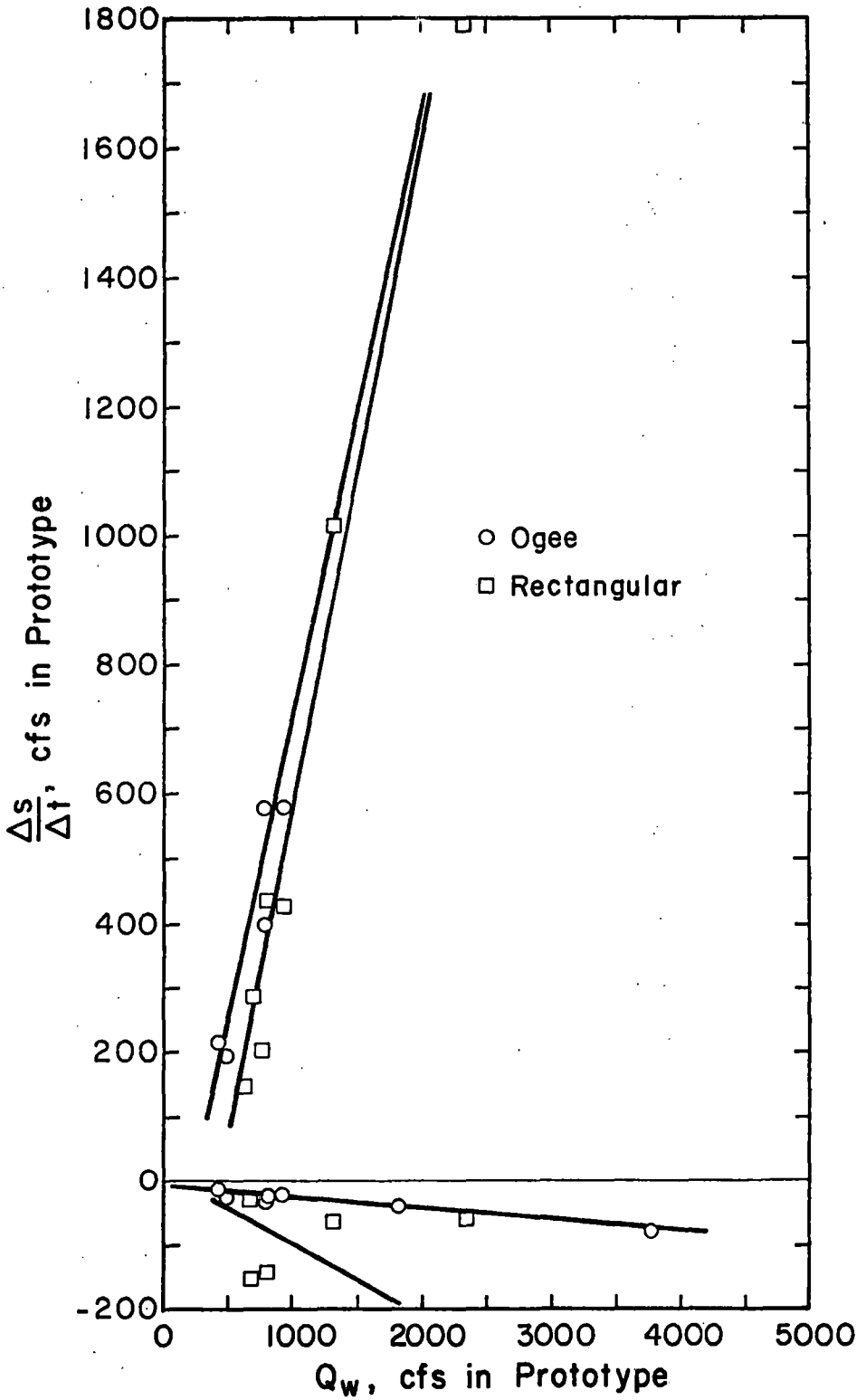

Figure 13. Comparison of loading and unloading rates for original ogee and rectangular dams at 25% slope (solid lines indicate trends in data).

no clogging was observed in the rectangular opening. In contrast, the ogee shape needed constant attention to avoid plugging that occurred as frequently as seven times during one unloading run.

PARTIAL SCOUR RUNS

Partial scour runs were conducted for both original dams at all three slopes. A partial scour run is defined as a run in which sediment is fed at one-half the transport capacity. These runs provided some interesting results for the original ogee and rectangular dams as shown in Figures 14 and 15 and listed in Table 5. In some runs, one-half of the sediment supply was large enough to produce filling. This is consistent with the observation that if the volume of sediment being transported into the backwater area behind the dam exceeds that passing through the dam, filling will occur. As in the loading and unloading runs, the rectangular-shaped dam tended to have a higher scour rate than did the ogee-shaped dam. (Low flows produced greater scour rates than high flows. This is in contrast to the no supply unloading rates.) Again, this is a function of the ports flow area and shape.

VEGETATIVE DEBRIS RUNS

Vegetative debris may clog the ports of any configuration of a split dam and thus may impair the dam's self-cleaning hydraulic characteristics. There were no definite observed differences between dams or between slopes in these runs. In the vegetative debris runs, simulated vegetation was introduced into clear water channel flow at 0.5 percent of the discharge rate. Table 6 lists the prototype debris sizes and corresponding model debris. Three flow levels were investigated. One level was at or near the bottom of the narrow split (Plate 30). The second level was just at the notched crest but below the top of the dam

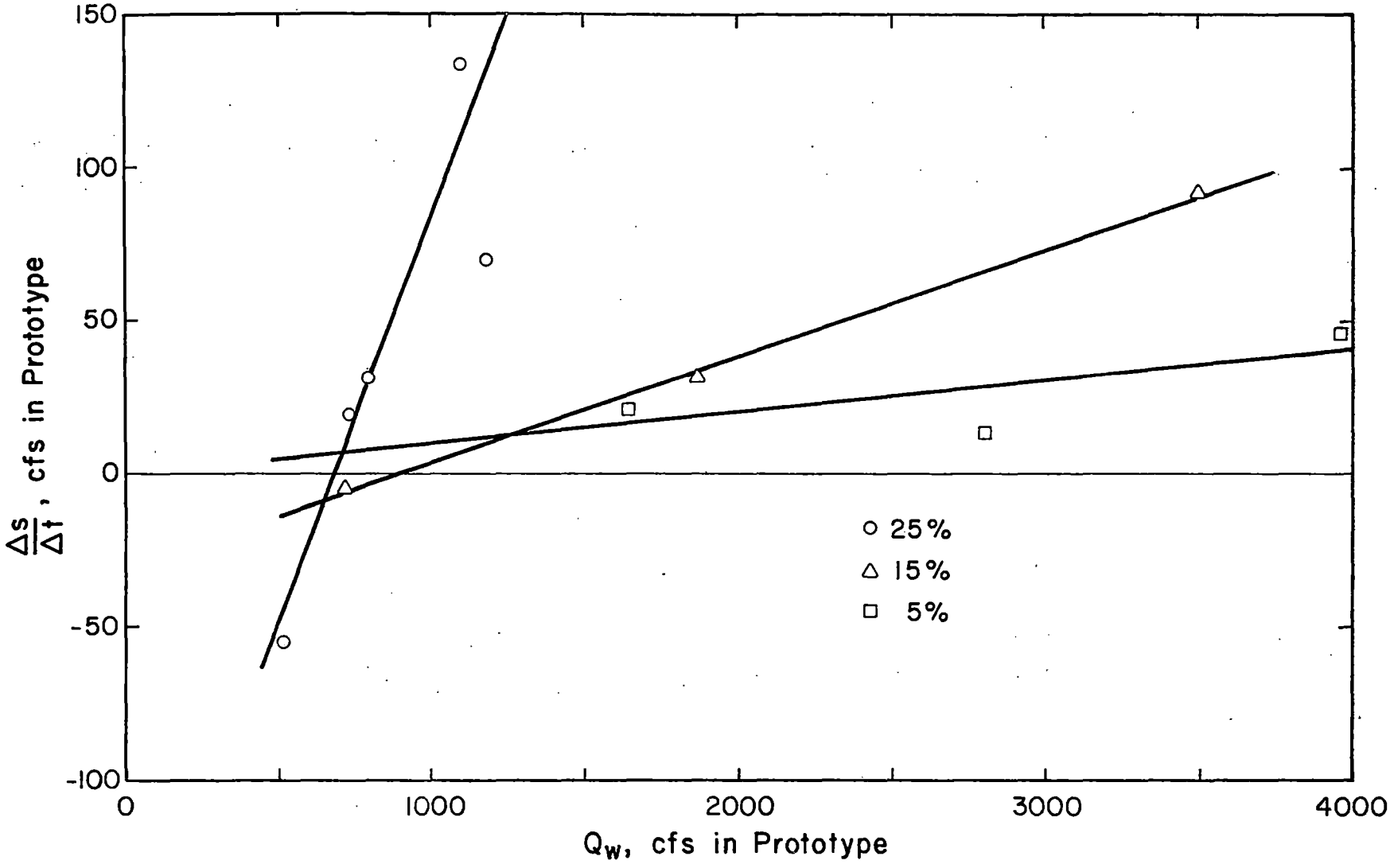

Figure 14. Partial scour rates for original ogee dam at the three slopes (solid lines indicate trends in data).

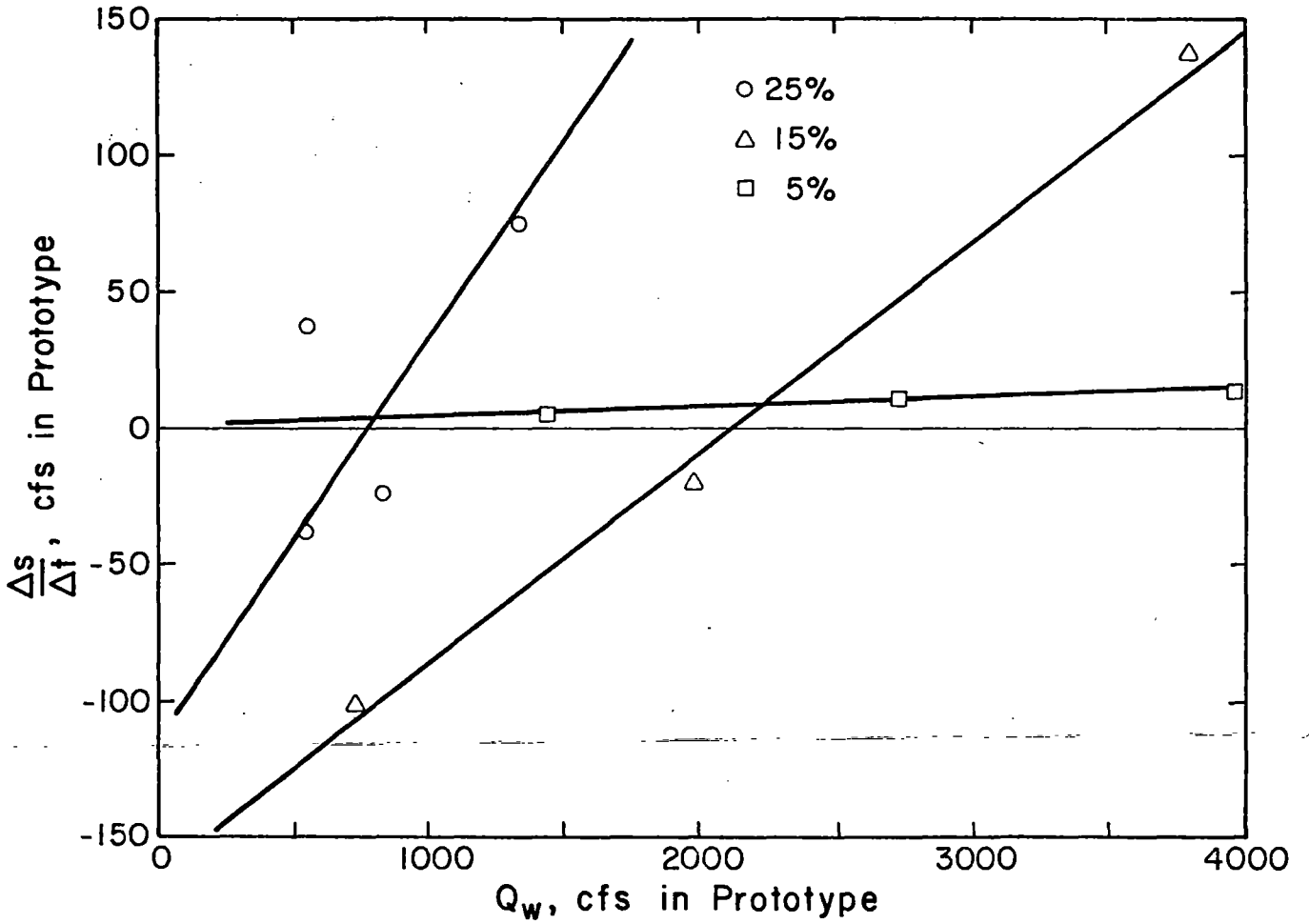

Figure 15. Partial scour rates for original rectangular dam at the three slopes (solid lines indicate trends in data).

Table 5. Results of partial scour runs.

Number	Dam[1]	Slope Percent	Q_{water} cfs	$\frac{\Delta s}{\Delta t}$ ft^3/sec
1	R	5	1432.22	5.71
2	R	5	2725.65	10.80
3	R	5	3962.29	14.53
4	O	5	3962.29	45.28
5	O	5	2817.27	13.27
6	O	5	1654.21	19.93
7	O	15	3494.55	91.47
8	O	15	1874.53	31.10
9	O	15	725.64	-5.64
10	R	15	725.64	-101.37
11	R	15	1990.85	-20.60
12	R	15	3802.51	137.33
13	R	25	1328.25	75.44
14	R	25	830.52	-24.20
15	R	25	545.48	-38.69
16	R	25	550.50	37.45
17	O	25	511.12	-55.42
18	O	25	798.80	31.09
19	O	25	1173.03	69.39
20	O	25	773.95	19.01
21	O	25	1103.46	134.54

[1] O = Ogee R = Rectangular

Table 6. Vegetative debris size distribution used in experiments.

Prototype Dimensions	Model Dimensions	Percent of Total	Material
11' x 1'	5-1/4" x 1/2"	10%	wooden dowel
10' x 3/4'	5" x 3/8"	15%	wooden dowel
12-1/2' x 1/2'	6" x 1/4"	15%	wooden dowel
5-1/4' x 1/4'	2-1/2" x 1/16"	20%	toothpick
2' x 1"	2-1/2" x 1/32"	40%	straw

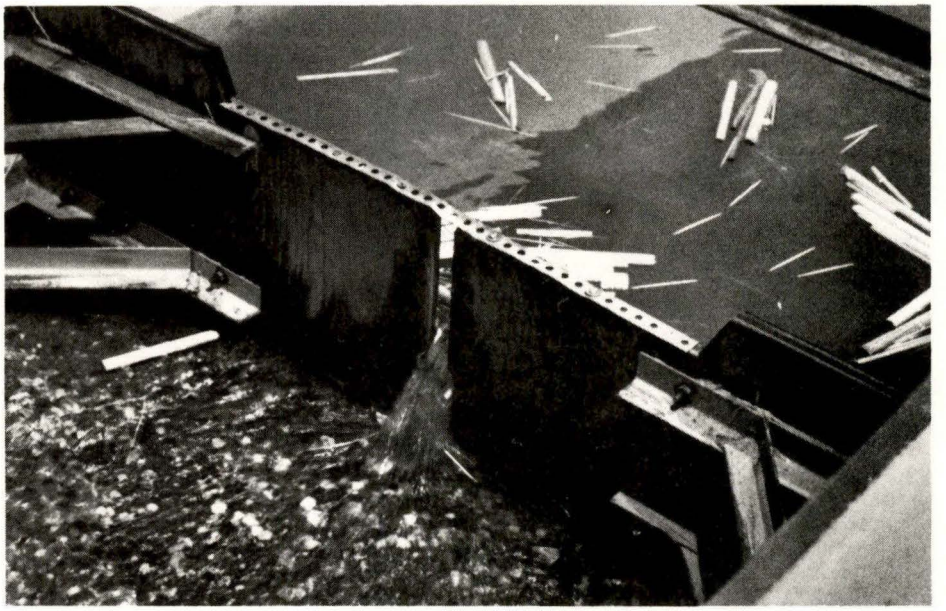

Plate 30. Vegetative debris run at low water level.

and the third level was just at the notched crest but below the top of the dam (Plates 31 and 32). After each run the volume of vegetative debris trapped behind the dam was compared with the volume of debris passing through or over the dam. Vegetative debris passing the dam and not trapped in the downstream channel was collected in a wire sampling basket (Plate 33). Comparison of post-run and pre-run debris volumes showed that complete recovery was attained at every run. Data for these vegetative debris trapping runs are also listed in Table 7 and shown in Figure 16. As this figure indicates, there is a general trend for less vegetative debris trapping at higher discharges. This trend is reasonable since higher water levels allow more debris to pass over the dam. In every run, however, clogging of the split occurred, even at the highest flow levels (Plate 34). Clogging occurred at higher flows due to submerged debris carried into the split. At low flow levels much of the debris appeared to be readily transported through the culvert openings until, by chance a simulated tree trunk or brush pile would lodge crosswise in the opening initiating further clogging. Thus, the sequence of events for flow levels below the crest of the notch were:

1. Debris transported through the split with simulated logs aligning in flow before passing through the opening,
2. A log or brush pile lodged crosswise in the split,
3. A debris jam from the crosswise log or brush developed upstream and below the water surface,
4. Debris carried below the water surface clogged the split and raised the water level,
5. The jam expanded upstream and below the water level until split was entirely clogged, and

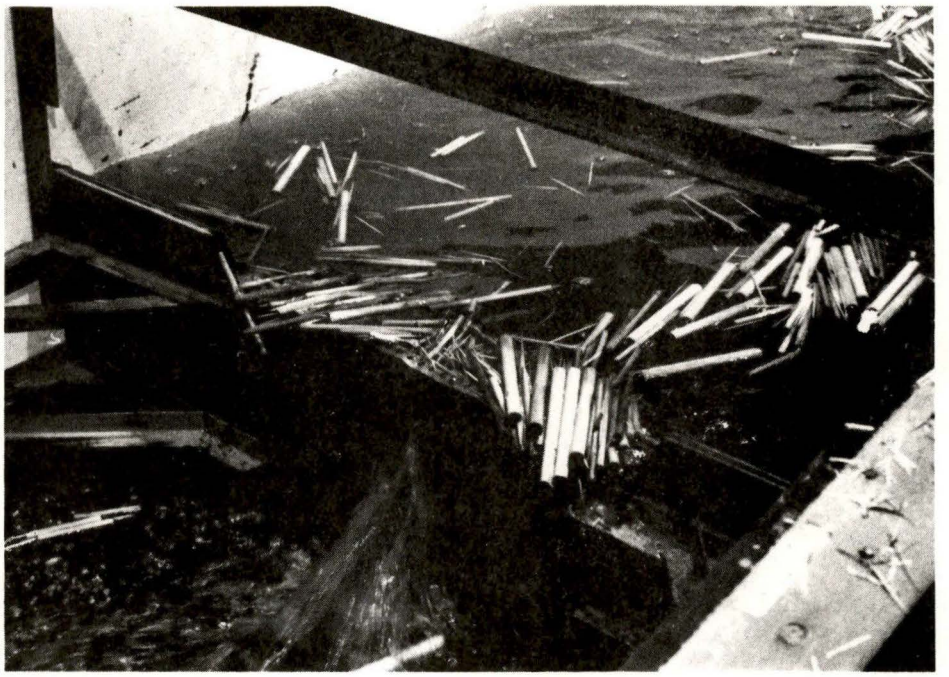

Plate 31. Vegetative debris run at medium water level.

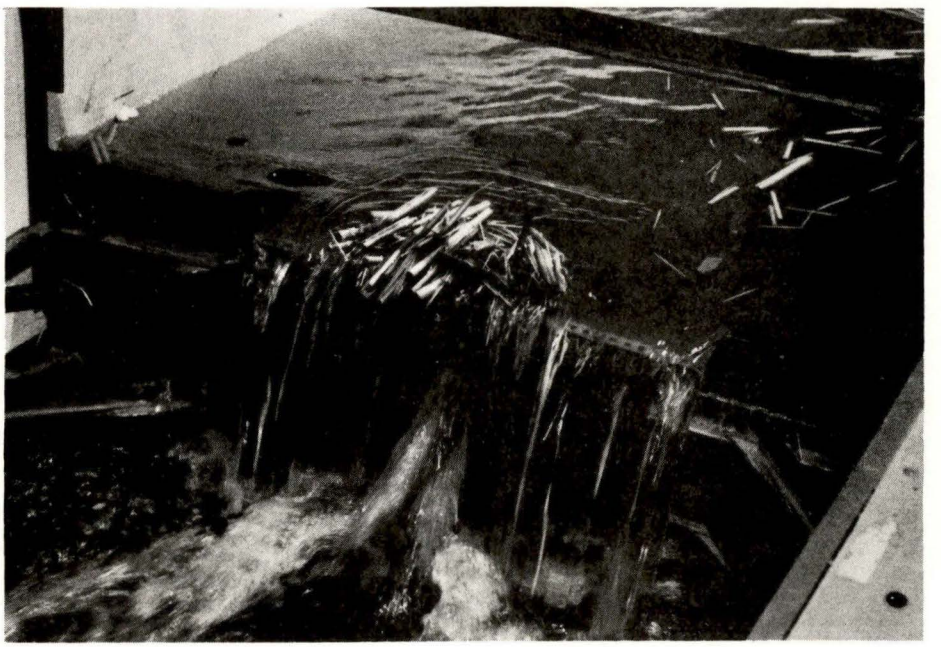

Plate 32. Vegetative debris run at high water level.

Plate 33. Sampling of vegetative debris.

Table 7. Results of vegetative debris runs.

Number	Dam	Slope Percent	Q_{water} cfs	Percent of Debris Trapped Behind Dam
1	O	25	965.00	75.68
2	O	25	1607.17	10.00
3	O	25	2726.81	0.99
4	O	25	478.73	98.33
5	R	25	375.17	62.50
6	R	25	1196.78	67.00
7	R	25	2701.41	10.00
8	R	15	2573.42	4.35
9	R	15	1406.39	18.80
10	R	15	386.89	91.10
11	O	15	350.74	80.00
12	O	15	1261.31	43.00
13	O	15	2413.19	6.00
14	O	5	2330.15	31.00
15	O	5	1212.46	53.00
16	O	5	403.50	74.00
17	O	5	362.47	51.00
18	O	5	1397.11	84.00
19	O	5	2486.47	24.00

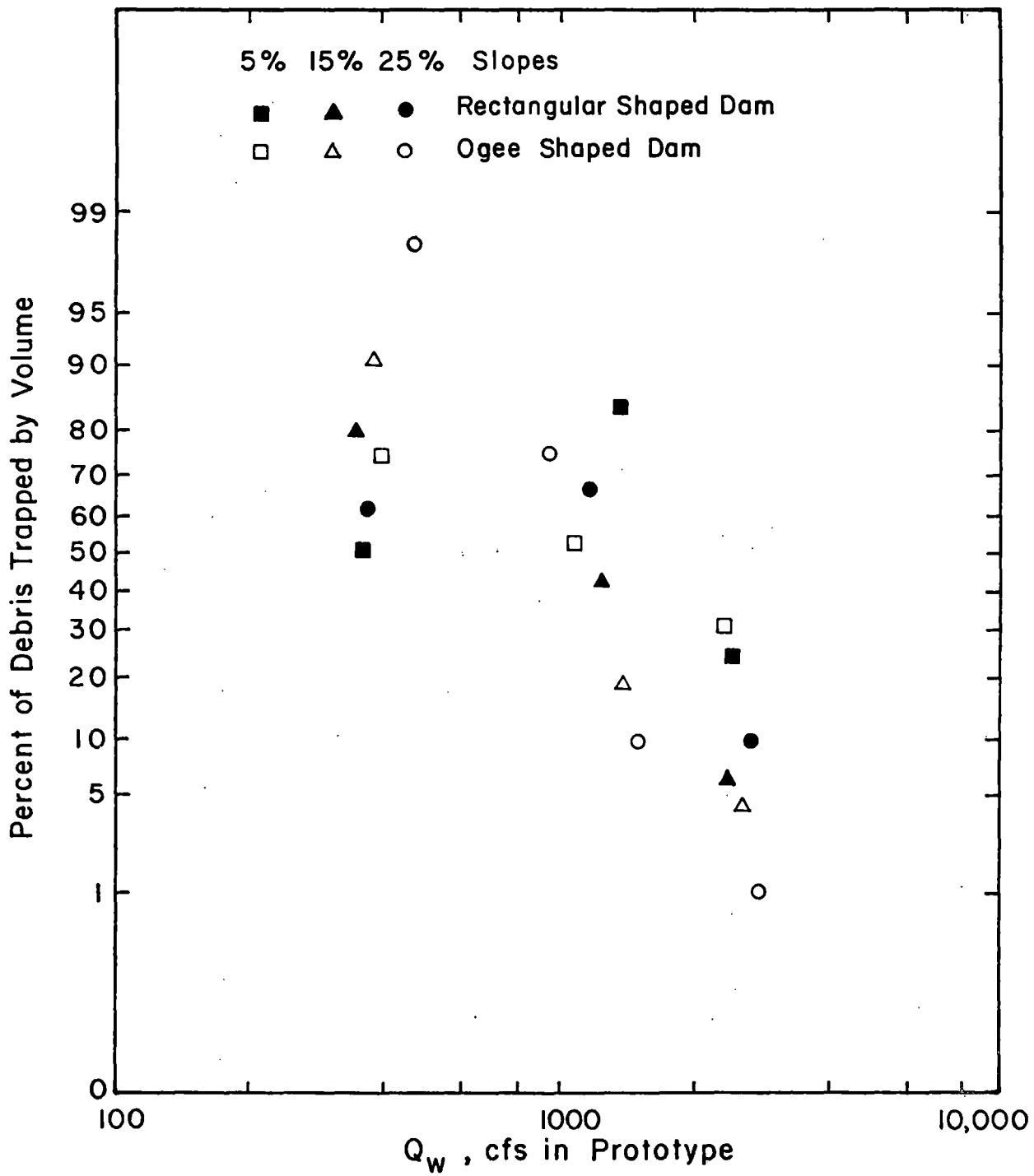

Figure 16. Percent of vegetative debris trapped compared to water discharge Q_w for original ogee- and rectangular-shaped dams.

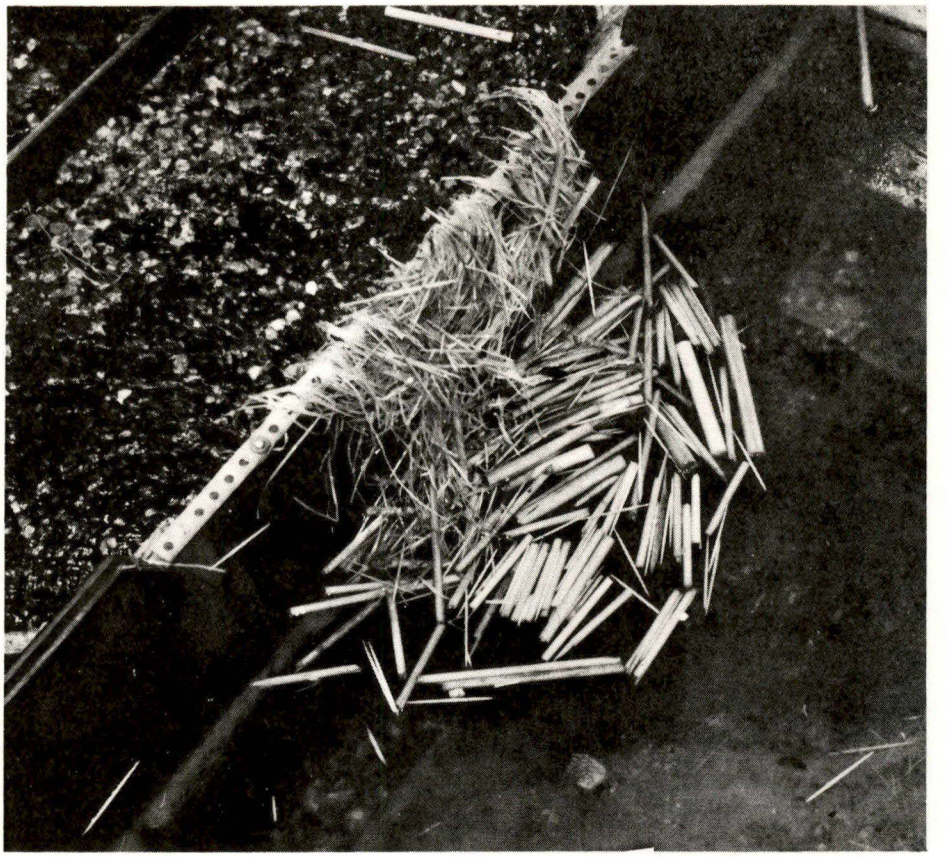

Plate 34. Split dam opening clogged by vegetative debris.

6. Debris flow through dam was essentially stopped.

Occurence of clogging is related to the probability that a log or brush pile will lodge in the split. At low flows where the split openings are wider, the chance of plugging may be less than at higher levels where the free water surface exits the dam through a narrower split (Figure 16).

For example, a higher percentage of debris was trapped behind the rectangular dam on the 5 and 25 percent slopes for flows of about 1500 cfs than for flows of about 400 cfs. In the former case the water surface is in the wide opening. In the latter case it is in the narrow slot. Counteracting this flow area problem is the increased velocity and streamlining of the opening that tend to pass more debris through the split dam. In general, the higher the discharge, the less likely is the chance of trapping debris. Since clogging occured in every run, some type of upstream debris catcher may be useful in preventing clogging.

TOP-TIE PILE WALL DAMS

Top-tie pile wall (solid) dams load rapidly, unload slowly and once full cannot be scoured enough to provide sediment trapping during future runoff events. A top-tie pile wall dam was studied on three slopes under a minimum of three flow conditions. Results of runs are listed in Table 8 and shown in Figure 17. Similar to the other dam types, higher slopes promoted faster loading rates. Once full, the newly modified channel gradient resisted erosion except at high flows where turbulent action at the upstream edge of the backwater produced some local scour and sediment transport. However, high flows without some sediment inflow from upstream are not realistic. Additional sediment inflow from

Table 8. Results of top-tie pile wall loading and unloading runs.

Number	Type of Run[1]	Slope Percent	Q_{water} cfs	$\frac{\Delta s}{\Delta t}$ ft^3/sec
1	F	25	916.42	864.33
2	S	25	916.42	-32.70
3	S	25	1969.39	-14.34
4	S	25	3913.95	-20.80
5	F	25	755.62	661.47
6	S	25	755.62	-39.40
7	F	25	407.39	252.45
8	S	15	4209.29	-15.77
9	S	15	985.93	-3.66
10	F	15	1916.35	543.53
11	S	15	1916.35	-23.89
12	F	15	1173.03	400.26
13	F	15	667.83	203.74
14	S	5	3317.12	-3.22
15	F	5	3159.26	122.05
16	S	5	5942.72	-36.86
17	F	5	2437.12	71.34
18	S	5	1397.05	-11.70
19	F	5	4209.29	167.99

[1]F = Fill S = Scour

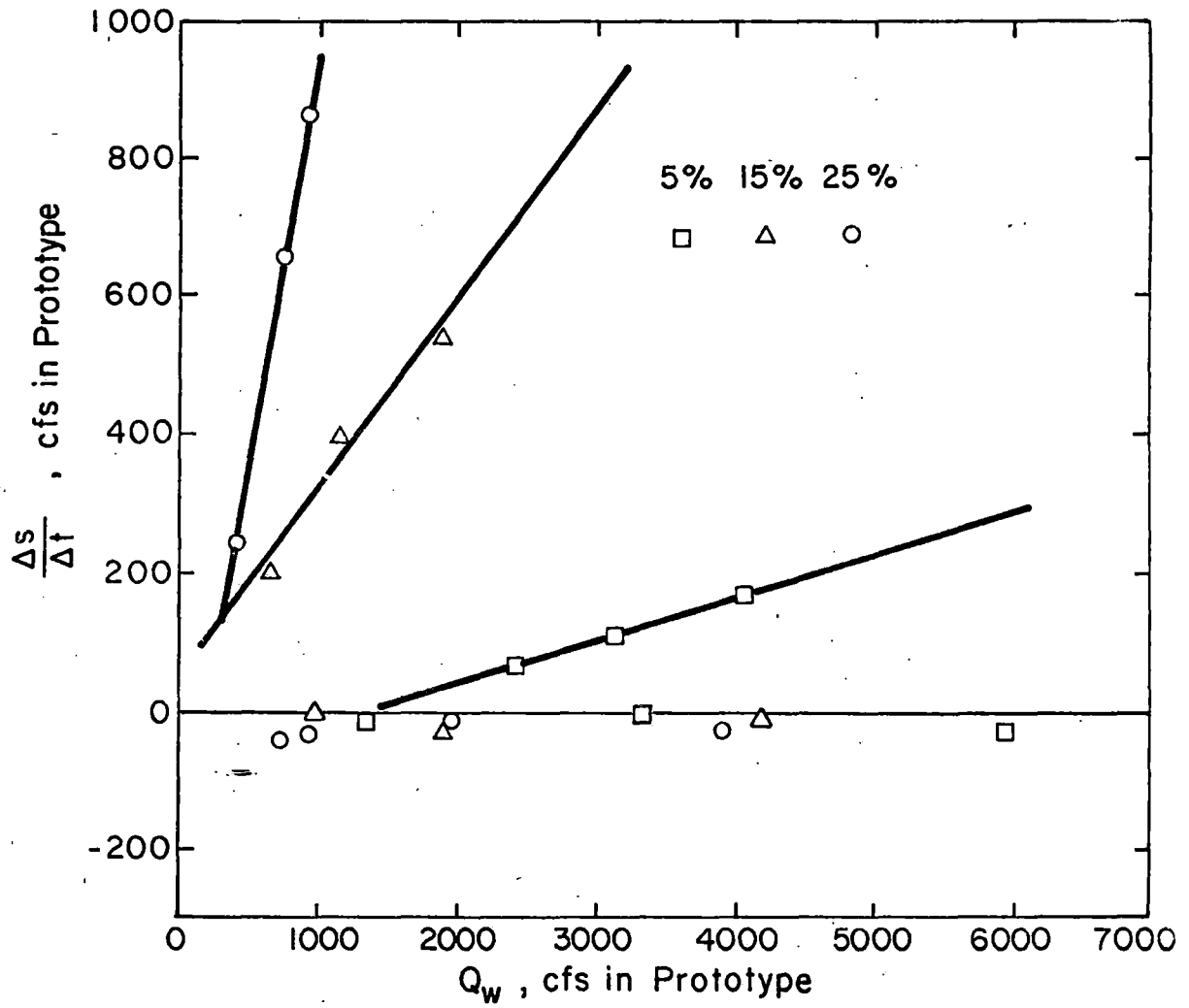

Figure 17. Comparison of loading and unloading rates $\Delta s/\Delta t$ for top-tie pile wall dam at the three slopes (solid lines indicate trends in data).

upstream reduces scouring potential caused by the turbulent action. As sediment was transported from the upstream end of the reservoir to the dam, an adverse or backslope (Plate 35) developed resembling those seen in the field.

Scour during unloading runs consistently progressed from the upstream end of the stored sediment toward the dam until a flow and channel bed gradient combination developed that reduced the unloading until little erosion occurred (Plate 36). On steeper slopes, erosion progressed further downstream than on less steep slopes. In general, the top-tie pile wall dam is an efficient sediment trap until it fills, after which it has only minimal effect on removing sediment from floodwaters.

COMPARISON OF SCOURING FOR ALL DAMS

The results of the scouring runs for the initial ogee and rectangular, top-tie pile wall, and new ogee and rectangular dams were analyzed to determine the extent of fill material removed during scour runs. The results of this analysis are shown in Table 9.

As this table shows, there is, as expected, an increasing amount of scour as slope increases, higher scour for the rectangular dams, and substantially higher scour for the split dams as compared to the top-tie pile wall dam. Because of individual differences in determining when to terminate scour runs, the values in Table 9 should only be used for relative comparisons. The data also indicated that there was no strong relationship between discharge and percent of material scoured. Scour was more strongly controlled by slope and split opening shape.

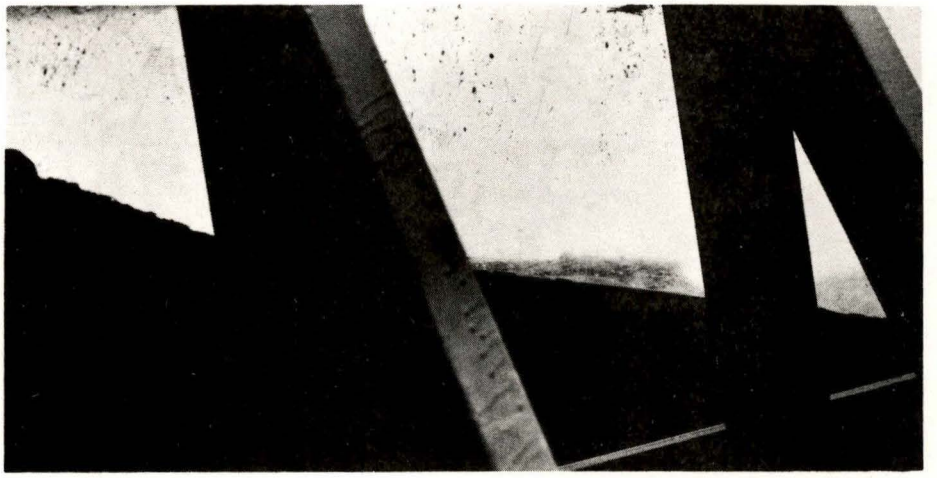

Plate 35. Adverse bed slope developed behind top-tie pile wall dam on 25% channel slope. Flow is from right to left. Sediment is black. The adverse slope on left is inclined in an upstream direction. Turbulent water (gray) in center.

Plate 36. Erosion at the upstream end of the deposited sediment behind top-tie pile wall dam occurring on 25% channel slope.

Table 9. Average percent of material removed by scour.

Dam	Slope		Average Percent of Fill Scoured
Old Ogee	.05		17
	.15		42
	.25		53
		average	37
Old Rectangular	.05		25
	.15		47*
	.25		70
		average	47*
Top-tie pile wall	.05		13
	.15		13
	.25		18
		average	15
New Ogee	.05		46
	.15		49
	.25		68
		average	54
New Rectangular	.05		60
	.15		72
	.25		81
		average	71

* Estimated because comparable data not available. This set of runs conducted during Phase I.

IV. ADAPTION OF SPLIT DAM DESIGN MATHEMATICAL MODEL

GENERAL

A mathematical model is a set of formulated equations that represent physical processes. Math models are available that simulate many types of natural processes. Included in these models are those that describe channel flow, sediment transport, and flow through and around structures. It must be realized that mathematical models are not exact because the natural phenomenon they represent are much more complex than can be adequately described by any type of formulation. However, models are often representative enough to sufficiently approximate a natural system. Therefore, models are widely utilized to help solve many problems associated with sediment transport and hydraulic structures. Mathematical models, if properly developed, can provide insight regarding how a system will respond to various natural and man-induced conditions. However, it should be noticed that mathematical models are only as good as the formulations used and the data required. If the model has been developed with the controlling physical processes as guidelines, then it should provide useful computations when supplied with good data.

In general, mathematical models go through at least four phases. First is conceptualization of the model with respect to the processes involved. Second, the model is developed or adapted from other existing models. Third, the model is tested and adjusted using a selected data base, and fourth, the model is used for prediction or application purposes.

SPLIT DAM MATH MODEL

The mathematical model for the split check dam was adapted from other existing models considering hydraulics of the dam opening, channel

flow and sediment transport, and sediment discharge from the dam. A full description of the math model is located in the appendix. To model discharge, the continuity and Manning's equations were used. For flow through the dam, the weir and orifice equations were used. A form of the Meyer-Peter, Müller bed load equation was used to define sediment transport capacity for a specific water inflow rate. A general sediment rating relationship between sediment discharge rate through the split and split geometry, channel slope, water depth, and characteristic height of the sediment concentration was adapted for use. Height of the sediment concentrations accounts for the fact that most of the sediment passing through the dam opening is located near the channel bed.

Weir and orifice relationships for stage height on the dam as a function of discharge and dam dimensions were checked against laboratory data. A discharge coefficient and a friction coefficient were varied until the computed and observed values were close (Figure 18).

Sediment inflow to the dam was simulated by adapting the Manning's open channel flow equation and Meyer-Peter, Müller's bed load sediment transport equation (USBR, 1960). Computed values were checked against transport rates measured in Phase I, Group II runs. Results of these simulations are presented in Figure 19. Relative closeness of the computed and measured values is quite good considering the numerous physical processes controlling sediment transport in steep channels.

Sediment outflow through the dam was estimated by relating calculated sediment discharge rate through the dam with flow depth at the dam, flow area through the dam and height of sediment concentration. In this way, effects of the dam opening shape and distribution of sediment in the flow were incorporated. Knowing the sediment inflow and

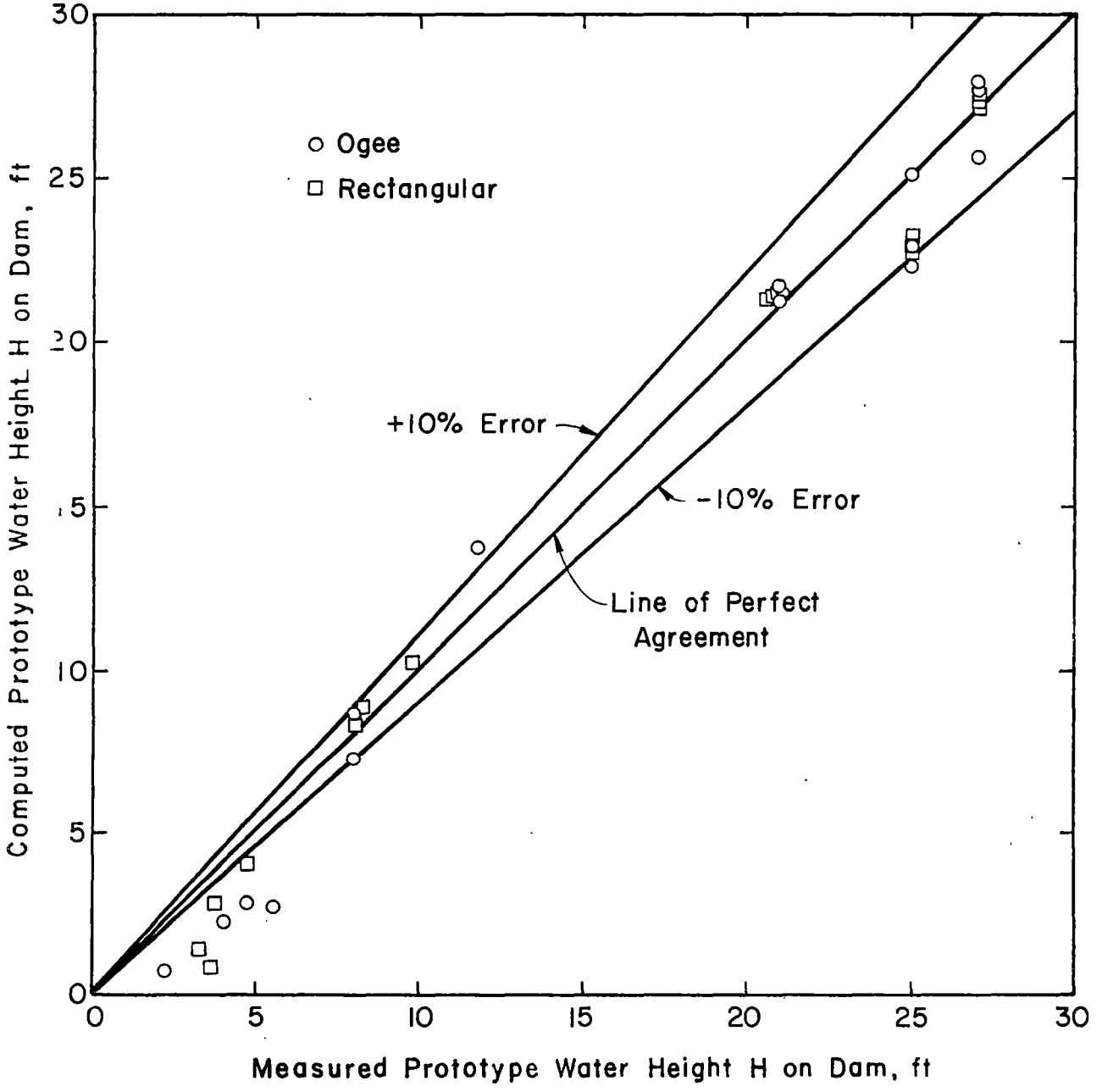

Figure 18. Comparison of computed and measured water level heights on dam.

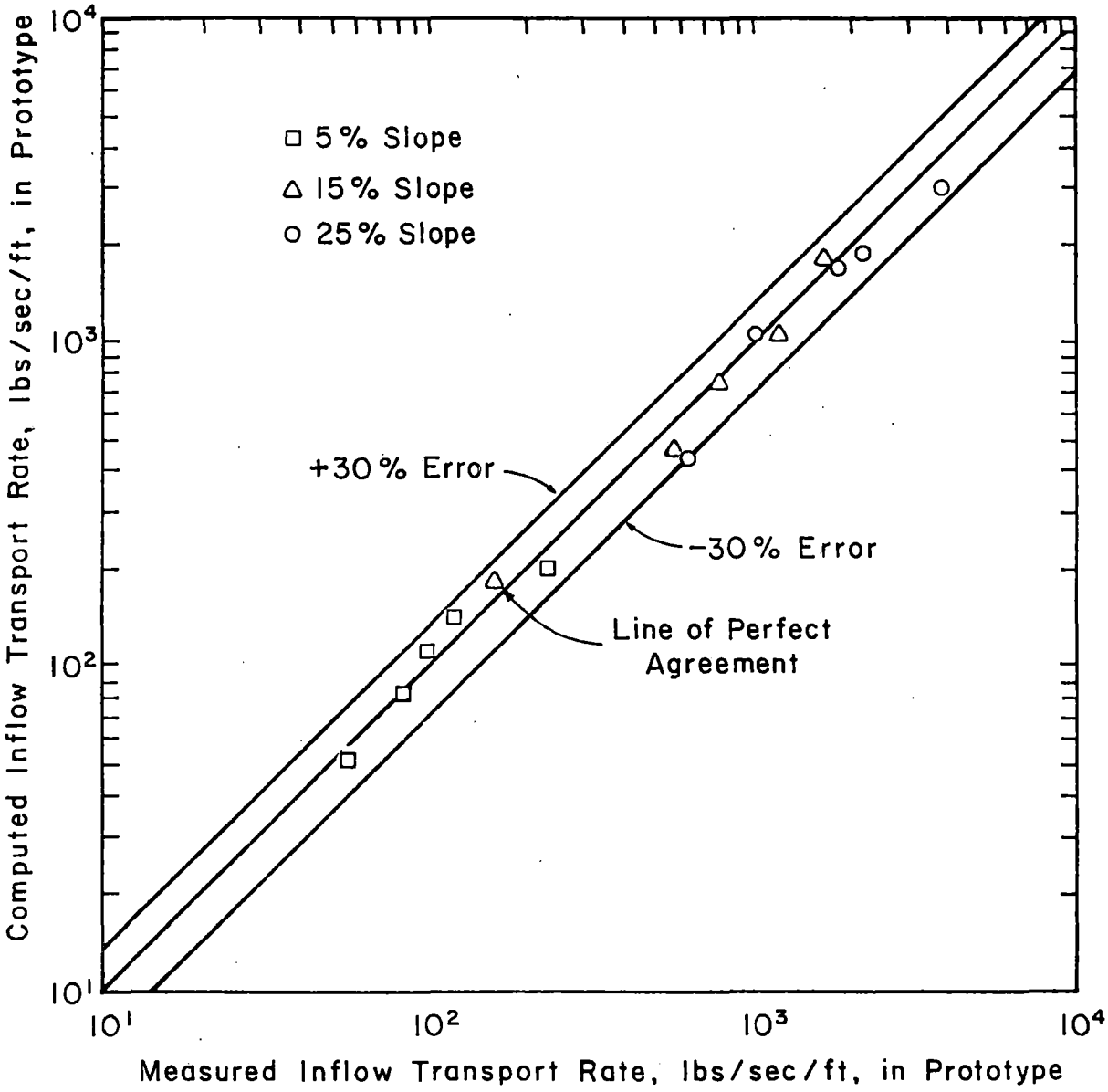

Figure 19. Comparison of computed and measured sediment transport rates using calibrated Meyer-Peter, Müller equation.

outflow rates allowed computation of the debris dam filling and scouring rates. A comparison of measured and computed filling and scouring rates for the porous or bulked sediment is shown in Figure 20 for the original ogee dam and Figure 21 for the original rectangular dam. These figures show that the model results are realistically close to the measured data.

The mathematical model was then verified by estimating filling and scouring rates for two new split dam opening shapes. Initial trials indicated that the model represented the filling and scouring rates very well. Because the dam openings were larger in the new models, the discharge coefficient became larger and the frictional or loss coefficient became smaller. Adjustment of these two coefficients provided better comparisons between model predictions and measured values. These comparisons of measured filling and scouring rates (bulked sediment) with model computed rates are shown in Figures 22 and 23 for the new ogee and new rectangular dams, respectively. Measured values for these dams are listed in Table 10. The model predicted trend lines and the measured values are presented in Figures 24 and 25 to indicate further that the mathematical model can be used to estimate the response of split dams. A tendency for overprediction on the lower slopes can be attributed to the method of selecting the best model coefficients that gave more emphasis to the higher filling rates at the 25% slope. Another value that can be used to adjust the model is the effective height of sediment in the flow. Adjustment using this value would provide better comparisons for the lower slopes and indicate more about the controlling sediment transport processes.

INCREMENTAL HYDROGRAPH

As an application of the mach model and in an attempt to gain insight about dam functioning, the new ogee-shaped dam was subjected to

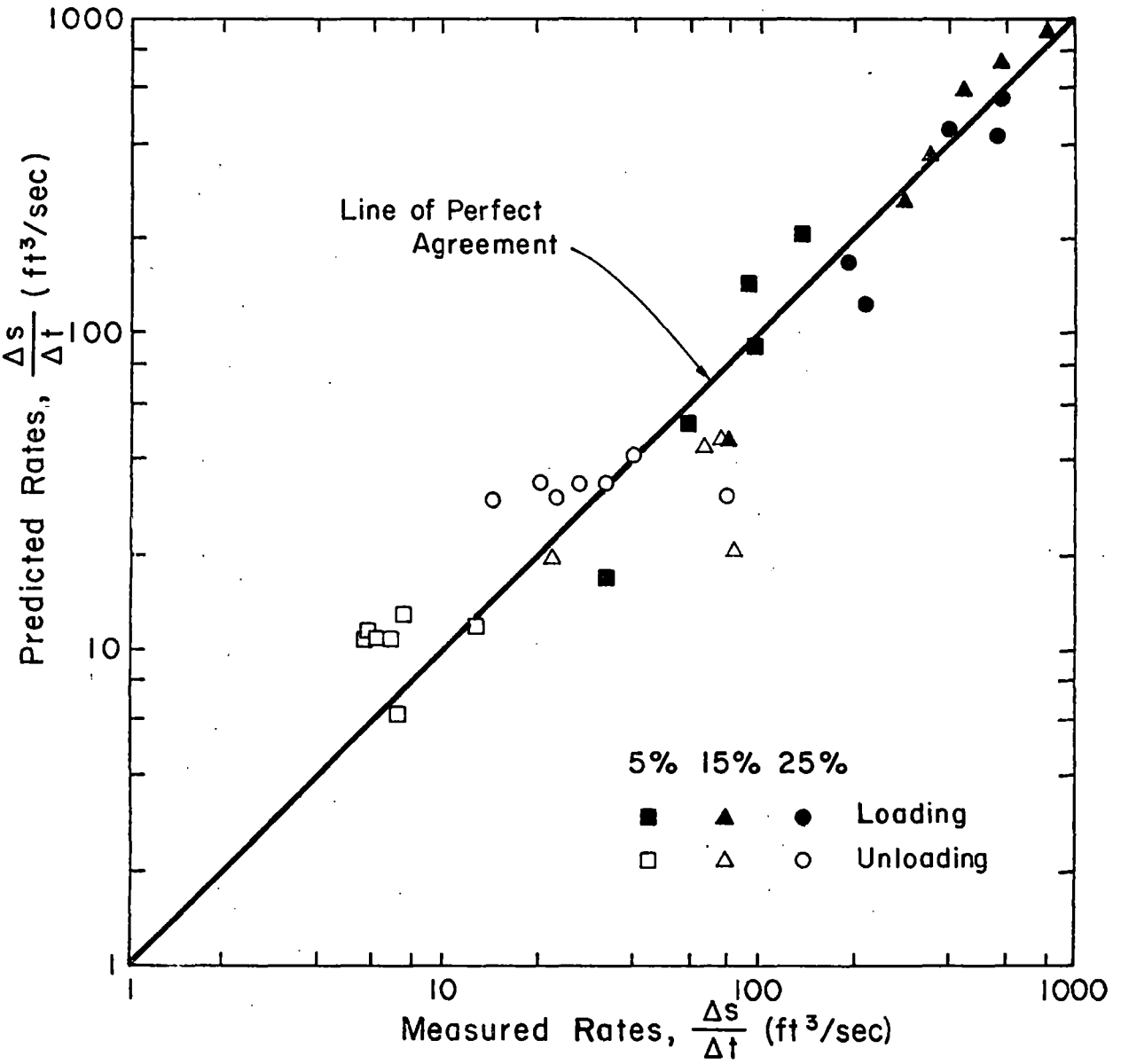

Figure 20. Comparison of measured and predicted loading and unloading rates $\Delta s/\Delta t$ for original ogee-shaped dam (prototype values).

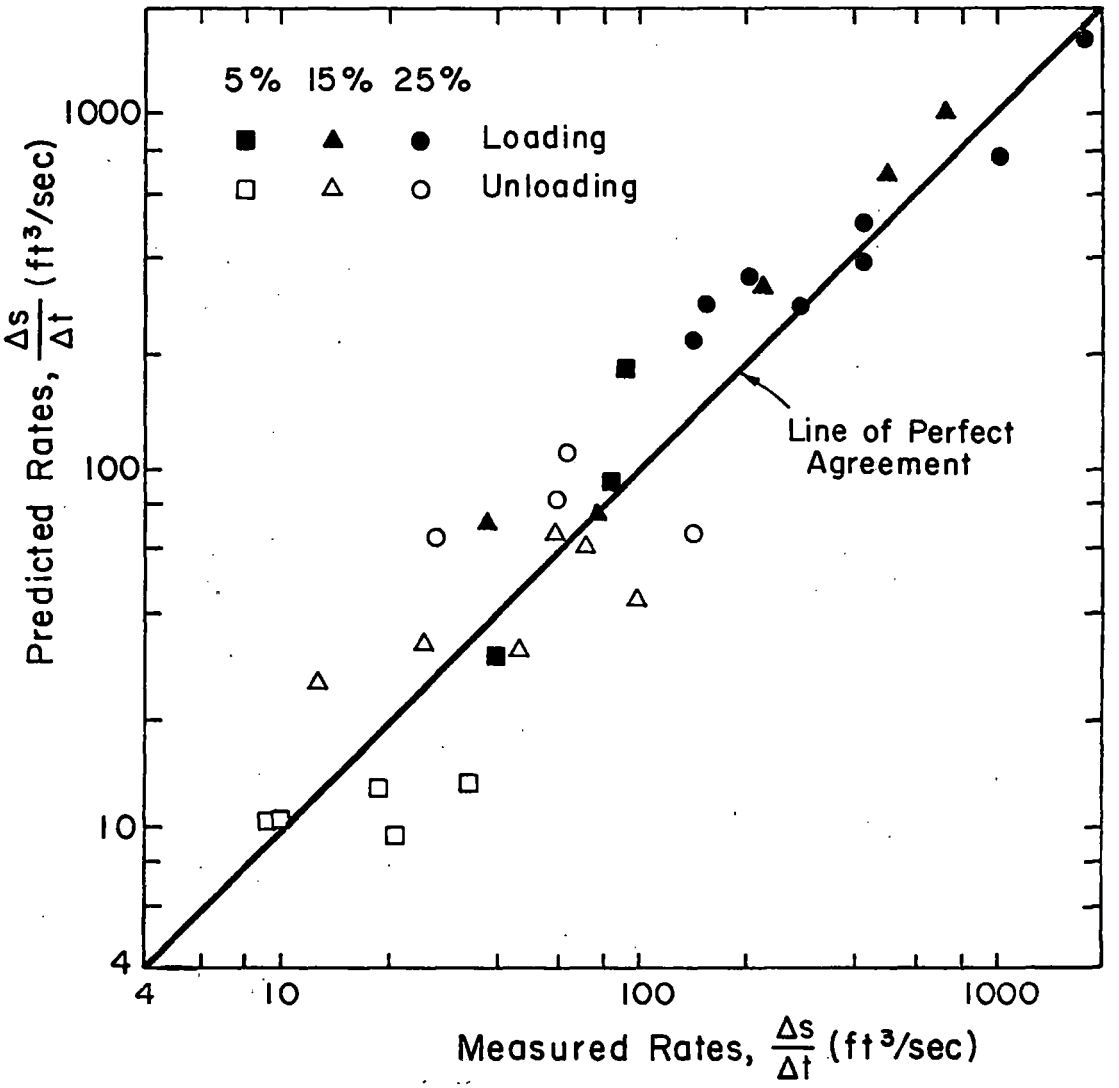

Figure 21. Comparison of measured and predicted loading and unloading rates $\Delta s/\Delta t$ for original rectangular-shaped dam (prototype values).

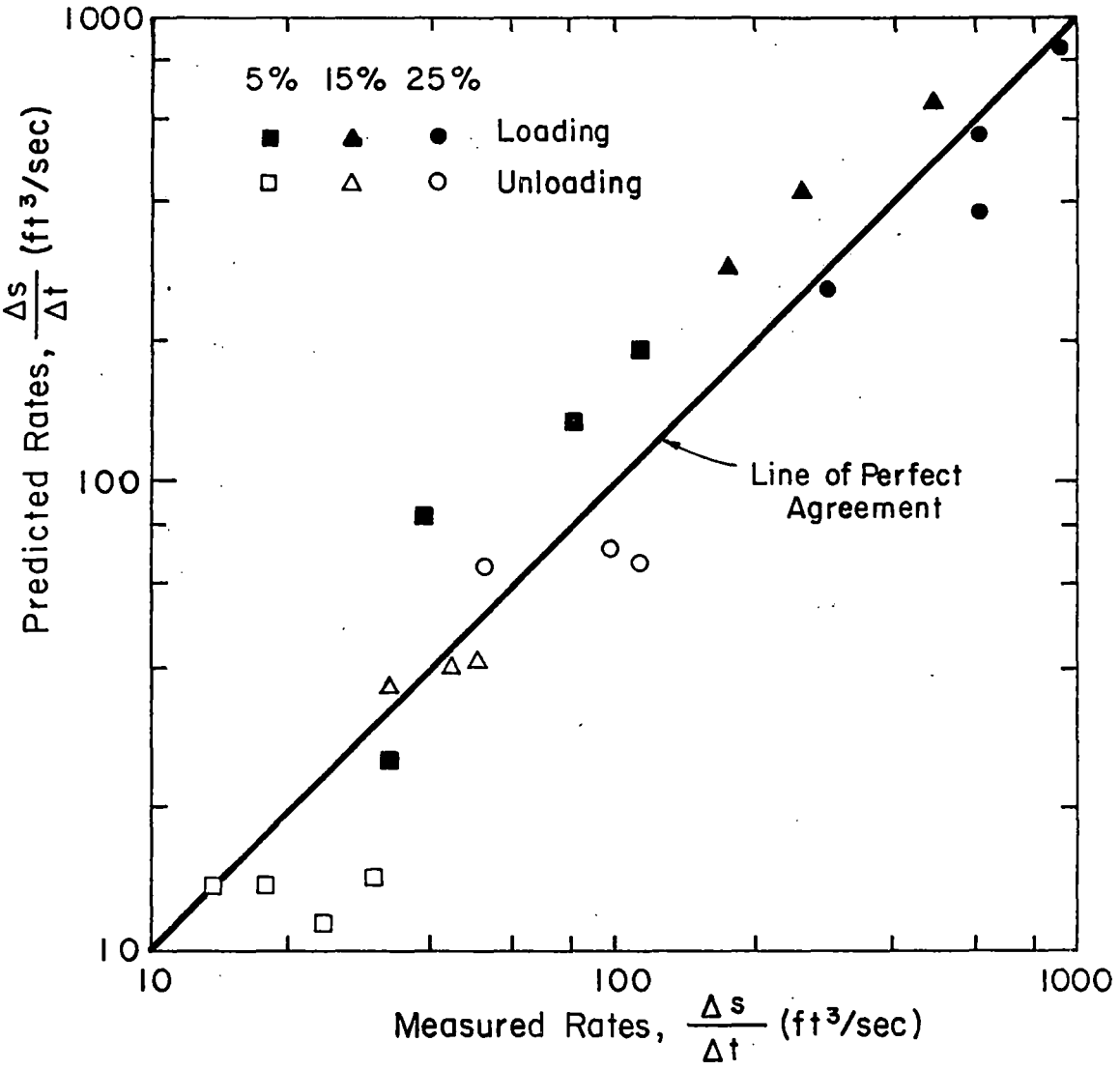

Figure 22. Comparison of measured and predicted loading and unloading rates $\Delta s/\Delta t$ for new ogee-shaped dam (prototype values).

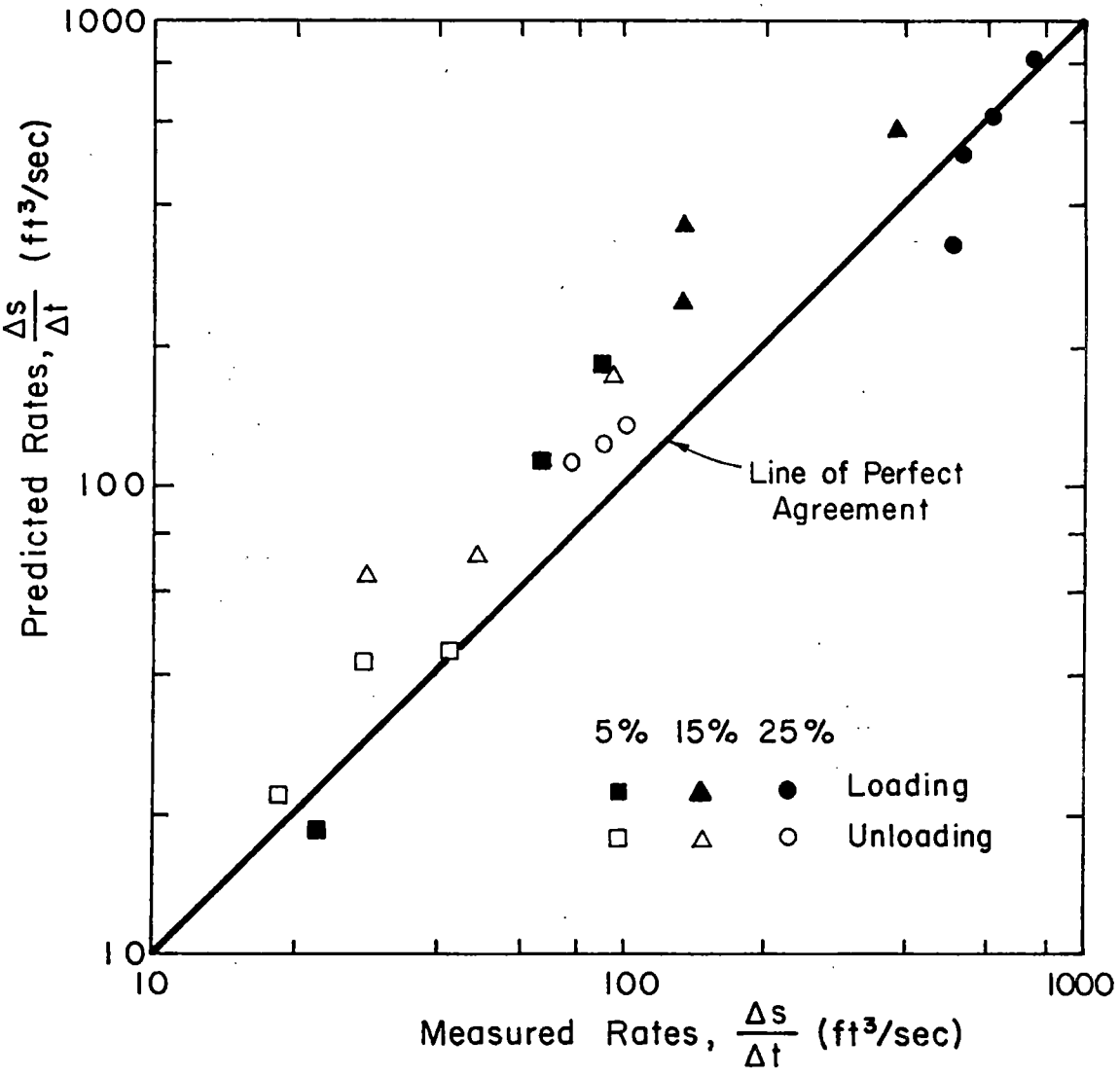

Figure 23. Comparison of measured and predicted loading and unloading rates $\Delta s/\Delta t$ for new rectangular-shaped dam (prototype values).

Table 10. Loading and unloading rates for new ogee and rectangular dams.

Number	Dam[1]	Type of Run[2]	Slope Percent	Q_{water} cfs	$\frac{\Delta s}{\Delta t}$ ft^3/sec
1	O	F	5	4293.59	110.64
2	O	S	5	4293.59	-31.77
3	O	S	5	2236.02	-14.01
4	O	F	5	2133.69	38.22
5	O	S	5	1051.07	-24.09
6	O	F	5	950.80	33.18
7	O	F	5	3145.13	81.36
8	O	S	5	3145.13	-18.26
9	R	F	5	899.45	22.66
10	R	S	5	899.45	-18.72
11	R	F	5	2870.44	67.62
12	R	S	5	2870.44	-28.16
13	R	F	5	4293.59	91.92
14	R	S	15	4293.59	-43.37
15	R	F	15	1606.60	394.16
16	R	S	15	1606.60	-95.43
17	R	F	15	1051.07	138.60
18	R	S	15	1051.07	-49.68
19	R	F	15	805.09	136.07
20	R	S	15	805.09	-28.71
21	O	F	15	856.42	173.89
22	O	S	15	856.42	-32.67
23	O	F	15	1134.07	254.12
24	O	S	15	1134.07	-44.09
25	O	F	15	1606.40	481.38
26	O	S	15	1606.40	-51.37
27	O	F	25	645.50	289.68
28	O	F	25	1007.37	607.36
29	O	S	25	1007.37	-110.72
30	O	F	25	780.12	603.94

Table 10 (continued)

Number	Dam[1]	Type of Run[2]	Slope Percent	Q_{water} cfs	$\frac{\Delta s}{\Delta t}$ ft^3/sec
31	O	S	25	780.12	-53.42
32	O	F	25	1353.81	919.46
33	O	S	25	1353.81	-98.13
34	R	F	25	1371.01	783.70
35	R	S	25	1371.01	-101.80
36	R	F	25	1000.19	541.25
37	R	S	25	1000.19	-92.43
38	R	F	25	792.55	503.28
39	R	S	25	792.55	-79.45
40	R	F	25	1118.70	601.28

[1] O = Ogee R = Rectangular

[2] F = Fill S = Scour

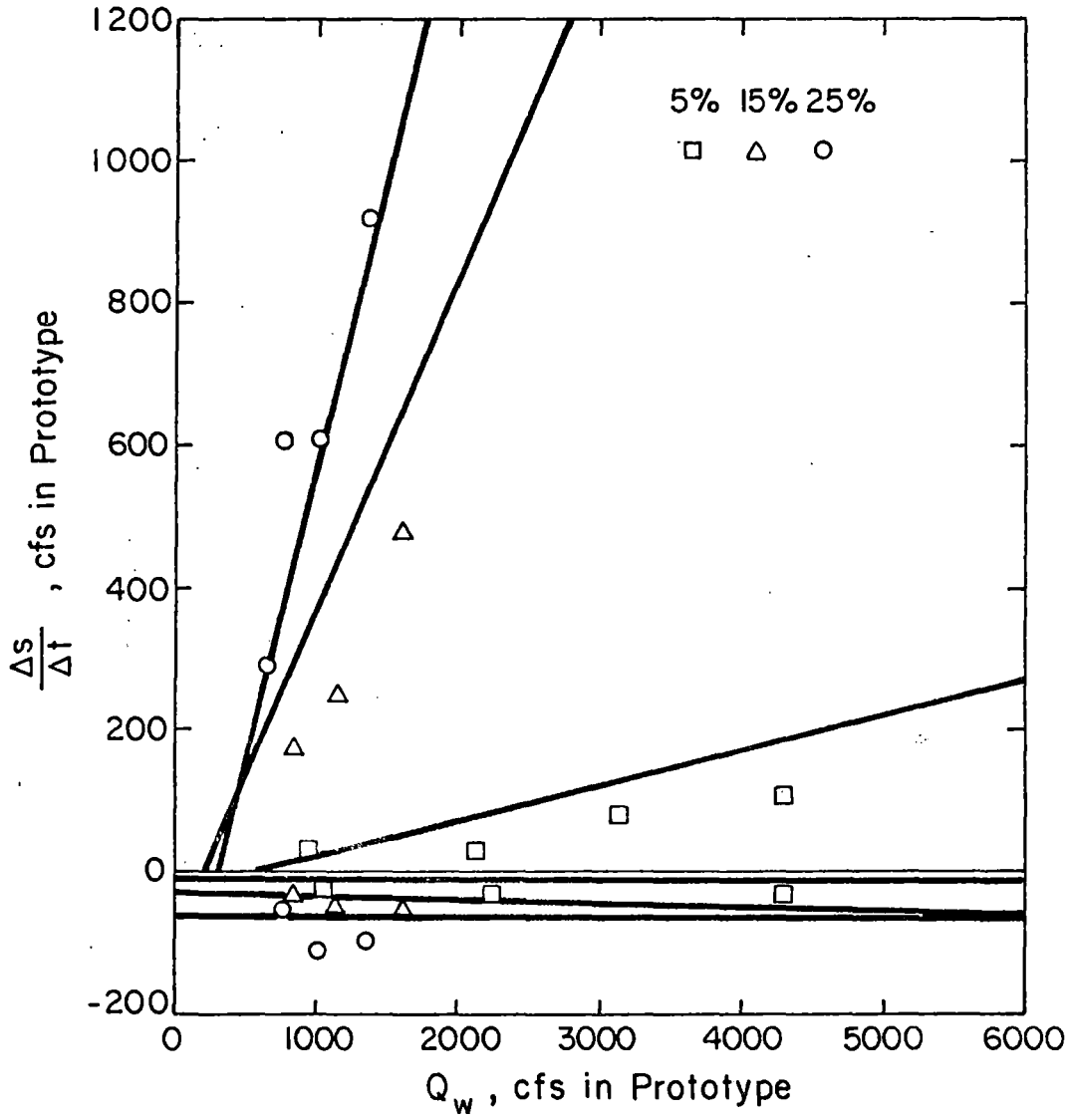

Figure 24. Measured filling and scouring rates (symbols) compared with predicted rates from mathematical model (solid lines) for new ogee-shaped dam (prototype values).

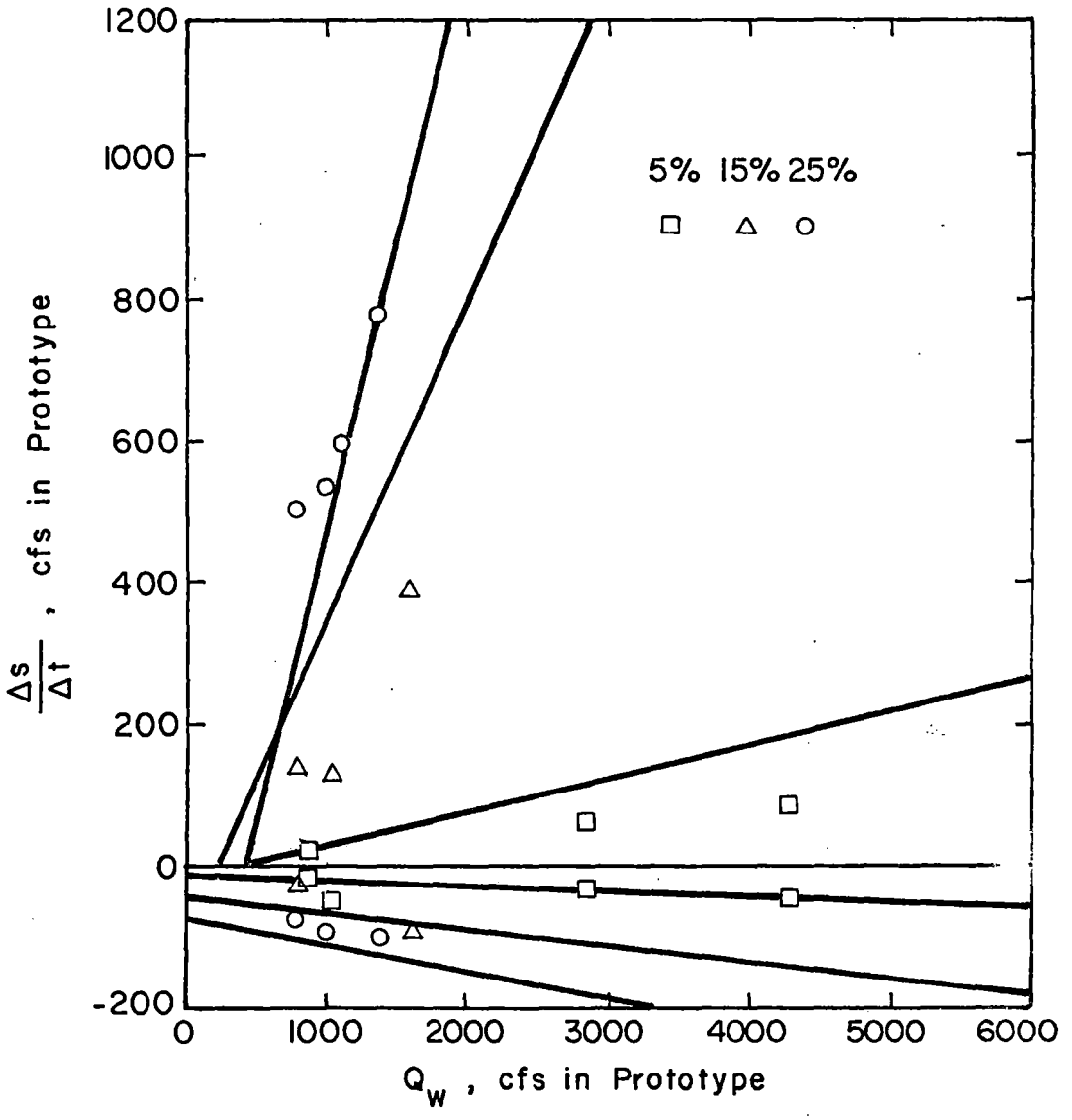

Figure 25. Measured filling and scouring rates (symbols) compared with predicted rates for mathematical model (solid lines) for new rectangular-shaped dam (prototype values).

a variable water discharge and variable sediment inflow rate hydrograph on the 15 percent slope. Three water discharges of 500, 1500, and 4400 cfs were used (Figure 26) (Plates 37, 38 and 39). The first part of the hydrograph was a loading sequence of 1500 cfs for five minutes (prototype) to approximately one-half sediment storage level, followed by 4400 cfs discharge for two minutes and thirty-five seconds (prototype) until the dam filled. A 100 percent sediment supply rate was used for both discharges. The second part was an unloading sequence of 4400 cfs at 10 percent sediment supply for five minutes (prototype), followed by a 1500 cfs discharge at 5 percent supply for 12.5 minutes (prototype), and finished by 500 cfs for 25 minutes (prototype) at no sediment supply.

Two runs were conducted. The first run was continuous discharge during the entire loading part, followed by sediment volume measurements, then continuous discharge during the entire unloading part, and measurements at the end of the run. Water discharge was varied by a butterfly valve on the water supply line and the sediment supply rate was varied by using the feeder belt attached to the supply hopper. The post-loading and post-unloading measurements were used for comparison with the mathematical model.

In the second test, an incremental run was conducted as a series of individual steps. Measurements were taken after each discharge-sediment supply step. Again this information was compared to model performance with results similar to the first run. The average volume of sediment at the end of the run was 12,700 cubic yards (prototype). The mathematical model was run in discrete steps of discharges for the same conditions to estimate the volume at the end of the run. The estimated volume from the mathematical model is 14,600 cubic yards. Although

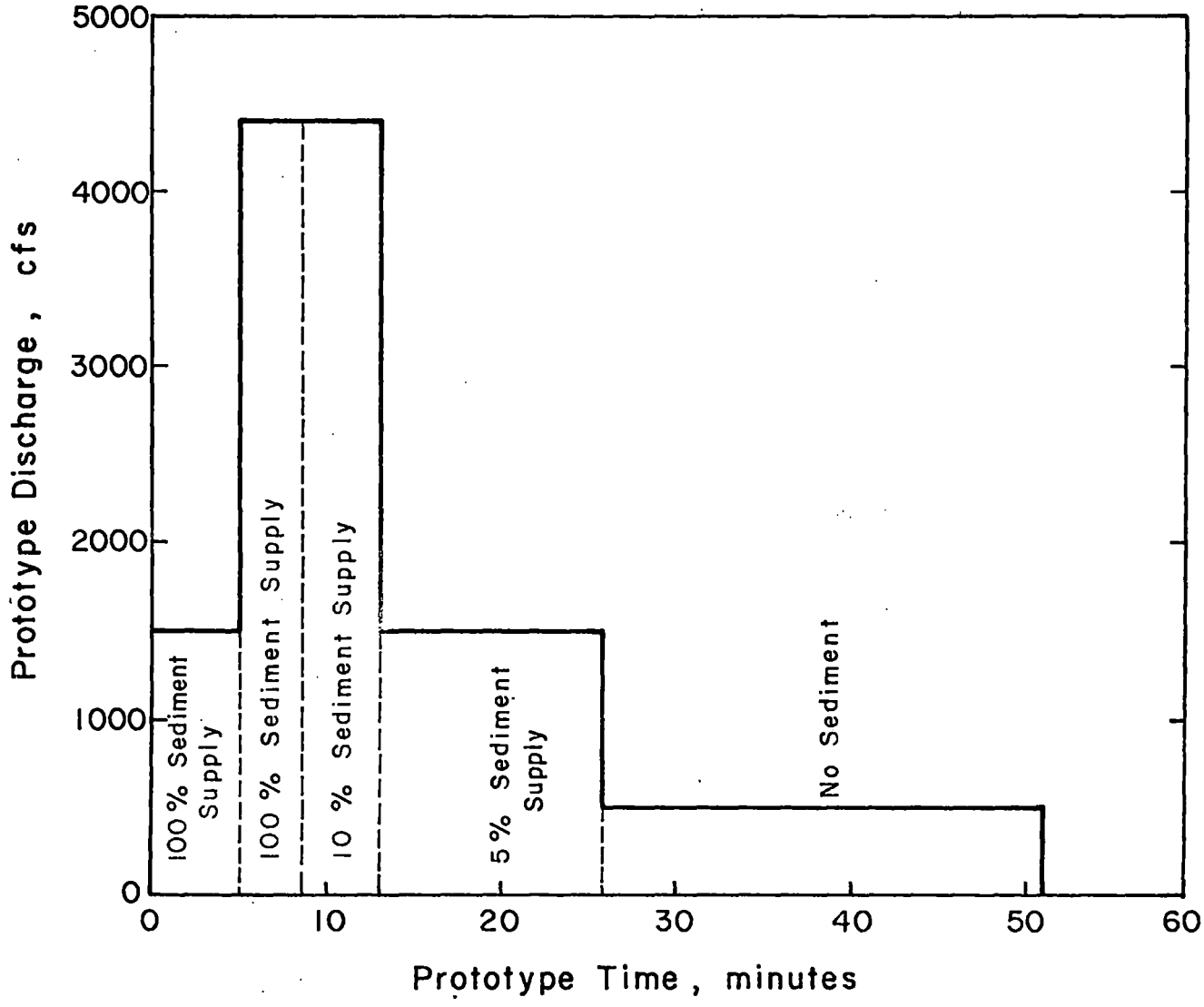

Figure 26. Prototype incremental hydrograph.

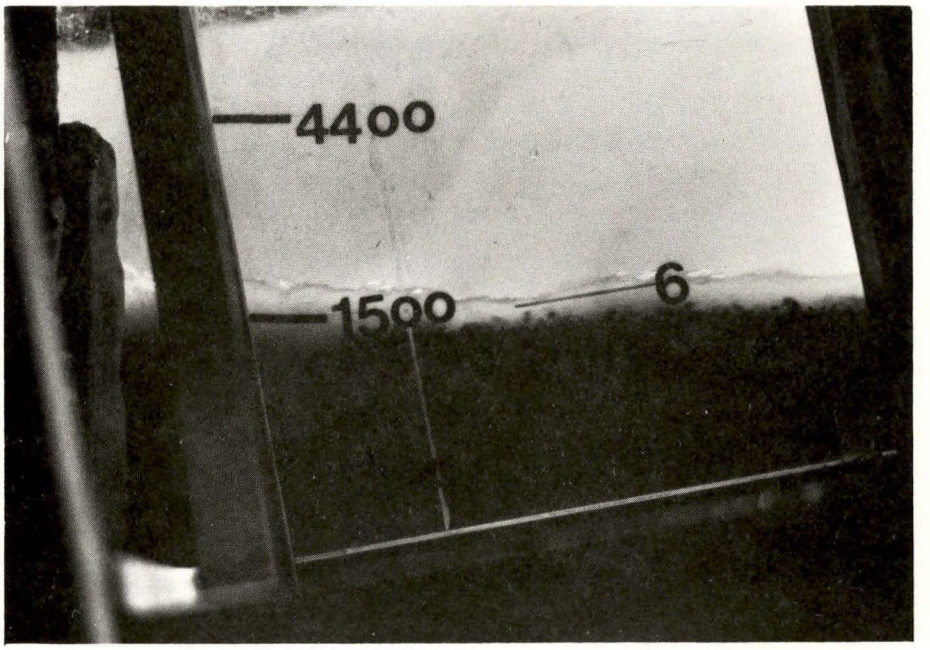

Plate 37. Incremental hydrograph run at 1500 cfs (prototype discharge). Sediment (black) layer under flowing water (gray) layer. (6 is six inch mark above bottom of flume).

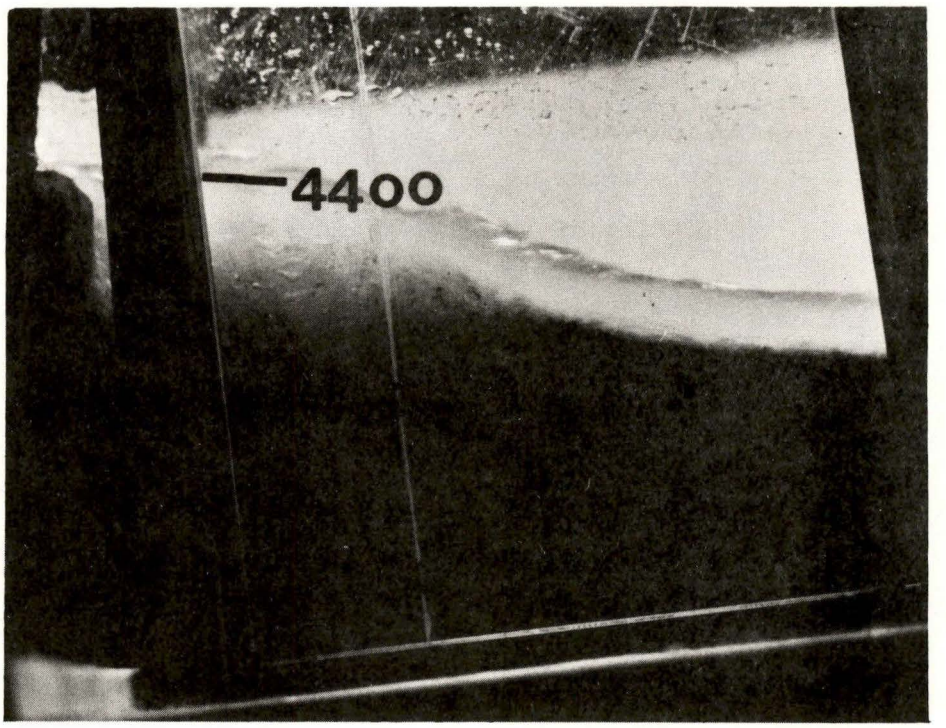

Plate 38. Incremental hydrograph run at 4400 cfs (prototype discharge).

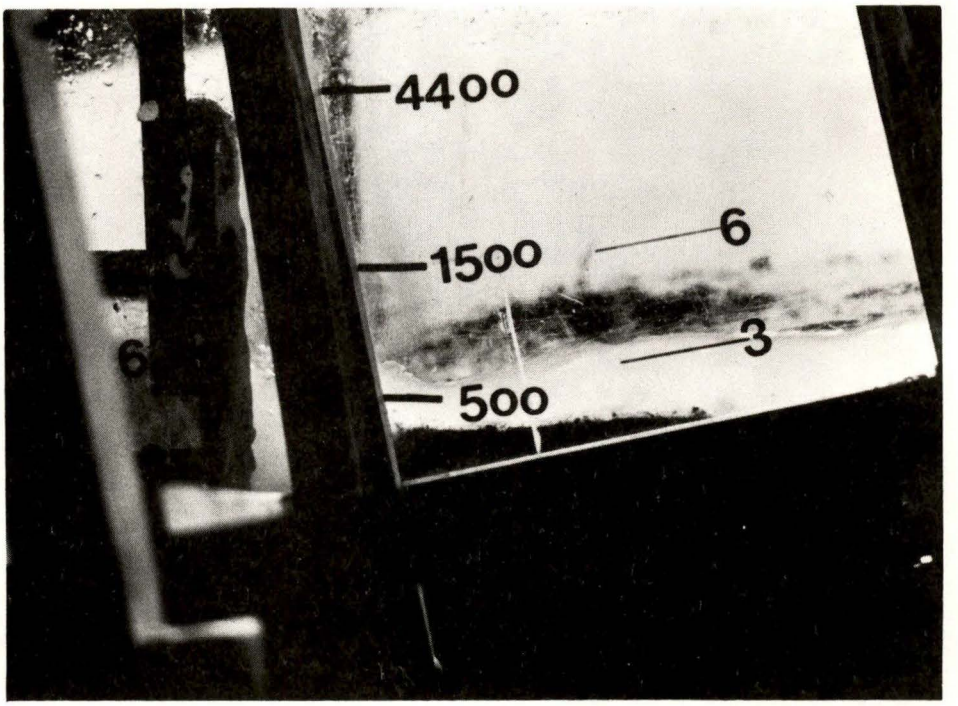

Plate 39. Incremental hydrograph run at 500 cfs (prototype discharge). (6 and 3 are six and three inch marks above bottom of flume).

almost identical, the difference between the physical model results and the mathematical model results may be caused by several factors. Important items that must be considered are the effects of stored sediment on outflow with partial sediment inflow supply, the effects of variable water and sediment discharge, or erroneous physical or mathematical model results. The physical and mathematical models do, however, show that a large amount of sediment will be left behind the dam after the assumed event (Plate 40).

Plate 40. Deposited sediment behind new ogee dam after an incremental hydrograph run for 15% channel slope. Note the steep gradient of remaining sediment deposit upstream (to the right) of the dam. Subsequent low frequency discharges will rapidly erode down into the sediment deposit because the downstream side of the deposit is so steep, thereby, facilitating self-cleaning of the dam.

V. SUMMARY AND CONCLUSIONS

Phase II experiments completed tests initiated in Phase I and several other new investigations. Results from experiments conducted in Phase I and Phase II indicate that split dams, particularly those with rectangular openings, are an efficient means for temporarily storing sediment in steep channels. However, vegetative debris can cause plugging that would prevent the split dam from functioning and must be considered in split dam design. Addition of trash racks to split dam facilities may somewhat alleviate this problem. Top-tie pile wall and catenary cable dams are not efficient at temporarily storing sediment. Top-tie pile wall dams fill rapidly and once full do not experience enough erosion to provide future sediment trapping capacity. Catenary cable dams that were tested did not produce flow conditions conducive to sediment transport from the dam for one design, and prevented adequate sediment deposition for the other design. Redesign and reevaluation of catenary cable dams may improve their effectiveness in efficiently controlling sediment movement. Use of existing hydrologic and hydraulic concepts for channel discharge, sediment transport, and flow through structural openings provided a mathematical model that was adapted to estimate split dam response for different designs when subjected to various water and sediment inflow conditions. The math model was verified for two new opening shapes by predicting dam response to selected conditions. Another application and test of the mathematical model was for estimation of stored sediment following a complex set of water and sediment discharge conditions. These results indicate that the mathematical model is a definite design aid, and also

points out which factors need further study. The hydraulic and mathematical model study has provided insights and increased understanding of steep channel hydraulics, the function of split dams, and directions for future research.

In addition to the general findings discussed above, there are some specific observations or results that should be listed or reiterated. These are:

1. This is one of the only, if not the only, set of experiments where sediment transport was measured and mathematically modeled for such steep bed slopes.
2. Measurement of sediment transport on high slopes is possible with a well organized data collection team and proper preparation of the sampling devices.
3. Bulking rates of sediment observed in the scale model are similar to those observed in the field.
4. Channel slope plays a significant role in sediment movement in the channel and through the dam.
5. Bed slopes created by deposition of sediment behind the dams affects local sediment transport rates and outflow rates through the dam.
6. Observations of downstream scour below the top-tie pile wall dam, depositional and erosional forms of the trapped sediments, armoring of the bed by larger particles, and creation of adverse or upstream facing bed slopes behind the dam were consistent with field experience.

7. Sediment transport through the dam is affected by opening shape and channel slope. The opening shape is related to the resistance to flow and the flow area at various water discharges.
8. Clogging of the split openings by debris is a function of the discharge and the probability that debris will become lodged in the opening thus catching more debris.
9. Mathematical modeling results were very close to measured values justifying use of the math model.

Other observations are presented in the body of this report.

VI. RECOMMENDATIONS FOR FUTURE WORK

The findings of this unique physical and mathematical model study have suggested several topics in need of further research. These topics include:

1. Expand the math model to include watershed characteristics in the formulation of split dam designs.
2. Improvement of split dam design to increase self cleaning efficiency and effective storage capacity.
3. Feasibility study using various structure designs and channel placements of structures for sorting transported sediments.
4. Response of the channel system to a series of structures placed at different locations. These structures may have alternating designs to affect storage efficiency.
5. Investigation and adaption of a methodology for estimating sediment movement following a dam failure.
6. Integration of watershed management concepts and control structure information for analyzing sediment movement in the entire watershed-channel system.
7. Investigate control strategies for avoiding negative effects of transported vegetative debris on split dams.
8. Further testing of split dam response to complex water and sediment inflow hydrographs.
9. Investigation of other split dam designs.
10. Presentation of a short course detailing the physical processes that govern functioning of debris dams and the planning necessary for devising an effective sediment control program utilizing these dams.

Of these ten possible study topics, the first three promise to provide the most immediate results.

VII. REFERENCES

Li, R. M., D. B. Simons, T. J. Ward, and K. S. Steele, 1977. Hydraulic Model Study of Flow Control Structures, Phase I Report, prepared for USDA Forest Service, Angeles National Forest and Rocky Mountain Forest and Range Experiment Station, Colorado State University CER77-78-RML-DBS-TJW-KSS15.

U.S. Bureau of Reclamation, 1960. Investigation of Meyer-Peter, Müller Bedload Formulas, Sedimentation Section, Hydrology Branch, Division of Project Investigations, U.S. Department of the Interior, Bureau of Reclamation.

APPENDIX A

FORMULATION OF THE MATHEMATICAL MODEL

The mathematical model describing the filling and scouring rates of sediment behind split opening check dams can be divided into four distinct parts. These are channel flow, channel sediment transport, flow through the split dam, and sediment transport through the dam. Formulations for each part are presented below.

Water flow in the stream channel was formulated using Manning's equation of

$$V = \frac{1.486}{n} R^{2/3} S^{1/2} \tag{A-1}$$

where V is average flow velocity, n is Manning's roughness number, R is hydraulic radius equal to $\frac{A}{P}$, A is flow area, P is wetted perimeter, and S is channel slope. If discharge Q is equal to flow area times average velocity, then equation A-1 can be rewritten as

$$Q = \frac{1.486}{n} R^{2/3} S^{1/2} A \tag{A-2}$$

For a wide rectangular channel (similar to those in this study) area can be expressed as

$$A = w \cdot d \tag{A-3}$$

and hydraulic radius as

$$R \tilde{\approx} d \tag{A-4}$$

where w is channel width. Substituting equations (A-3) and (A-4) into (A-2) and rearranging gives

$$\frac{Q}{w} = \frac{1.486}{n} d^{5/3} S^{1/2} \tag{A-5}$$

which can be used to compute the depth of flow as

$$d = \left(\frac{Q\, n}{1.486 w S^{\frac{1}{2}}} \right)^{0.6} \tag{A-6}$$

Therefore, Q, n, W, and S, known variables, can be used to solve for d.

Channel sediment transport is found from a form of the Meyer-Peter, Müller equation

$$q_s = a(\tau-\tau_c)^b \tag{A-7}$$

where q_s is sediment transport per unit of width, τ is the shear stress acting on a particle, τ_c is the critical shear necessary for particle movement and a and b are empirical constants. A value for b of 1.5 is used in this study, while the value of a is calibrated. Sediment transport is computed by sizes and the fraction of each size is accounted for in the total transport as

$$Q_s = w \sum_{i=1}^{N} q_{si} \, Pi \tag{A-8}$$

where Q_s is total transport rate, q_{si} is the transport rate for representative size i from equation (A-7) and Pi is the percent of representative size i. For example in the physical model, only about 10% of the sediment was of a size greater than approximately 8 mm. Therefore, the representative size for this upper 10 percent, which may be about 10 mm, must be multiplied by a factor of 0.10 to indicate the actual transport. In wide steep mountain channels, the shear stress acting on the bed is

$$\tau = \gamma \; d \; S \tag{A-9}$$

where τ is the shear stress, γ is the unit weight of water, d is depth of flow (replaces R for wide channels) and S is the channel slope. The value of S is the tangent of the channel inclination ψ. For small slopes

$$S = \tan \psi \tilde{\simeq} \text{Sine } \psi \tag{A-10}$$

For steep slopes where $\tan \psi \geq 0.25$ or $\psi \geq 14.04°$, the slope should be used as S = Sine ψ = 0.24.

This keeps approximation errors in (A-10) reasonable. The critical shear τ_c can be written as

$$\tau_c = 0.047 \ (\gamma_s - \gamma) \ D_s \qquad \text{(A-11)}$$

where γ_s is the unit weight of sediment and D_s is the particle size. For steep slopes τ is much greater than τ_c and equation (A-7) becomes

$$q_s \cong a \ \tau^b = a \ (\gamma dS)^b = K_1 d^b \qquad \text{(A-12)}$$

where K_1 is a product of variables for a particular flow. Equation (A-6) shows that

$$d = K_2 \ Q^{0.6} \qquad \text{(A-13)}$$

where K_w is another product of variables.

Substituting (A-13) into (A-12) yields

$$q_s = K_3 \ (Q^{0.6})^b \qquad \text{(A-14)}$$

if b is 1.5 or 3/2 then (A-14) becomes

$$q_s = K_3 \ Q^{0.9} \qquad \text{(A-15)}$$

where K_3 is a product of variables. The power on Q is approximately 1.0 as was found in the physical model tests. The theoretical results shown in equation (A-15) coupled with the physical model findings support the use of the Meyer-Peter, Müller form of the sediment transport relationships with the "a" coefficient equal to 16.05.

Water height at the dam was calculated from the discharge using a reformulation of the generalized weir equation given as

$$Q = C_d \sqrt{2g} \ \int_o^h (h-y) \ W(y) \ dy \qquad \text{(A-16)}$$

where C_d is a discharge coefficient, h is the height of water at the dam, W(y) is the opening width as a function of the flow depth y. The acceleration of gravity is included as g. This equation is solved for h at each section of the opening.

Each opening shape can be divided into three zones; a lower part below the narrower "slit," the slit portion, and the crest portion above the slit. Solutions to this equation for each zone require trial and error or convergence type algorithms and are not detailed in here. This height determination component of the model was calibrated for C_d using data from Group I runs. The calibrated C_d value for both original dams was 0.633.

Water height at the dam does not completely describe the physical processes controlling sediment transport through the dam. A better indicator is the effective height of sediment transport through the dam. This height is found from the depth and sediment concentration profile proposed by Rouse (1937) and represents the height below which most of the sediment is transported. It is this height which is used to compute hydraulic geometry at the opening. The concentration curve can be written as

$$\frac{C_{h_s}}{C_a'} = C_k = \left[\frac{h-h_s}{h_s}\,\frac{a'}{h-a'}\right]^{Z'} \qquad \text{(A-17)}$$

where C_{h_s} is the sediment concentration in the flow at height h_s above the bed, C_a' is the measured concentration at height a', a' is chosen as $2D_s$, C_k is a value based on the slope and was developed for this application, and Z' is a function of particle fall velocity and water discharge characteristics. The value of Z' can be computed from

$$Z' = \frac{w}{\beta\kappa U_*} \qquad \text{(A-18)}$$

where w is the fall velocity of the sediment particle, β relates the diffusion coefficient to the kinematic eddy viscosity for diffusion in turbulent flow, κ is von Karman's coefficient, and U_* is the shear

velocity (Simons and Sentürk, 1977). Fall velocity is determined by particle size and shape and water properties. Fall velocity of the median grain size is used in the model. The value of β is chosen as 1.0 and κ is 0.4. Shear velocity through the opening is computed as

$$U_* = \left(\frac{f_c}{8}\right)^{\frac{1}{2}} \bar{U} \tag{A-19}$$

where f_c is a resistance parameter for the opening, similar to a drag coefficient, and U is the average velocity through the opening based on water depth, discharge, and flow area. The average velocity is

$$\bar{U} = \frac{Q}{A} \tag{A-20}$$

where A is the flow area through the opening. The value of C_k is estimated as a function of slope and represents the ratio of concentration at height h_s to that at a'. On steep slopes this value will be larger than at low slopes because of changes in flow depth, velocity, and turbulence. For the model, C_k variation was selected by observation of model predictions and measured data. A reasonable variation is

$$C_k = 0.0011 + 0.0495\ (S-0.05) \tag{A-21}$$

or at a 5 percent slope $C_k = 0.0011$ and $C_k = 0.011$ at a 25 percent slope. The effective sediment height can be found from equation (A-17) as

$$h_s = \frac{h\ a'}{C_k^{1/Z'}\ (h-a') + a'} \tag{A-22}$$

Height h_s is then used to compute flow area, effective depth of flow, hydraulic radius, effective width of the opening, and the conveyance.

Sediment outflow from the dam was computed as the difference between the sediment inflow rate and change in storage. These outflow

rates were regressed against the calculated hydraulic parameters to yield nonlinear equations of the form

$$Q_{so} = a_1(W_e)^{a_2} (K_o)^{a_3} (S)^{a_4} \quad \text{(A-23)}$$

where Q_{so} is the sediment outflow rate, W_e is the effective width, K_o is a conveyance, S is channel slope, and a_1, a_2, a_3 and a_4 are regression parameters. Because of the different characteristics of filling and scouring outflow rates, two equations were developed; one for each type of outflow. In general, sediment outflow during filling was higher than during scour because sediment was already moving within the flow, the gradient of stored sediment was steeper, and flow did not channelize the stored sediment as occurred during scouring experiments. The regression parameters of a_1, a_2, a_3, and a_4 for the filling experiment outflows were computed as 145098.78, 0.322, 0.076, and 1.826. For the scouring outflows, these parameters were 1458.76, 1.073, 0.226, and 1.179. The model was calibrated for f_c using the correlation coefficients from these two regressions. The best value of f_c was selected as 0.6 for the original dams.

The math model computes filling and scouring rates for a selected split dam configuration as the difference between sediment inflow and outflow. Inflow is computed from discharge characteristics, channel geometry, and the sediment size distribution. Outflow is computed as a function of sediment size, hydraulic variables of the opening, and slope. Comparison of measured and predicted sediment filling rates for the ogee and rectangular dams indicate that even with the variability in the system being analyzed, results are quite good.

Two parameters were recognized as being important in model adjustment. One value was the discharge coefficient. As the opening gets

larger the discharge coefficient should increase to reflect lower losses through the opening. Similarly, the resistance coefficient f_c should decrease. Calibration of the model to measured data for the new dams showed this was the case as C_d became 0.88 and f_c was computed as 0.27. It is believed that both parameters are related to flow area through the opening and opening shape. However, this observation cannot be substantiated because of lack of comparable information for these types of dams. It is also believed that the model can give even better results if the C_k value in equation (A-21) is adjusted.

REFERENCES FOR APPENDIX A

Rouse, H., 1937. Modern Conceptions of the Mechanics of Turbulence, Transactions, ASCE, Vol. 102.

Simons, D. B. and F. Sentürk, 1977. Sediment Transport Technology, Water Resource Publications, Fort Collins, Colorado.

APPENDIX B

LISTING OF THE SPLIT DAM MATHEMATICAL MODEL

The following is a computer listing of the split dam interactive mathematical model. The model is constructed in a modular form so that each process is separated from the others for ease of isolation, checking, and changing if necessary. The interactive model is designed to allow user input of split opening dimensions, ten water discharge values, initial channel slope, and Manning's n for the channel. Grain size distribution, discharge coefficient, and resistance parameter must be included in the program before operation. Manning's n was included as input even though it is reset in the program in order to provide a useable feature at a later date. Filling and scouring rates are computed for each of the ten discharges for three slopes, original input slope, input slope plus 0.1, and input slope plus 0.2. Input information is listed by the program. A sample input output sequence follows the listing. Note that in some low flow cases the fill rate is negative. This occurs because the fill rate is the difference between sediment inflow and outflow rates and the outflow rate determination may be higher at low flows. Observations of the physical model indicate that at low flows there is a possibility of scour from the concentration of the low channel flows through the split opening. Therefore negative fill rates are reasonable at low flows.

Listing of Program SFMOD:

```
      PROGRAM SFMOD(INPUT,OUTPUT)
      COMMON/ABC/A,B,C,D,E,F,G,W,Z
      DIMENSION DS(10),P(10),Q(10)
C
C   SFMOD IS DESIGNED TO SIMULATE THE HYDRAULIC CHARACTERISTICS
C   OF STEEP CHANNEL CONTROL STRUCTURES.  IN SEPARATE SUBROUTINES
C   AND FUNCTIONS, THE MODEL COMPUTES FLOW DEPTH,
C   SEDIMENT TRANSPORT, HEIGHT OF FLOW ON THE STRUCTURE, AND
C   THE SEDIMENT OUTFLOW THROUGH THE STRUCTURE.
C   THE MAIN PROGRAM  COMPUTES THE CHANGE IN THE SEDIMENT
C   VOLUME BEHIND THE BACKWATER OF THE CHECK DAM
C   FOR EITHER FILL OR SCOUR TYPE RUNS.
C
C   IN RUNNING THE MODEL IT IS NECESSARY TO INPUT THE PROTOTYPE
C   STRUCTURE DIMENSIONS, THE SEDIMENT SIZE GRADATION, MANNING@S
C   N, CHANNEL SLOPE, AND HYDROGRAPH DISCHARGE VALUES.
C
C   DIMENSION A IS HEIGHT OF THE LOWER OPENING
C   DIMENSION B IS HEIGHT OF THE SLIT
C   DIMENSION C IS HEIGHT OF THE WEIR SECTION
C   DIMENSION D IS WIDTH OF THE LOWER OPENING
C   DIMENSION E IS WIDTH OF THE SLIT
C   DIMENSION F IS WIDTH OF THE WEIR AT THE BOTTOM
C   DIMENSION G IS WIDTH OF THE WEIR AT THE TOP
C   DIMENSION W IS WIDTH OF THE CHANNEL OR DAM
C   DIMENSION Z IS HEIGHT OF THE DAM
C
C   CALIBRATED COEFFICIENTS USED IN THE MODEL ARE THE
C   SEDIMENT RESISTANCE AND TRANSPORT COEFFICIENTS, FC AND
C   CSED, RESPECTIVELY, AND THE CONTROL STRUCTURE
C   DISCHARGE COEFFICIENT, CDIS.
C
C   STATEMENTS TO INPUT CONTROL STRUCTURE SHAPE
C   AND HYDROGRAPH DISCHARGES
C
      PRINT 100
  100 FORMAT (5X,*INPUT VALUES TO DEFINE THE CONTROL STRUCTURE SHAPE*,
     C   /,5X,* A,B,C,D,E,F,G,W,Z*)
      READ*,A,B,C,D,E,F,G,W,Z
      PRINT 110
  110 FORMAT (/,5X,*INPUT TEN  VALUES FOR DISCHARGE,Q*,/,5X,
     C   *NOTE: THERE MUST BE EXACILY 10 VALUES*)
      READ *, (Q(I),I=1,10)
C
C   SEDIMENT SIZE GRADATION INPUT CHANGE AS NECESSARY
C   DS IN MILLIMETERS
C   P IN DECIMAL FRACTION
C
      DATA DS/2.75,7.00,11.00,16.50,23.25,32.00,45.50,
     C   70.25,123.75,401.75/
      DATA P/.1,.1,.1,.1,.1,.1,.1,.1,.1,.1/
C
C   INPUT STATEMENTS FOR SLOPE AND MANNING@S N
C
      PRINT 120
  120 FORMAT(/,5X,*INPUT VALUES FOR SLOPE,S, AND*,/,
     C   5X,*MANNINGS N,XN*)
      READ *, S,XN
      PRINT 130, A,B,C,D,E,F,G,W,Z
  130 FORMAT(///,20X,*STRUCTURE DIMENSIONS:  A,B,C,D,E,F,G,W,Z*,
     C   /,5X,9F8.1,/)
C
C   DO LOOP EXECUTES 3 TIMES INCREASING
C   SLOPE EACH TIME BY 10%.
C
```

Listing of Program SFMOD (continued):

```
      DO 300 K=1,3
      IF(S.LT.0.03) GO TO 250
      CK = 0.0011 + 0.0495 * (S - 0.05)
C
C     STATEMENTS FOR OUTPUT AND HEADING
C
      PRINT 140, S,CK
  140 FORMAT(/,20X,*SLOPE = *,F7.3,7X,*CK = *,F8.4)
      PRINT 150
  150 FORMAT(/,5X,*Q*,7X,*Y*,5X,*H*,5X,*CON*,12X,*QSI*,11X,
     C   *FILL*,10X,*SCOUR*,11X,*HSED*,/)
C
C     CALIBRATED PARAMETERS FOR SEDIMENT DISCHARGE,
C     DISCHARGE COEFFICIENT, AND RESISTANCE, RESPECTIVELY
      CDSED = 16.05
      CDIS = 0.880
      FC = 0.27
C
      DO 200 I=1,10
C
C     COMPUTING CHANNEL DEPTH
C
      Y=0.0
      XN = 0.07
      IF(S.EQ.0.05) XN = 0.025
      QN = Q(I)
      CALL DEPTH(QN,S,W,XN,Y)
C
C     COMPUTING THEORETICAL SEDIMENT TRANSPORT
C
      VAVG = 10.0
      NSED = 10
      QSI=0.0
      CALL MPM(S,Y,CSED,NSED,DS,P,QSI)
      QSI = QSI * W
C
C     COMPUTING THE HEIGHT OF FLOW AT THE CONTROL STRUCTURE
C
      H=10.
      CALL HEIGHT(QN,H,CDIS,VAVG)
C
C     COMPUTING THE SEDIMENT TRANSPORT CARRIED THROUGH THE STRUCTURE
C
      CON=25.0 $ EFW=10.0
      QSOF=100.0 $ QSOS=100.0
      HS = 5.0
      CALL SEDOUT (QN,H,QSOF,QSOS,CDIS,S,CON,EFW,Y,CK,HS,VAVG,FC)
C
C     COMPUTING THE SEDIMENT TRANSPORT FILL AND SCOUR RATES
C
      DSDTF = QSI-QSOF
      DSDTS = -QSOS
      QSI = QSI / (2.65*62.4*.56)
      DSDTF = DSDTF / (2.65*62.4*.56)
      DSDTS = DSDTS / (2.65*62.4*.56)
      PRINT 160, QN,Y,H,CON,QSI,DSDTF,DSDTS,HS
  160 FORMAT(F8.2,3F7.2,6F15.3)
  200 CONTINUE
  250 S = S + 0.10
  300 CONTINUE
      STOP
      END
C
C     *****     *****     *****     *****     END MAIN PROGRAM
C
```

Listing of Program SFMOD (continued):

```
      SUBROUTINE DEPTH(Q,S,W,XN,Y)
C
C    SUBROUTINE COMPUTES THE CHANNEL DEPTH USING
C    THE MANNINGS EQUATION AND MANNINGS N VALUES
C    OF 0.025 FOR 5% SLOPE AND 0.07 FOR GREATER
C    CHANNEL SLOPES.
C
      Y=((Q*XN)/(1.486*W*S**0.5))**0.6
      RETURN
      END
C
C    *****     *****     *****     ***.**     END DEPTH
C
```

Listing of Program SFMOD (continued):

```
      SUBROUTINE MPM(S,Y,CSED,NSED,DS,P,QSI)
C
C   SUBROUTINE COMPUTES THE CHANNEL TRANSPORT
C   UTILIZING MEYER-PETER,MULLER THEORY
C   AND CALIBRATED EQUATIONS.
C
      DIMENSION DS(10),P(10)
      TAU=62.4*Y*S
      DO 400 I=1,NSED
      TAUC=0.05*(165.36-62.4)*DS(I)/304.8
      IF(TAU.LE.TAUC) GO TO 400
      QS=CSED*(TAU-TAUC)**1.5
      QSI=QSI+QS*P(I)
  400 CONTINUE
      RETURN
      END
C
C   *****     *****     *****     **.**     END MPM
C
```

Listing of Program SFMOD (continued):

```
      SUBROUTINE HEIGHT (Q,H,CDIS,VAVG)
C
C   SUBROUTINE EQUATES THE HEIGHT ON THE CONTROL
C   STRUCTURE TO THE DISCHARGE FROM CALIBRATED ORIFICE
C   EQUATIONS FOR EACH SECTION OF THE CHECK DAM
C
      COMMON/ABC/A,B,C,D,E,F,G,W,Z
      REAL K1,K2,K5,KW
      GR =32.2
C
C   STATEMENTS TO FIND HEIGHT OF FLOW
C   BELOW THE CONTROL STRUCTURE SLIT
C
      K1=2./3.*CDIS*(2.*GR)**0.5*D
      K2=K1*E/D
      KW=(2.*GR)**0.5*(F+G)/3.
      HP1=A**1.5-Q/K1
      IF(HP1.LE.0.) GO TO 510
      H1=A - HP1**.6667
      H=H1
      AREA = D*H
      GO TO 550
C
C   WITHIN THE SLIT SECTION
C
  510 Q1=A**1.5*K1
      Q=Q - Q1
      HP2=B**1.5-Q/K2
      IF (HP2.LE.0.) GO TO 520
      H2=A+B-HP2**.6667
      H=H2
      Q=Q+Q1
      AREA = D*A + (H-A)*E
      GO TO 550
C
C   WITHIN THE WEIR SECTION
C
  520 Q2=B**1.5*K2
      Q=Q - Q2
      Q3=C**1.5*KW
      QCHECK=Q-Q3
      IF(QCHECK.GT.0.0) GO TO 530
      HP3=H3(Q)
      H=HP3
      Q=Q+Q1+Q2
      AREA = D*A + E*B + (H-A-B)*(F + 0.5*(H-A-B))
      GO TO 550
C
C   ABOVE THE WEIR SECTION
C
  530 Q=Q - Q3
      K5=(2.*GR)**0.5*W*2./3.
      H4=Z + (Q/K5)**.6667
      H=H4
      Q=Q+Q1+Q2+Q3
      AREA = D*A + E*B  + C*0.5*(F+G) +(H-Z)*W
  550 CONTINUE
      VAVG = Q/AREA
      RETURN
      END
C
C   *****     *****     *****     **.**     END HEIGHT
C
```

Listing of Program SFMOD (continued):

```
      FUNCTION H3(Q)
      COMMON/ABC/A,B,C,D,E,F,G,W,Z
      REAL K3,K4
C
C     FUNCTION COMPUTES THE DISCHARGE- HEIGHT FOR
C     THE TRAPEZOIDAL WEIR SECTION OF THE DAM
C
      GR=32.2
      K3=(2.*GR)**0.5
      K4=K3*F*2./3.
      CONST1=2.*K3/15.*(2.*(A+B+C)+3.*(A+B))
      CONST2=2.*K3/15.* 2.*(A+B+C)+ K4
      ICOUNT=0
      H3=21.
  600 CHECK=(A+B+C)-H3
      IF(CHECK.LE.0.0) H3=A+B+C
      IF(CHECK.LE.0.0) GO TO 650
      FUN=Q-C**1.5*(CONST1+K4)+CONST2*((A+B+C)-H3)**1.5
     C  +2.*K3*H3/5.*((A+B+C)-H3)**1.5
      IF(ABS(FUN).LT..001) GO TO 650
      FP=-3./2.*CONST2*((A+B+C)-H3)**.5-3./5.*K3*H3*
     C  ((A+B+C)-H3)**.5+((A+B+C)-H3)**1.5*(2.*K3/5.)
      ICOUNT=ICOUNT+1
      IF (ICOUNT.GE.10) GO TO 650
      HN3=H3-FUN/FP
      H3=HN3
      GO TO 600
  650 CONTINUE
      RETURN
      END

C
C    *****      *****      *****      **.**      END WEIR FUNCTION
C
```

Listing of Program SFMOD (continued):

```
      SUBROUTINE SEDOUT (Q,H,QSOF,QSOS,CDIS,S,CON,EFW,Y,CK,HS,VAVG,FC)
C
C   THE SEDOUT SUBROUTINE COMPUTES THE VOLUME OF SEDIMENT
C   TRANSPORTED THROUGH THE STRUCTURE USING THE HYDRAULIC
C   PARAMETERS OF EFFECTIVE SEDIMENT TRANSPORT HEIGHT AND
C   CONVEYANCE OF THE CONTROL STRUCTURE OPENING
C
      COMMON/ABC/A,B,C,D,E,F,G,W,Z
      HS = HSED(S,H,Y,CK,VAVG,FC)
      IF(HS.GT.A) GO TO 710
C
C   FOR HEIGHT OF FLOWS WITHIN THE BOTTOM SECTION
C   OF THE CONTROL STRUCTURE THE FOLLOWING EQUATIONS APPLY
C
      AREA  = HS*D
      WP  = 2.*HS + D
      EFD = HS
      GO TO 740
  710 IF (HS.GT.(A+B)) GO TO 720
C
C   FOR HEIGHT OF FLOWS WITHIN THE SLIT SECTION OF THE
C   STRUCTURE THE FOLLOWING EQUATIONS APPLY
C
      W1 = W3 = (D-E)/2.
      W2 = E
      WP1 = WP3 = A + D - E
      WP2 = 2.*(HS-A) + W2
      WP = WP1 + WP2 + WP3
      A1 = A3 = W1*A
      A2 = HS*W2
      AREA = A1 + A2 + A3
      R1 = A1/WP1
      R2 = A2/W2
      R3 = R1
      EFD = (2.*(HS-A/2.)*W1*R1**.6667 + HS/2.*W2*R2**.6667) /
     C    (W1*R1**.6667 + W2*R2**.6667 + W3*R3**.6667)
      GO TO 740
  720 IF (HS.GT.Z) GO TO 730
C
C   FOR HEIGHT OF FLOWS WITHIN THE WEIR SECTION
C   OF THE STRUCTURE THE FOLLOWING EQUATIONS APPLY
C
      W1 = W3 = (D-E)/2.
      W2 = E
      W4 = F + 0.5*(HS-A-B)
      A1 = A3 = W1*A
      A2 = (A+B)*W2
      A4 = (HS-A-B)*W4
      AREA = A1 + A2 + A3 + A4
      WP1 = WP3 = A + D - E
      WP2 = 2.*B + E
      WP4 = F - E + (HS-A-B)*SQRT(5.0)
      WP = WP1 + WP2 + WP3 + WP4
      R1 = A1 / WP1
      R2 = A2 / WP2
      R3 = A3 / WP3
      R4 = A4 / WP4
      EFD = (2.*(HS-A/2.)*W1*R1**.6667 + (HS-(A+B)/2.)*W2*R2**.6667 +
     C     .5*(HS-A-B)*W4*R4**.6667) / (W1*R1**.6667 + W2*R2**.6667 +
     C     W3*R3**.6667 + W4*R4**.6667)
      GO TO 740
C
C   FOR HEIGHT OF FLOWS OVER THE TOP OF
C   THE CONTROL STRUCTURE THE FOLLOWING
C   EQUATIONS APPLY
C
```

Listing of Program SFMOD (continued):

```
      GO TO 740
C
C   FOR HEIGHT OF FLOWS OVER THE TOP OF
C   THE CONTROL STRUCTURE THE FOLLOWING
C   EQUATIONS APPLY
C
  730 W1 = W3 = (D-E)/2.
      W2 = E
      W4 = (F+G)*0.5
      W5 = W
      A1 = A3 = W1*A
      A2 = (A+B)*W2
      A4 = C*W4
      A5 = W*(HS-Z)
      AREA = A1 + A2 + A3 + A4 + A5
      WP1 = WP3 = A + D - E
      WP2 = 2.*B + E
      WP4 = C*SQRT(5.0) + F - E
      WP5 = 2.*(HS-Z) + W - G
      WP = WP1 + WP2 + WP3 + WP4 + Wp5
      R1 = A1 / WP1
      R2 = A2 / WP2
      R3 = A3 / WP3
      R4 = A4 / WP4
      R5 = A5 / WP5
      EFD = (2.*(HS- A/2.)*W1*R1**.6667 + (HS-(A+B)/2.)*W2*R2**.6667 +
     C     (HS-(A+B)-C/2.)*W4*R4**.6667 + ((HS-Z)/2.)*W5*R5**.6667) /
     C     (W1*R1**.6667 + W2*R2**.6667 + W3*R3**.6667 +
     C     W4*R4**.6667 + W5*R5**.6667)
  740 R = AREA / WP
      EFW = AREA / EFD
      CON=AREA*R**.6667
C
C  SEDIMENT OUTFLOW EQUATIONS FOR SPLIT OPENING
C
      QSOF = 145098.78 * EFW**(0.32193) * CON**(0.07561) * S**(1.82643)
      QSOS =   1458.76 * EFW**(1.07288) * CON**(0.22632) * S**(1.17933)
      RETURN
      END
C
C   *****     *****     *****     **.**     END SEDOUT
C
```

Listing of Program SFMOD (continued):

```
      FUNCTION HSED(S,H,Y,CK,VAVG,FC)
C
C   FUNCTION COMPUTES THE EFFECTIVE HEIGHT OF FLOW
C   FOR A GIVEN SEDIMENT CONCENTRATION
C
      GR = 32.2
      USTAR = ((FC/8.)**0.5) * VAVG
      AP = 0.18
      C2 = AP /(H-AP)
      VS = 1.80
      WEX = VS /(0.4*USTAR)
      EXP = 1.0 / WEX
      C1 = CK**EXP / C2
      HSED = H / (C1 + 1.0)
      END
C
C   *****     *****     *****     *****     END SED FUNCTION
```

Input Output Sequence Sample:

```
     INPUT VALUES FOR A,B,C,D,E,F,G,W,Z
? 14,7,4,8,6,42,46,96,25

     INPUT VALUES FOR Q
     NOTE: THERE MUST BE EXACTLY 10 VALUES
? 100,200,500,1000,1500,2000,2500,3000,3500,4000

     INPUT VALUES FOR SLOPE,S, AND
     MANNINGS N,XN
? .05,.025
```

STRUCTURE DIMENSIONS: A,B,C,D,E,F,G,W,Z

14.0 7.0 4.0 8.0 6.0 42.0 46.0 96.0 25.0

SLOPE = .050 CK = .0011

Q	Y	H	CON	QSI	FILL	SCOUR	HSED
100.00	.22	.48	2.15	2.856	-10.777	-5.093	.475
200.00	.33	.96	6.46	7.032	-7.786	-6.535	.958
500.00	.57	2.48	25.89	21.205	4.747	-8.949	2.449
1000.00	.86	5.26	69.31	46.326	28.595	-11.183	5.068
1500.00	1.10	8.60	118.48	72.092	53.628	-12.625	7.755
2000.00	1.31	14.24	142.23	97.706	78.985	-13.158	9.013
2500.00	1.50	21.00	146.63	123.079	104.315	-13.249	9.244
3000.00	1.67	21.51	172.95	148.206	129.206	-13.754	10.617
3500.00	1.83	22.06	190.60	173.102	153.962	-14.059	11.531
4000.00	1.98	22.65	199.89	197.784	178.576	-14.212	12.010

SLOPE = .150 CK = .0061

Q	Y	H	CON	QSI	FILL	SCOUR	HSED
100.00	.29	.48	2.13	46.778	-54.551	-18.568	.472
200.00	.44	.96	6.30	98.602	-11.402	-23.743	.943
500.00	.76	2.48	24.03	249.018	127.300	-32.143	2.323
1000.00	1.15	5.26	57.42	499.314	369.306	-39.150	4.388
1500.00	1.47	8.60	81.51	744.201	610.703	-42.380	5.750
2000.00	1.75	14.24	64.27	983.867	852.747	-40.160	4.781
2500.00	2.00	21.00	55.19	1219.247	1089.628	-38.801	4.258
3000.00	2.23	21.51	66.80	1451.054	1319.552	-40.513	4.925
3500.00	2.44	22.06	74.76	1679.815	1547.187	-41.559	5.374
4000.00	2.65	22.65	78.53	1905.927	1772.806	-42.024	5.584

SLOPE = .250 CK = .0110

Q	Y	H	CON	QSI	FILL	SCOUR	HSED
100.00	.25	.48	2.11	89.060	-168.340	-33.840	.469
200.00	.38	.96	6.14	181.095	-98.009	-43.119	.928
500.00	.65	2.48	22.32	453.308	145.601	-57.743	2.207
1000.00	.99	5.26	48.80	895.629	569.180	-68.922	3.881
1500.00	1.26	8.60	62.22	1322.654	990.151	-72.819	4.664
2000.00	1.50	14.24	42.83	1738.644	1415.399	-66.917	3.523
2500.00	1.71	21.00	35.48	2146.152	1827.473	-64.127	3.070
3000.00	1.91	21.51	42.80	2546.807	2223.578	-66.907	3.521
3500.00	2.10	22.06	47.82	2941.726	2615.773	-68.609	3.823
4000.00	2.27	22.65	50.14	3331.724	3004.603	-69.348	3.961

AD-33 Bookplate
(1-63)
U. S. FOREST SERVICE
NATIONAL F.C.
AGRICULTURAL
LIBRARY
LIBRARY COPY
ROCKY MT. FOREST & RANGE
EXPERIMENT STATION